IRAM Annual Report 2015

iram
Institut de
Radioastronomie
Millimétrique

IRAM Annual Report 2015

Published by IRAM ©2015
Director of publication Karl-Friedrich Schuster
Edited by Cathy Berjaud, Roberto Neri, Karin Zacher

With contributions from:
Sébastien Blanchet, Walter Brunswig, Isabelle Delaunay, Eduard Driessen, Bertrand Gautier, Olivier Gentaz, Frédéric Gueth, Carsten Kramer, Bastien Lefranc, Santiago Navarro, Roberto Neri, Juan Peñalver, Karl-Friedrich Schuster

Contents

Introduction

We are proud to present the IRAM 2015 annual report. Such a report is not only a valuable internal exercise and a duty defined in our statutes but also useful to document how IRAM evolves over the years and how the great trust our partners put into the institute results in excellence science.

The selection of science topics presented in this report represents only a very small fraction of the huge number of scientific results from the IRAM instruments published every year. Research on galactic and extragalactic star formation and the formation of galaxies themselves throughout cosmological timescales remain at the center of the astronomy done with IRAM. An increasingly important branch of IRAM's science however also is related to the search and identification of complex organic molecules in the solar system and galactic star formation regions. This particular part of millimeter astronomy has recently created spectacular synergy with laboratory experiments such as, for example the investigation of radiation-induced synthesis of complex molecules on ice mantles of dust. In particular the unique frequency coverage and the sensitivity of NOEMA and the 30-meter telescope will revolutionize research in this area. The extended instrumental capabilities of IRAM have also supported the expansion of IRAM's activities into new fields such as the high signal to noise mapping of SZ sources, millimeter VLBI for imaging of supermassive black holes and detection of pulsars at millimeter wavelengths.

Representatives from IRAM, CNRS, MPG and Leitner Ropeways inaugurating on Oct 2, 2015, the new cable-car system of the NOEMA observatory. From left to right: E. Rolland (Leitner Ropeways), D. Mourard (CNRS), D. Ribot (Leitner Ropeways), K. Schuster (IRAM), M. Schleier (MPG)

In 2015, IRAM has seen several extremely important steps taken. Unsurprisingly, NOEMA and its progress is at the center of all our attention. With the commissioning and science verification of the first NOEMA antenna 7 in early 2015, the project has shown that two key elements of the NOEMA concept, new antennas and ultra-broad band receivers, have made the transition from concept to reality and at the same time show excellent performance. The extension of the existing correlator WIDEX to an eight antenna configuration was successful thanks to forward looking decisions made nearly ten years ago, well before the greenlight for the NOEMA project. This tells us to remain ambitious with visions extending beyond near term goals. The focus shifts now towards streamlining and optimizing the construction and integration of the following antennas and their equipment including the new NOEMA correlator. During 2015, the construction of antenna 8 has progressed extremely well and at the moment of editing this report, the antenna has actually entered commissioning.

At the same time IRAM has now to care about optimization of the sometimes challenging compromise between upgrading and science operation. We hope that the steep progress in the NOEMA project does compensate our users for the various restrictions that exist in the current transitional phase.

This brings me to another important event that is intimately linked to the rapid progress made during the last twelve months. On August 2015 the new cable car started its operation for transport of persons and material.

Meanwhile, at the IRAM 30-meter telescope in October 2015, NIKA 2, simply spoken the most powerful millimeter wave continuum imager of all times, has seen a very smooth installation. The complex preparation of the receiver cabin with a new Nasmyth-Optics and the very numerous constraints in space and environmental as well as boundary conditions with other instruments, made this installation a major challenge. First light was obtained only two weeks later and confirms a very promising behavior of NIKA 2. However testing and commissioning of this complex instrument will need clearly more time than anticipated and user software is bound to be on a very basic level for the start of the instrument. The success achieved so far is due, in large part, to the very close and fruitful collaboration between the NIKA 2 PI team and IRAM.

IRAM's success is not without generating quite some attention worldwide and IRAM is proud that in September 2015 a collaboration agreement between the University of Michigan Ann Arbor and IRAM could be concluded. This agreement will not only help to further develop NOEMA but will greatly foster scientific collaboration across the Atlantic.

Finally, 2015 was completed with the great news that the Max-Planck-Society could identify the necessary resources to build the NOEMA baseline extension. IRAM will therefore be able to keep on track with its declared plans and continue to generate excellence for its user community.

With best regards

Karl-Friedrich Schuster
Director

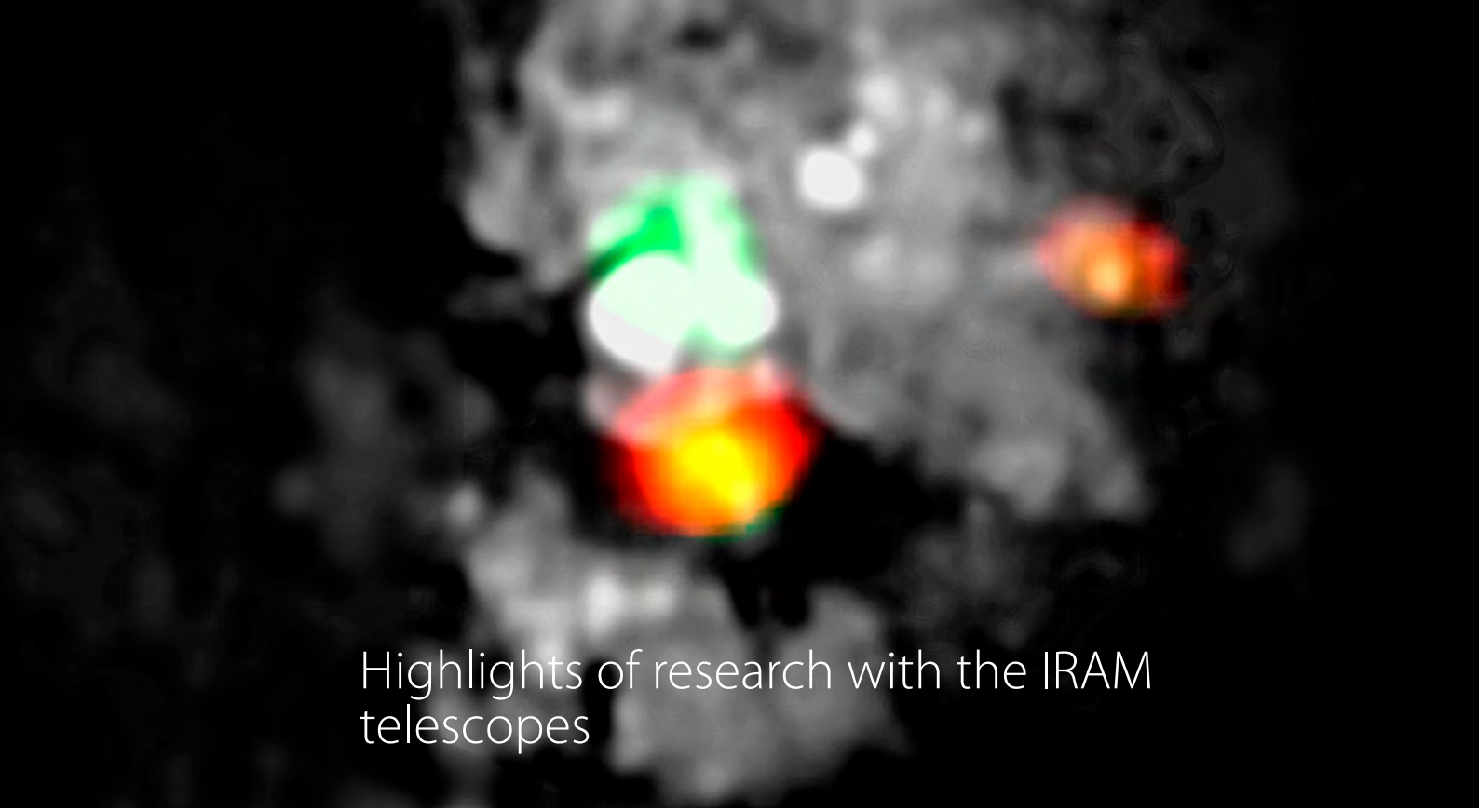

Highlights of research with the IRAM telescopes

ETHYL ALCOHOL AND SUGAR IN COMET LOVEJOY (C/2014Q2)

Comets are among the most pristine bodies of the solar system. As primordial remnants of our solar system, they are a unique source of information on the physics and chemistry of the protosolar nebula from which the solar system has formed, and very likely an important source of prebiotic molecules for the building blocks of life on Earth. When a comet comes close to the Sun, the ices of its nucleus sublimate to form an atmosphere rich in molecules that can be probed from the ground with instruments such as EMIR at the IRAM 30-meter radiotelescope. Among the molecules identified in comets, the most important are water, simple hydrocarbons, oxygen, sulfur, nitrogen-bearing species, as well as a few complex organic molecules (COMs), such as ethylene glycol and glycine.

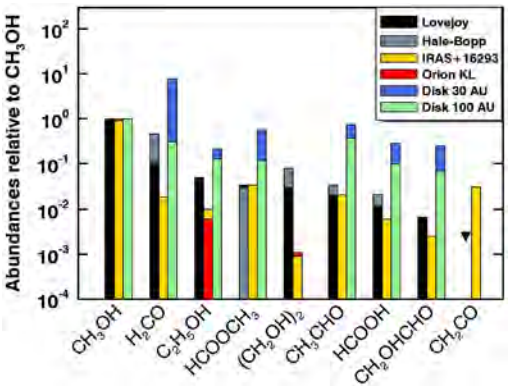

Abundances (relative to methanol) measured in comets Lovejoy and Hale-Bopp, as compared to two regions of star formation, Orion KL and IRAS 16293-2422. The figure also shows the results of simulations of organic synthesis in a protoplanetary disk at 30 and 100 AU from the protostar (Walsh et al. 2014).
Work by Biver et al. 2015, Science Advances, 1, 9

As part of a recent EMIR campaign to survey the chemical composition of comet C/2014 Q2 in the 210-272 GHz spectral domain, Nicolas Biver (LESIA) and collaborators reported the detection of 21 molecules including the first identification of ethanol (C_2H_5OH) and the simplest monosaccharide sugar glycolaldehyde (CH_2OHCHO) in a comet. They found that the abundances of ethanol and glycolaldehyde, respectively 5 and 0.8% relative to methanol (0.12 and 0.02% relative to water), were somewhat higher than the values measured in solar-type protostars. Such a high abundance of COMs in the atmosphere of C/2014 Q2 is suggestive of the formation of COMs through grain-surface reactions in the protoplanetary disk of the primordial solar system. The authors conclude that the relatively high abundance of these molecules in C/2014 Q2 in comparison to what is measured in regions of star formation, is also hinting to the possibility that an important part of the organic synthesis of these compounds has taken place in the outskirts of the protosolar nebula.

A SEARCH FOR FORMAMIDE (NH_2CHO), A KEY PREBIOTIC PRECURSOR

The origin of life on Earth is today one of the biggest unsolved questions of science. Addressing this fascinating issue is the job not only of biologists or biochemists, but also of astrochemists. Indeed, astrochemistry can help understanding to what extent organic matter may have been exogenously delivered onto the young Earth, or how organic chemistry works elsewhere in space. For this reason,

the search for biochemically relevant molecules in comets and star-forming regions is one of the main targets of astrochemistry.

One of such molecules is formamide (NH_2CHO), believed to have played a key role in the context of the origin of life on Earth due to its chemical versatility, which can result in a variety of prebiotic molecules such as sugars, amino acids, and nucleic bases. While this molecule has been observed in space, most of its detections correspond to massive star-forming regions. Motivated by this lack of investigation in the low-mass regime, Ana López Sepulcre (IPAG/U.Tokyo) and collaborators performed a search for NH_2CHO in 10 solar-mass pre- and proto-stellar objects. This study is part of the IRAM 30-meter telescope Large Programme Astrochemical Surveys At IRAM (ASAI). Thanks to the superb frequency coverage of the spectral observations carried out within ASAI, López Sepulcre and collaborators were able to evaluate the detectability of multiple molecular transitions of NH_2CHO. They detected formamide in five targets, and found that its abundance is tightly correlated with that of HNCO. On the other hand, the five sources with no formamide detection, which are also the coldest, display an excess of HNCO relative to NH_2CHO. These results suggest that, while HNCO can form efficiently in the gas phase during the cold phases of star formation, NH_2CHO predominantly forms on the icy mantles of dust grains, until the temperature rises sufficiently to sublimate them and release formamide into the gas. While the authors propose hydrogenation of HNCO as a likely route of NH_2CHO formation, recent experimental results challenge this conclusion. However, the strong abundance correlation between the two species places solid constraints and remains to be explained in future studies, perhaps with the aid of interferometric observations.

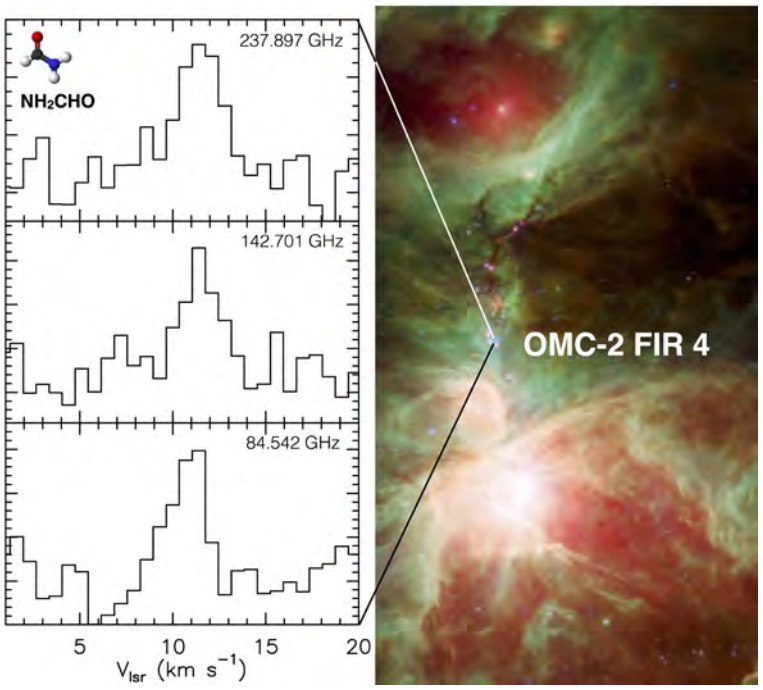

Three of the NH_2CHO lines detected in OMC-2 FIR 4, one of the targets of the study. A Spitzer composite image around this region at 2.2, 3.6, and 4.5 µm is also shown. Work by López Sepulcre et al. 2015, MNRAS, 449, 2438

This study proves that key prebiotic precursors such as formamide can be synthesized in solar-mass star-forming regions at a relatively early stage. It also highlights the importance of communication among observers, theoretical chemists, and experimentalists, in order to make progress in astrochemistry.

A LARGE RESERVOIR OF ORGANIC MATERIAL IN L1544

Complex organic molecules (COMs) are of particular interest for their potential relation with the origin of life on Earth. COMs were first detected in hot cores associated with high-mass, star-forming regions, then in a variety of environments such as low-mass hot-corinos, cold envelopes, Galactic center cold clouds and prestellar cores. Given the key role that COMs in prestellar cores have for our understanding of the general mechanisms of their formation, it is important to establish a census, as complete as possible, of the COMs in prestellar cores, and better characterize the regions where they are observed, and, as a consequence, better estimate their abundances.

Placed in the Taurus star-forming region, at about 450 light-years from Earth, L1544 is the prototype of prestellar cores, the cold gas condensations on the verge of collapsing to form new stars.

Charlotte Vastel (IRAP) and collaborators used the data collected on L1544 in the frame of ASAI, an IRAM 30-meter telescope Large Program aimed at providing a full census of oxygen bearing COMs in its central region. These observations were made with EMIR and led to the detection of many complex molecules.

Tricarbon monoxide (C_3O), methanol (CH_3OH), acetalhehyde (CH_3CHO), formic acid (HCOOH), ketene (H_2CCO) and propyne (CH_3CCH) were detected with abundances ranging from $5x10^{-11}$ to $5x10^{-9}$. In order to explain the methanol abundance, the authors argue that the ices, where methanol has formed, are desorbed through non-thermal processes in an outer layer of the dense core, where the far ultraviolet radiation can penetrate. They also suggest that it is likely that water and the other COMs detected have the same origin. Even more

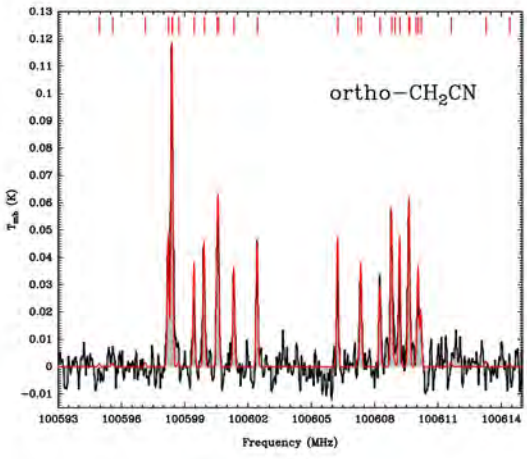

Spectral profile of the ortho-CH_2CN transitions around 100.6 GHz (in black) superposed with the results of LTE modeling (in red). Work by Vastel et al. 2015, A&A Letters, 582, L3, and 2014, ApJL, 582, L2

recently, complex spectral patterns near 100.6 GHz for which the authors suspected the presence of hyperfine structures, have been identified with the lines of the ortho and para forms of the cyanomethyl radical CH_2CN.

The results from LTE radiative transfer modeling of CH_2CN show that the spectra are perfectly reproduced using a column density of the ortho and para forms of 3.5×10^{11} cm^{-2} for an excitation temperature of 10 K, using a full width at half maximum of 0.3 km s^{-1} at a systemic velocity of 7.25 km s^{-1}. The results also show that the hyperfine structure of the ortho form of CH_2CN is clearly identified, while the hyperfine structure of the para form is only marginally detected. This suggests that the ortho-to-para ratio of CH_2CN in L1544 is close to unity. The abundance, which is estimated between 1.9×10^{-12} (at 15 K) and 1.6×10^{-10} (at 5 K), is found to vary with the C/O ratio.

All in all, these ASAI observations reveal a very rich organic content in the L1544 prestellar core. Although it is difficult to predict all the chemical processes to which these organic molecules will be subjected during the formation of a new star and planetary system, upon viewing of these rich molecular spectra it is tempting to suggest that the prebiotic chemistry can be rooted in the interstellar medium, at very early stages of the star formation process.

HIERARCHICAL FRAGMENTATION IN IRDC 18310-4

The initial conditions required to allow high-mass star formation are still poorly characterized but recent studies suggest the time span during which massive gas clumps exist without embedded star formation is of the order of 50 000 yr. The same studies raise questions, however, about how fragmentation of high-mass clumps to individual star forming cores is initiated during the earliest evolutionary stages, and about the specifics and kinematic properties of these regions.

To address these questions, a group of researchers led by Henrik Beuther (MPIA) used NOEMA and the IRAM 30-meter telescope to observe IRDC 18310-4, a 70 µm dark starless region. The aim was to investigate the earliest evolutionary of high-mass

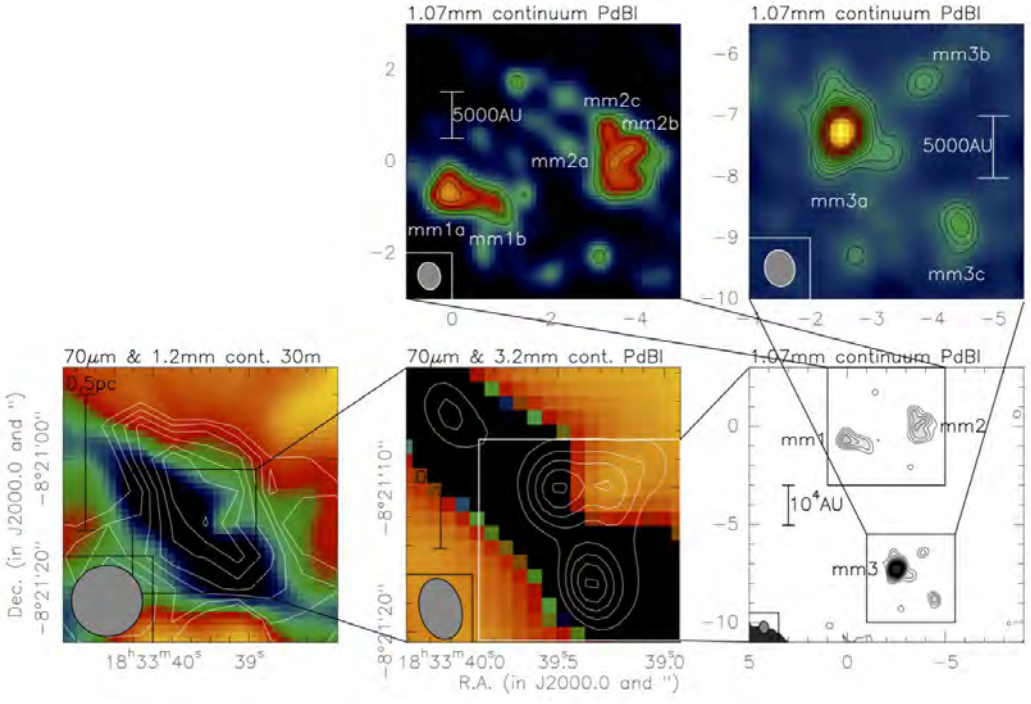

Continuum images in IRDC18310-4. The bottom left and middle panels show in color the Herschel 70 µm image with a wedge going dark for low values. The white contours in the left panel show the 1.2mm MAMBO continuum maps obtained at the IRAM 30-meter telescope. The contours in the bottom middle panel show the NOEMA 3.2mm continuum. The bottom right panel then shows the NOEMA 1.07mm continuum. The two top panels show zooms of the 1.07mm continuum data with a different color wedge to highlight the substructures. Work by Beuther et al. 2015, A&A, 581, A119

star formation prior to the existence of embedded heating and outflow sources that could quickly destroy any signatures of the early kinematic and fragmentation properties. The researchers aimed at resolving the length scales for filament formation and fragmentation (resolution ≤0.1 pc), in particular the Jeans length and cylinder fragmentation scale.

By zooming through different size scales from single-dish data to intermediate and high angular resolution observations, Beuther and collaborators show that the resolved entities always fragment hierarchically into smaller substructures at the higher spatial resolution. While the fragment separations are still in approximate agreement with thermal Jeans fragmentation, the observed core masses are orders of magnitude larger than the estimated Jeans masses at the given densities and temperatures. However, the data can be reconciled with models using non-homogeneous initial density structures, turbulence, and/or magnetic fields. While most sub-cores remain (far-)infrared dark even at 70 µm, they identify weak 70 µm emission toward one core with a comparably low luminosity of ~16 $L_\odot$. The spectral line data show multiple spectral components toward each core with comparably small line widths for the individual components (in the 0.3 to 1.0 km s^{-1} regime). Based on single-dish $C^{18}O$ (2–1) data, a virial-to-gas-mass ratio of ≤0.25 is estimated. The authors propose that the likely origin of these spectral properties may be the global collapse of the original gas clump that results in multiple spectral components along each line of sight. Even within this dynamic picture the individual collapsing gas cores appear to have very low levels of internal turbulence. Beuther and coworkers conclude that the IRDC 18223-04 3.2 mm continuum data are consistent with thermal fragmentation of a gravitationally bound and compressible gas cylinder.

A MULTI-OBSERVATORY, MULTI-TRANSITION STUDY OF THE PROTOSTELLAR OUTFLOW CEPHEUS E

It is now well established that the formation of protostars powers fast jets surrounded by wide-angle winds that impact the high-density parent cloud. These jets interact through shock fronts that compress and heat the ambient gas while driving the formation of low-velocity bipolar outflows. While the low-excitation lines of CO have been the privileged tools of the study of protostellar outflows for decades, the Herschel Space Observatory and SOFIA have made it possible to observe in a systematic way the CO ladder up to very high energy levels. This allows a much more accurate determination of the physical conditions and the origin of the high-temperature gas in protostellar outflows.

To perform such multi-transition study of the CO rotational ladder from millimeter to far-infrared wavelengths of a protostellar outflow, Bertrand Lefloch (IPAG) and collaborators embarked on a study of the outflow of the intermediate-mass Class 0 protostar Cepheus E. The goal was to determine the structure of the outflow and to constrain the physical conditions of the various components in order to understand the origin of the mass-loss phenomenon. The team observed several rotational transitions of CO with GREAT/SOFIA, with HIFI/Herschel towards the position of the terminal bowshock HH377, and produced large CO maps with the IRAM 30-meter telescope, the NOEMA interferometer (J = 2–1), and the James Clerk Maxwell Telescope.

The protostellar outflow shows three main components: the jet, the cavity, and the bowshock, with a typical size of 1.7″ × 21″, 4.5″, and 22″ × 10″, respectively. In the jet, the emission from the low-J CO lines is dominated by a gas layer at T_{kin} = 80–100 K, column density $N_{CO} = 9 \times 10^{16}$ cm^{-2}, and density $n(H_2) = (0.5–1) \times 10^5$ cm^{-3}; the emission of the high-J CO lines is found to arise from a warmer (T_{kin} = 400–750 K), denser ($n(H_2) = (0.5–1) \times 10^6$ cm^{-3}), lower column density ($N_{CO} = 1.5 \times 10^{16}$ cm^{-2}) gas component. Similarly, in the outflow cavity, two components are detected: the emission of the low-J lines is dominated by a gas layer of column density $N_{CO} = 7 \times 10^{17}$ cm^{-2} at T_{kin} = 55–85 K and density in the range $(1–8) \times 10^5$ cm^{-3}; the emission of the high-J lines is dominated by a hot, denser

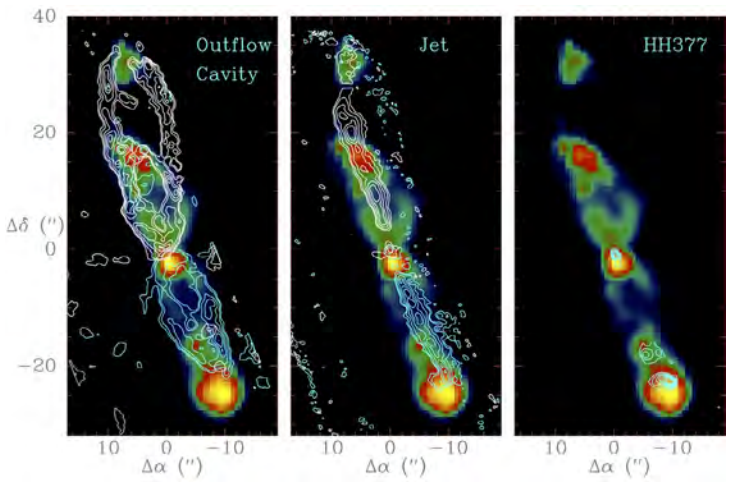

Cepheus E outflow emission observed in the CO J = 2–1 line with NOEMA at 1″ resolution (contours) and with IRAC/Spitzer H24.5 µm line (color). Each panel shows the emission associated with each of the three outflow components identified: (left) outflow cavity walls emission, integrated between −15.2 and −8.7 km s^{-1} in the southern lobe (blue contours) and between −2.2 and −8.7 km s^{-1} in the northern lobe (white contours); (center) jet emission integrated between −135 and −110 km s^{-1} and between +40 and +80 km s^{-1} towards the southern (blue contours) and northern lobes (white contours), respectively; (right) HH377 bowshock emission integrated between −77 and −64 km s^{-1} (blue contours).
Work by Lefloch et al. 2015, A&A, 581, A4

gas layer with T_{kin} = 500–1500K, $n(H_2) = (1–5) \times 10^6$ cm^{-3}, and $N_{CO} = 6 \times 10^{16}$ cm^{-2}. A temperature gradient, as a function of the velocity, is found in the high-excitation gas component. In the terminal bowshock HH377, the authors detect gas of moderate excitation, with a temperature in the range $T_{kin} \approx$ 400–500 K, density $n(H_2) \simeq (1–2) \times 10^6$ cm^{-3} and column density $N_{CO} = 10^{17}$ cm^{-2}. The amounts of momentum carried away in the jet and in the entrained ambient medium are similar. Comparison with time-dependent shock models shows that the hot gas emission in the jet is well accounted for by a magnetized shock with an age of 220–740 yr propagating at 20–30 km s^{-1} in a medium of density $n(H_2) = (0.5–1) \times 10^5$ cm^{-3} consistent with that of the bulk material.

According to the researchers, the observations trace the recent impact of the protostellar jet into the ambient cloud, producing a non-stationary magnetized shock, which drives the formation of an outflow cavity. They conclude that the Cepheus E protostellar outflow appears to be a convincing case of a jet bowshock driven outflow.

CLOCKING THE SPIN OF A MAGNETAR

Average pulse profiles of SGR J1745-2900 at 2.54, 4.85, 8.35, 87, 101, 138, 154, 209 and 225 GHz.
Work by Torne et al. 2015, MNRAS, 451, l50

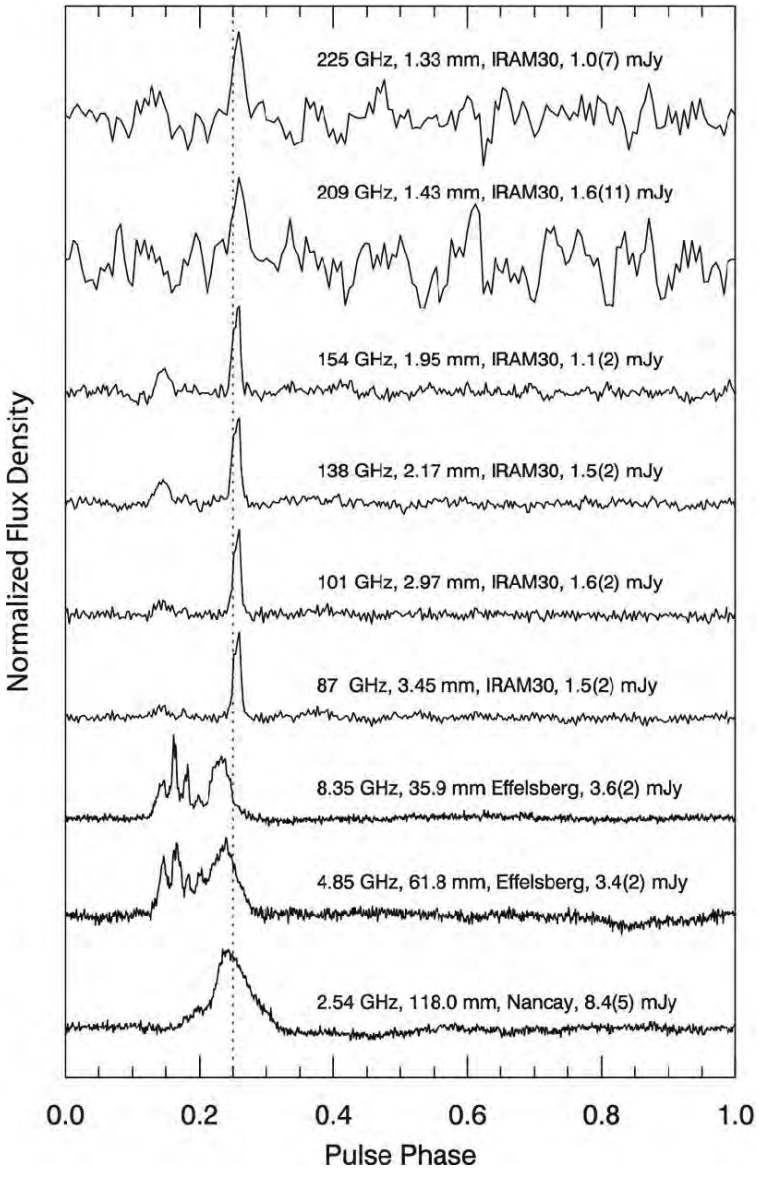

Magnetars are the strongest magnets in the present universe and the combination of extreme magnetic field, gravity and density makes them unique laboratories to probe physical theories from quantum electrodynamics to general relativity. They are observed as slowly rotating, bursting X-ray pulsars, and are usually classified as anomalous X-ray pulsars (AXPs) and soft gamma repeaters (SGRs). Among them is J1745-2900, a radio-loud SGR in the vicinity of Sgr A*, the supermassive black hole candidate in the Galactic Center (GC). Being a precise timekeeper, any deviation or bending of the radiation caused by Sgr A* could be used to test theories of gravity to the highest precision. To investigate its interest as a tool to probe fundamental physics such as general relativity, gravitational waves and nuclear interaction, Pablo Torne (MPIfR) and collaborators have employed the Effelsberg, Nançay and IRAM 30-meter telescopes and reported multi-frequency data of SGR J1745-2900.

The authors detect SGR J1745-2900 up to 225 GHz, the highest radio frequency detection of pulsed emission from a neutron star to date. The detections set a new record for the detection of pulsed emission from a neutron star in the radio band. The high measured flux densities of SGR J1745−2900, on average S = 1.4 ± 0.2mJy between 87 and 225 GHz, and the numerous strong single-pulses detected up to 154 GHz show that SGR J1745-2900 can be, at least during some periods of activity, an efficient producer of radiation at very high radio frequencies.

These detections suggest that emission at very high radio frequencies from radio-loud magnetars might be a frequent characteristic of these objects. And a key advantage of pulsar searches at millimeter wavelengths is that deleterious effects caused by the GC interstellar medium, like pulse scattering and dispersion, can be fully neglected. The high luminosity of SGR J1745-2900 in the millimeter band suggests that the detection of a less-luminous population of magnetars with the higher sensitivity of facilities, such as NOEMA and ALMA, is likely to be very promising.

AN EXTREME STAR FORMATION REGION IN THE "EYE OF MEDUSA"

The focus on studies of galaxy mergers often lies on major mergers and their evolution, but the impact of minor mergers on the stellar evolution of galaxies is expected to be more important than that of major mergers. Understanding how minor mergers trigger star formation is therefore key to our understanding of galaxy evolution.

In an attempt to address this question, Sabine König (IRAM) and collaborators (France, Sweden, UK, Germany, US) have used the NOEMA array to observe the nearby Medusa galaxy (NGC 4194), a minor merger with an exceptionally fast growing stellar component. The aim was to determine the distribution of the dense gas by using the HCN and HCO^+ (1-0) transitions as tracers. These lines originate generally in gas that is up to 2-3 orders of magnitude denser than gas traced by the corresponding rotational CO transition lines. Contrary to ULIRGs, the Medusa shows a low CO/HCN (1–0) luminosity ratio indicating that the fraction of dense gas is significantly higher despite similar star formation efficiency. A possible reason for this difference is that HCN in the Medusa is not tracing star formation directly, but rather is formed as a result of the feedback of the young star-forming regions on their surrounding medium.

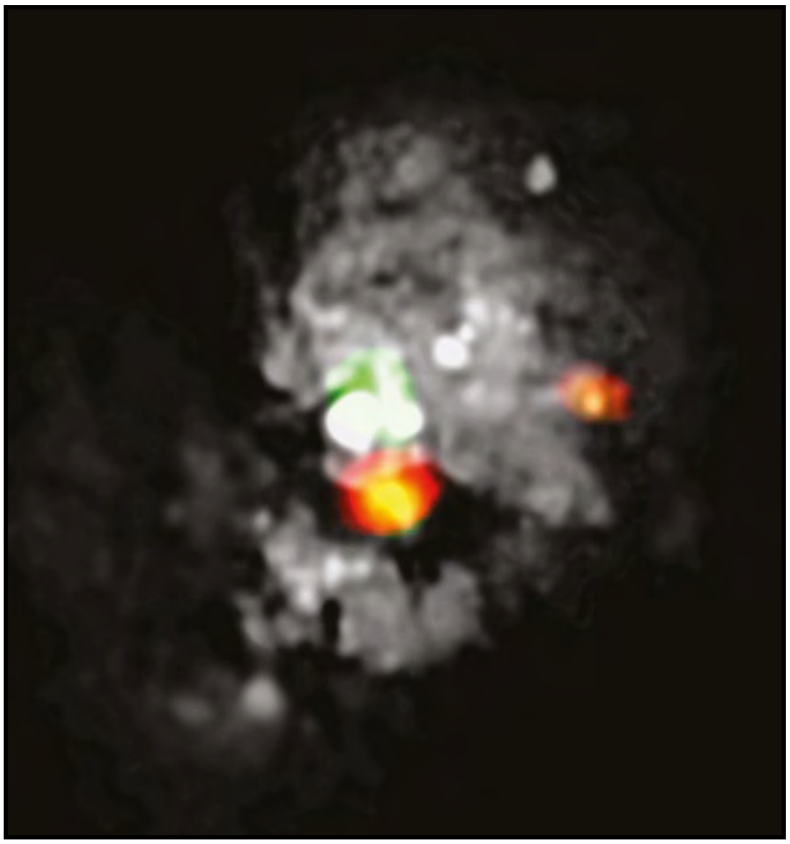

The multi-wavelength image shows the 'Eye of Medusa' (orange) located directly below the black hole at the center of NGC 4194 (white and green). Credits: IRAM/ NASA/ESA Hubble Space Telescope, Hubble Legacy Archive.
Work by König et al. 2015, IRAM Press Release

The observations of the Medusa revealed a giant region, about 500 light years across, of recently formed massive stars at the center of the 'Eye of Medusa', the central gas-rich region of the merger. The stars appear to be still wrapped in their dusty birth clouds and completely hidden from view in visible light.

The discovery demonstrates that star development can be probed in stages of formation, which are currently not detectable by tracing carbon monoxide. By successfully detecting other molecules, the extreme star formation observed in the Medusa demonstrates the existence of more complex chemical formulations than previously thought. This discovery means our understanding of the chemical formation of stars can be hugely expanded upon.

MASSIVE OUTFLOWS SHAPING MERGER EVOLUTION

Massive gas outflows powered by active galactic nuclei (AGN) and nuclear starbursts are intimately linked to the growth of black holes and their hosts galaxies - they prevent galaxies from becoming overly massive and help regulate the fueling of both the star formation and the nuclear activity. Studies are showing that, regardless of the driving mechanism, these outflows affect all phases of the interstellar medium (ISM) out of which stars forms and hence the overall evolution of the galaxy.

To shed new light on the specific role that star formation and AGN feedback can have in launching and maintaining molecular outflows in mergers, an international team of astronomers led by García-Burillo (OAN) has used the NOEMA interferometer to map the ^{12}CO emission in the two starburst-dominated LIRGs NGC 1614 and IRAS 17208-0014.

The data suggest most of the ^{12}CO emission stems from spatially resolved (~2–3 kpc-diameter) rotating disks but also provide significant evidence for the presence of high-velocity line gas that extend up to ±500–700 km s^{-1}, well beyond the estimated virial range associated with rotation and turbulence. The kinematic major axis of the line-wing emission is tilted by ~90° in NGC 1614 and by ~180° in IRAS 17208-0014 relative to the major axes of their

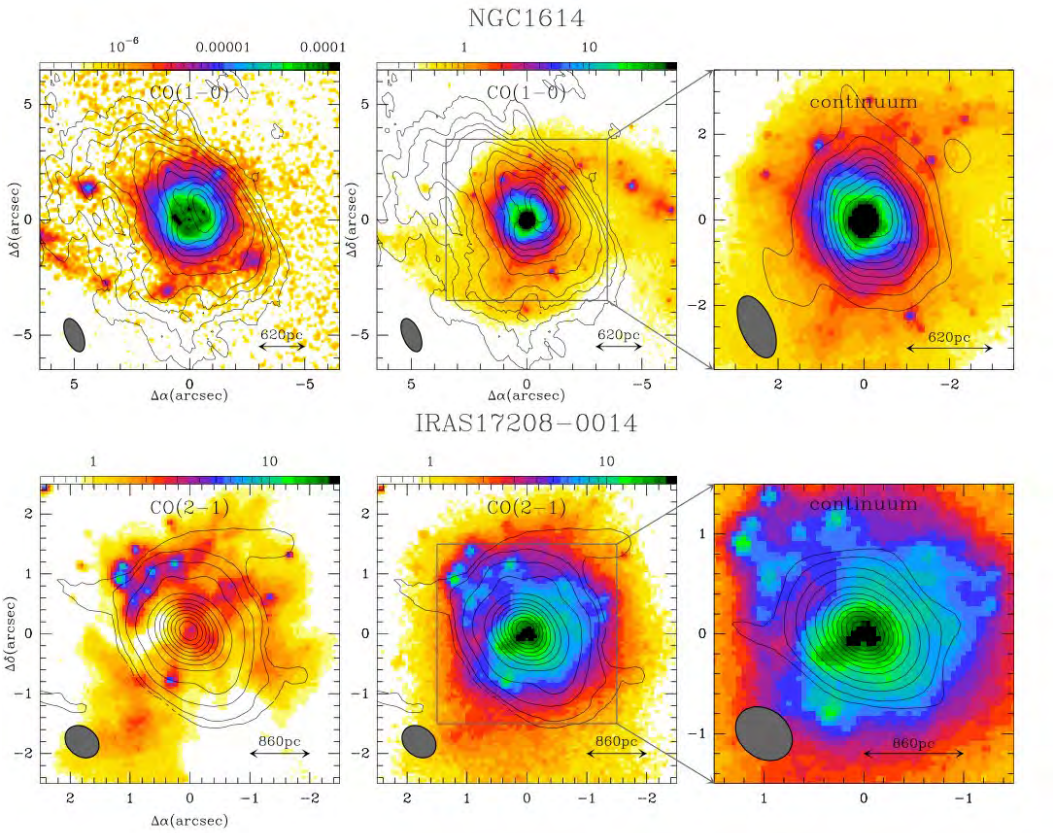

Top row: overlay of the NOEMA ^{12}CO(1–0) intensity contours on the HST Paα (left) and HST F160W emission (middle), and overlay of the NOEMA 3mm continuum on the zoomed-in NICMOS image (right). Bottom row: overlay of the NOEMA ^{12}CO(2-1) on the HST F814W (left) and HST/NICMOS F160W (middle), and overlay of the 1.4 mm continuum on the zoomed-in NICMOS image. Work by García-Burillo et al. 2015, A&A, 580, A35

respective rotating disks. These results suggests the existence of non-coplanar molecular outflows in both systems: the outflow axis being nearly perpendicular to the rotating disk in NGC 1614, and tilted relative to the angular momentum axis of the rotating disk in IRAS 17028-0014.

In stark contrast to NGC 1614, where star formation alone can drive its molecular outflow, the mass, energy, and momentum budget requirements of the molecular outflow in IRAS 17208-0014 can be best accounted for by the existence of a so far undetected AGN of 7×10^{11} $L_\odot$. The geometry of the molecular outflow in IRAS 17208-0014 suggests a non-coplanar disk that may be associated with a buried AGN in the western nucleus is launching the outflow. Higher resolution observations are necessary now to unambiguously identify the outflow-launching region.

WEIGHING THE BLACK HOLE IN NGC 1277

Supermassive black holes (SMBH) exhibit masses of several millions to tens of billions of solar masses. The existence of a correlation between the SMBH's mass and the mass/luminosity of the host galaxy's central bulge, strongly suggests that SMBHs play a key role in the growth and evolution of galaxies. While the mass of SMBHs is generally 0.2-1% of the galaxy's bulge mass, recent results on SMBHs of galaxy clusters provide supporting evidence for the existence of over-massive black holes with masses about 100 times the expected value. The existence of such massive SMBHs suggests part of the galaxy's stellar mass was stripped by tidal interactions with the cluster potential after the black hole had formed.

The most extreme candidate for harboring an ultra-massive black hole so far is NGC 1277, a compact lenticular galaxy with a stellar mass of 1.2×10^{11} $M_\odot$ and a central SMBH with a mass of 1.7×10^{10} $M_\odot$, about half the mass of the galaxy's bulge (van den Bosch et al. 2012). To corroborate (or not) the presence of such a supermassive black hole in the center of NGC 1277, an international team of astronomers led by Julia Scharwächter (LERMA) used NOEMA to obtain an independent constraint on its mass. Scharwächter and collaborators aimed at characterizing the gas kinematics by using the ^{12}CO(1-0) transition as a tracer of the gravitational potential. According to the authors, the molecular emission is most likely originating from the dust lane encompassing the galaxy nucleus at a distance of 0.9" (~320 pc). The double-horned ^{12}CO(1-0) profile found at 2.9" resolution traces 1.5×10^{8} $M_\odot$ of molecular gas, likely orbiting in the dust lane at

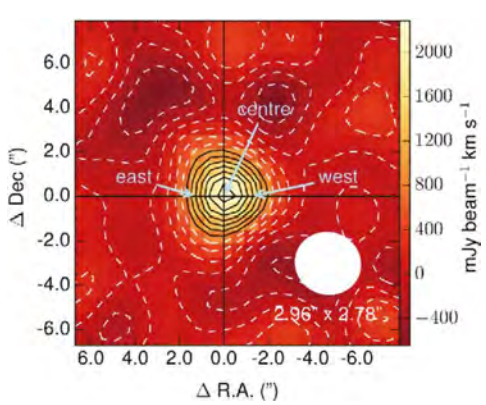

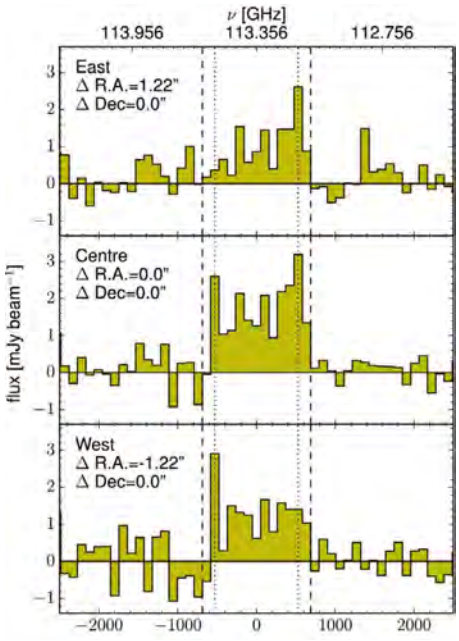

Left: Velocity integrated ^{12}CO(1-0) emission map obtained towards NGC 1277 in NOEMA's most compact configuration. 'East', 'Centre', and 'West' are the locations from which the spectra shown on the left were extracted.
Work by Scharwächter et al. 2015, MNRAS, 457, 4272
Right: Spectra extracted from an eastern, central, and western pixel in the ^{12}CO(1-0) emission peak.

~550 km s^{-1}, which suggests a total enclosed mass of ~2×10^{10} M$_\odot$. At 1" resolution, the ^{12}CO(1-0) emission appears spatially resolved along the dust lane in the East–West direction.

The authors conclude that the SMBH's mass estimate derived from the kinematics of the surrounding molecular emission and M/L$_V$=6.3 is indeed compatible with the high value found by van den Bosch et al. (2012), and that it would still be 15% for M/L$_V$=10.

While the molecular gas reservoir may be associated with a low-level star formation activity, the extended 2.6-mm continuum emission is likely to originate from a weak AGN with an inverted radio-to-millimeter spectral energy distribution.

THE GMVA SHEDS NEW LIGHT ON THE FLARES OF S5 0716+714

The combination of very long baseline interferometry (VLBI) images and broadband flux density variability is a unique and powerful way to unlock the emission mechanisms near the base of jets in active galactic nuclei (AGN). Radio flares, which are often found to be connected to the ejection of varying jet components, are therefore expected to provide key information on the structural evolution of the parsec-scale structure of AGN. In an attempt to explore the inner jet kinematics and its relation of the observed broadband flux variability, Rani (MPIfR) and collaborators embarked on 3mm Global Millimeter VLBI Array (GMVA) observations to observe the BL Lac object S5 0716+714 and measure size, brightness temperature, magnetic field, and motion of the jet emission regions.

According to the researchers, the jet shows significant non-radial motions with an exceptionally high superluminal speed of up to ~37c in the radial direction. The jet flow reveals a complex pattern with a roughly stationary feature ~0.15 mas downstream of the core. The long-term fits to the component trajectories reveal acceleration in the submas region of the jet. The study suggests a connection between jet kinematics and the observed broadband flaring activity. Rani and collaborators suggest a moving disturbance or a shock wave from the base of the jet has been producing high-energy optical to γ-ray variations upstream of the 7mm core and has been at the origin of an outburst in the core. Repetitive optical/γ-ray flares and the curved trajectories of the associated components suggest that the shock front propagates along a bent trajectory or helical path. Sharper γ-ray flares could be related to the passage of moving disturbances through the stationary feature.

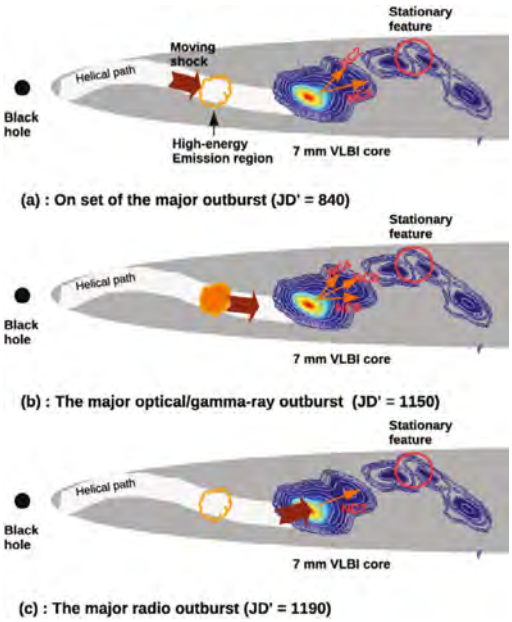

A shock propagates down the jet along a helical path, producing a major optical/γ-ray outburst upstream of the 7 mm VLBI core and later a major radio outburst accompanied by ejection of components from the core.
Work by Rani et al. 2015, A&A, 578, A123

A DISTANT GALAXY CLUSTER MERGER

Forming from the largest fluctuations in the primordial matter power spectrum, galaxy clusters are among the most massive gravitationally bound objects. The distribution of clusters as a function of mass and redshift shows clusters can be used as sensitive cosmological probes. Recent efforts exploiting the redshift-independent surface brightness of the Sunyaev-Zel'dovich effect (SZ) have detected ~1000 previously unknown clusters. While the Planck satellite is not well suited for the detection of high-*z*-systems whose SZ signal is heavily diluted inside Planck's beams. Planck's high-*z* detections are likely dynamically disturbed massive systems, which are far from being virialized and, on average, less X-ray luminous than X-ray selected clusters of the same mass.

Of the previously unknown clusters that Planck found, Tony Mroczkowski from Naval Research Lab and collaborators using the Goddard-IRAM Superconducting 2-Millimeter Observer (GISMO) on the IRAM 30-meter radiotelescope selected one spectacular candidate to image at 30 times higher resolution than Planck's original detection. The cluster they observed, called PLCK G147.3-16.6, was known from early X-ray follow-up observations to be a merger of two smaller clusters at z=0.645.

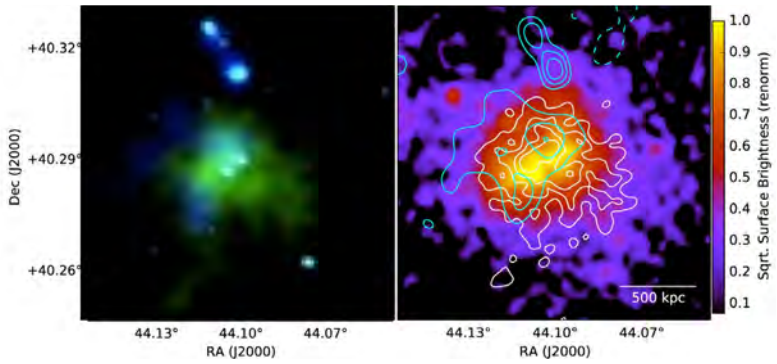

Left: PLCK G147.3-16.6 in the GISMO SZ imaging (green) and overlaid with GMRT 610 MHz radio emission (blue). Right: XMM-Newton SX image overlaid with GMRT (cyan) and GISMO contours (white). The image, shown on a square root scale (μ density), is smoothed with a 10" FWHM Gaussian.
Work by Mroczkowski et al. 2015, ApJ Letters, 808, L6

To the surprise of the scientists, the ground based imaging took less than 1/3 the time of the space-based X-ray observations and revealed most of the same structure seen in the X-ray observations. In the cluster core, however, the authors find that the SZ and X-ray peaks are somewhat offset. The location of the SZ signal at >6-σ broadly agrees with the location of the hottest gas found in the temperature and pseudo-pressure maps, but the authors find no clear evidence for shock-heated gas at the resolution of the X-ray spectroscopy and only a marginal enhancement of T_X = 11.33 keV over the global temperature T_X = 8.74 keV, in good agreement with the results found by the Planck Collaboration IV.

This leaves the possibility that the SZ/X-ray offset is due to an irregular gas distribution along the line of sight or the breakdown of the assumption that pseudo-pressure and SZ features should directly match. They conclude that while any contamination by the cosmic IR and microwave backgrounds is expected to be very marginal, differences in temperature or density substructure due to the on-going merging event are a more likely explanation.

A NEW TAKE ON THE 'SCALING RELATIONS' IN MAIN-SEQUENCE SFGS

Reinhard Genzel (MPE) and collaborators embarked on PHIBSS, a NOEMA Legacy Program, to pursue a comprehensive and systematic study of the molecular content of galaxies during the epochs associated with the rapid build-up (z>2), peak, and subsequent winding down (z<1) of star formation in the Universe. The aim of the program is to relate the physical properties of the gas content of galaxies to the cosmic evolution of the star formation rates (SFRs) with the goal of understanding the underlying physical processes, including the accretion and fragmentation of gas, star formation, wind outflows, and the final quenching of star formation.

The researchers used data from PHIBSS, COLDGASS and other surveys, to constrain the CO- and Herschel far-IR dust-based scaling relations of the molecular gas-mass depletion time, of the molecular gas mass to stellar mass ratio, and of the dust temperature as a function of redshift, specific star-formation rate (sSFR) offset, and stellar mass, for a sample of ~500 massive SFG (or stacks of SFGs) between z~0 and 3, with a focus on the near-main-sequence population. This is the first time that both dust and CO data have been compared in a large sample and on an equal footing across such a wide redshift range, spanning three orders of magnitude in sSFR and 1.8 orders of magnitude in stellar mass. In particular, the comparison of the CO and dust data allowed the researchers to derive quantitative constraints on the dependence of the CO conversion factor on redshift, sSFR offset from the main sequence (ms), and stellar mass (M*).

They found that the CO- and dust-based scaling relations agree remarkably well. This suggests that the CO/H_2 mass conversion factor varies little within ±0.6 dex of the main sequence (sSFR(ms,z,M*)), and less than 0.3 dex throughout the z~0 to 3 redshift range. They find that the gas depletion time scales

as $(1+z)^{-0.3}\times(sSFR/sSFR(ms, z,M^*))^{-0.5}$, with little dependence on M*. The resulting steep redshift dependence of Mmol gas/M* ≈ $(1+z)^3$ mirrors that of the sSFR and probably reflects the gas supply rate. The decreasing gas fractions at high M* are driven by the flattening of the SFR–M* relation. Throughout the probed redshift range a combination of an increasing gas fraction and a decreasing depletion timescale causes a larger sSFR at constant M*. As a result, galaxy integrated samples of the molecular gas mass to SFR rate relation exhibit a super-linear slope, which increases with the range of sSFR. With these new relations it is now possible to determine the molecular gas mass of near-main-sequence SFGs with an accuracy of ±0.1 dex in relative terms, and ±0.2 dex including systematic uncertainties.

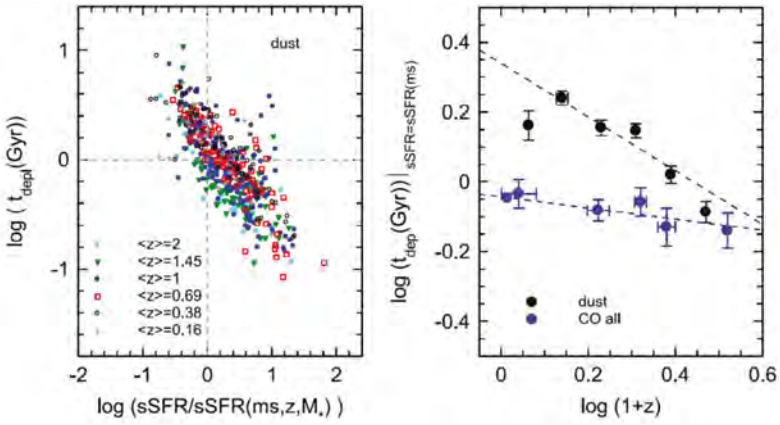

Left panel: dust-based molecular gas depletion time vs specific star-formation rate (sSFR) normalized to the main-sequence mid-line value at each redshift, for six redshift bins. Right panel: dependence of the CO-based (blue) and dust-based (black) molecular gas depletion time at the main-sequence mid-line on redshift, obtained from the zero-point offsets of the linear fits to the -0.59 slope in the log–log distributions in the left panel. Work by Genzel et al. 2015, ApJ, 800, 20

GALACTIC 'HAILSTORM' IN THE EARLY UNIVERSE

Two teams of astronomers led by Claudia Cicone and Tiago Costa from the University of Cambridge have looked back nearly 13 billion years, when the Universe was less than 10 percent its present age, to develop a better understanding of how quasars regulate the formation of stars and the build-up of the most massive galaxies. Using a combination of data gathered from the NOEMA interferometer and supercomputer simulations, the teams found that SDSS J1148+5251 at z~6.4 spits out cold gas at speeds up to 2000 km s^{-1}, and up to distances of nearly 30 kpc from the nucleus – much farther than has been observed before.

How this cold gas can be accelerated to such high speeds had remained a mystery. According to the authors, the gas is first heated to temperatures of $\geq 10^{6-7}$ K by the energy released by the supermassive black hole powering the quasar. This enormous build-up of pressure accelerates the hot gas and pushes it to the outskirts of the galaxy. The supercomputer simulations show that on its way out of the parent galaxy, there is just enough time for some of the hot gas to cool to temperatures low enough to be observable with radio telescopes.

Based on the spatially resolved [CII] observations. Cicone and collaborators estimate the median outflow dynamical time scale to 25 Myr. The distribution of the dynamical time scale within the outflow, however, is quite broad, ranging from 4 Myr to 100 Myr. This suggests the outflow has been in place for at least 100 Myr, which is a non-negligible fraction of the age of the Universe at this redshift, and that the ejection of gas in this source has not occurred at a constant rate, but most likely through multiple outflow events. The authors estimate the lower limits on the integrated mass-loss rate, momentum rate and kinetic power of the outflow to 1400 ± 300 $M_\odot$ yr^{-1}, (1.00 ± 0.14) L_{AGN}/c and (1.6 ± 0.2) × $10^{-3}L_{AGN}$, respectively.

The simulations by Tiago and collaborators have shown that radiative cooling of the hot shocked outflowing material can account in QSO at z~6 for the formation of entrained cold gas in both supernovae- and AGN-driven outflows at such distances. The large observed velocities (≥1000 km s^{-1}), however, require a combination of both. In the absence of supernovae feedback, the AGN-driven outflows that preferentially expand into the voids encounter gas of too low density and metallicity for sufficient cooling to take place and result in less vigorous, cold and dense outflows.

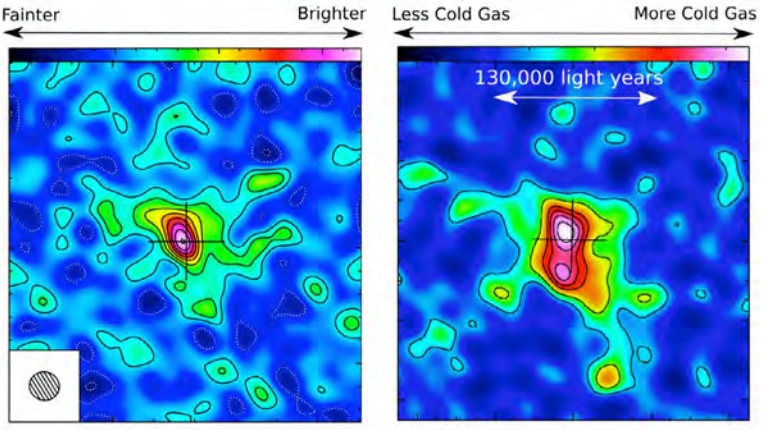

Left: IRAM NOEMA velocity integrated map of the total [C II] 158 µm emission of SDSS J1148+5251. Right: 'zoom-in' cosmological simulations of a z~6 QSO and its environment, following black hole growth and feedback via energy-driven outflows.
Work by Cicone et al. 2015, A&A, 574, A14 and Costa et al. 2015, MNRAS, 448, L30

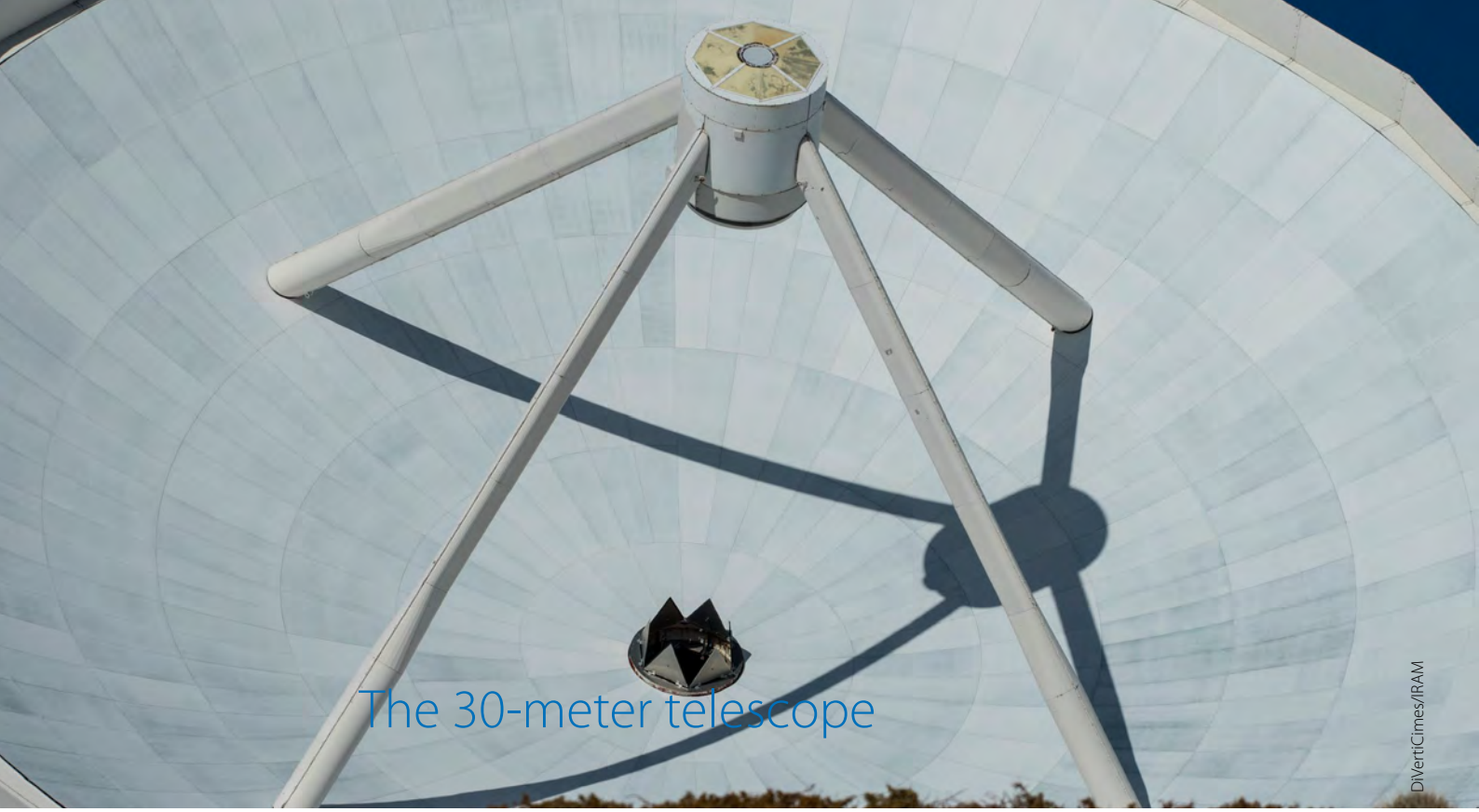

The 30-meter telescope

DiVertiCimes/IRAM

NIKA2, the 2nd generation New IRAM KID Array, was successfully installed in October 2015, followed by first very encouraging test and commissioning observations. These first-light observations finished a busy year at the telescope, which had started with the upgrade of the receiver cabin optics in April 2015, followed by the installation of a new cooling system for the NIKA2 compressors, and many other steps upfront of its installation. Here, we describe these important but intermediate steps towards making NIKA2 a large, new facility instrument at the 30-meter telescope.

The new receiver cabin optics, with its two large Nasmyth mirrors, allow for a large field-of-view of up to 7′, not only preparing for NIKA2 but also for the planned heterodyne array cameras at 3mm and at 1mm. Careful commissioning of the new optics with EMIR and HERA showed that the new configuration is stable and telescope efficiencies remain unchanged.

Frequency survey of the carbon-rich AGB star IRC+10216 between 70.3 and 117.5 GHz, observed with the upgraded EMIR band 1, the 3mm band E090.

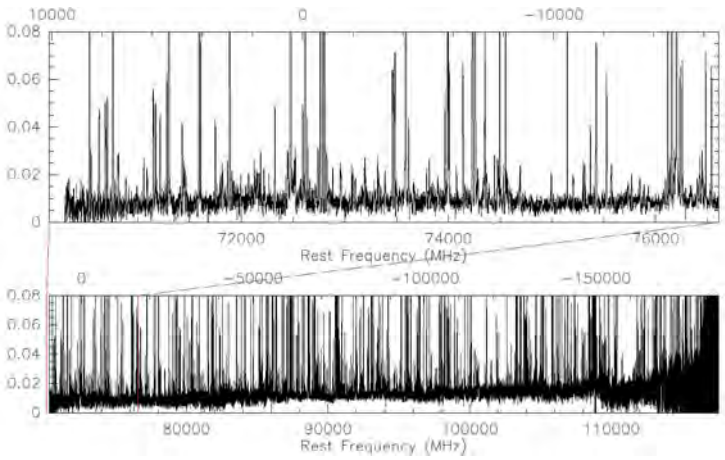

An international consortium led by the Institute Néel (Grenoble/France) is building NIKA2. The dual band camera, which is based on large arrays of superconducting Kinetic Inductance Detectors (KID) operating at a temperature of 150mK, observes simultaneously at 150 and 260 GHz. It is equipped with three arrays: one 1020 pixels array for imaging at 150 GHz and two arrays of 1140 pixels each for imaging at 260 GHz, allowing for polarimetry at the latter frequency. NIKA2's field of view has a diameter of 6.5′ and angular resolutions of 12″ and 18″, at the high and low frequency, respectively. The IDL data pipeline developed by Néel institute for the NIKA prototype camera, has been adapted and upgraded for NIKA2 to handle the online quick data reduction and also the offline data processing. Further upgrades of hard- and software, and in-depth characterization and commissioning of the instrument will take place in 2016.

The workhorse for most heterodyne observations is the Eight Mixer Receiver EMIR together with 24 broad-band fast fourier transform spectrometers covering a total bandwidth of 32 GHz. EMIR was installed in 2009 and continuously upgraded since then. The most recent upgrade was conducted in November/December 2015, by replacing the band 1 mixers against NOEMA-type mixers and by installing an ortho-mode transducer (OMT) for band 1. By splitting the two polarisations received via only one horn, the OMT ensures a perfect co-alignment of both polarisations. This upgrade extends the available frequency range down to 73 GHz without impinging on the upper frequency limit. Though the atmospheric transmission slowly degrades when going from 81 to 73 GHz due to an atmospheric

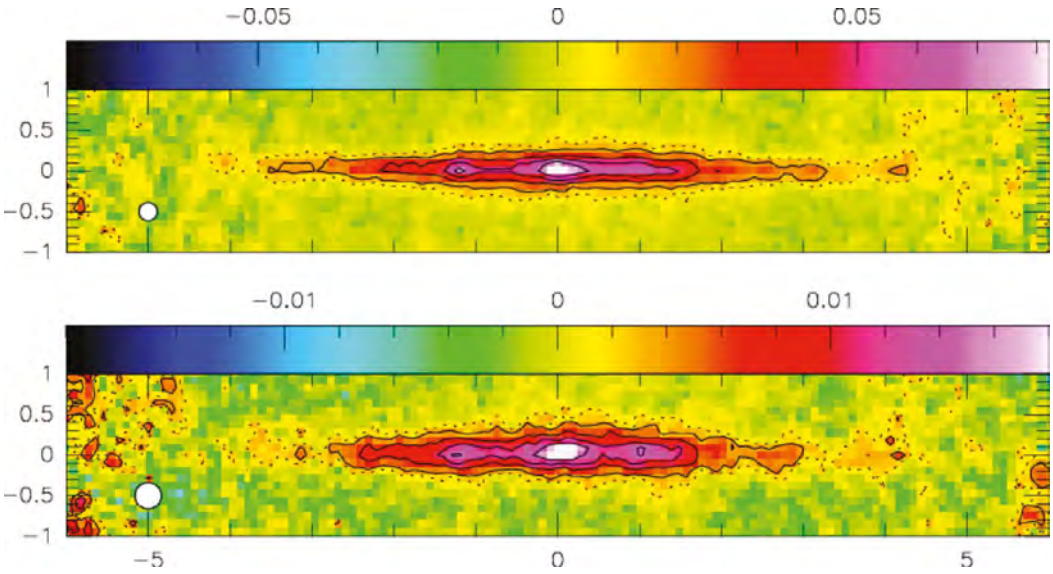

NIKA2 maps of NGC891 at 1mm (Upper) and at 2mm (Lower), taken in November 2015 during the initial testing phase. The maps cover a 12'x2' area. Half-power beamwidths of 12" and 18" are shown. Contours are at 10% (dashed), and 20% to 80% in steps of 20% (drawn) of the peak flux densities.

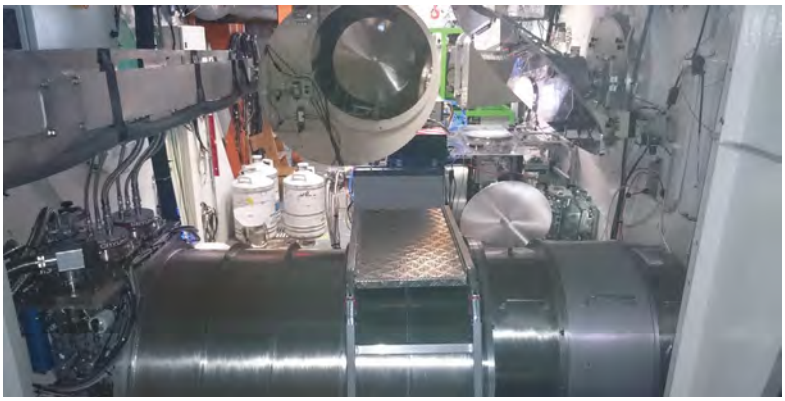

NIKA2 and the new optics inside the receiver cabin of the 30-meter telescope seen from the Vertex window of the primary mirror.

oxygen line at 60 GHz, the atmospheric transmission is robust against changing weather conditions. This frequency range can now be reached with excellent receiver temperatures and well determined image band rejections, allowing well calibrated observations of bright cooling lines of redshifted objects and access to a number of important chemical tracers of local molecular clouds like the low lying rotational transitions of deuterated species, e.g. DCO^+, DCN, DC_3N, DNC, N_2D^+, CH_3OD, or of other heavy rotators. During this upgrade, NOEMA-type mixers replaced the band 2 mixers.

In two observing campaigns in May and June 2015, phase coherent holography measurements were conducted, mapping the beacon of the ESA Alphasat satellite at 39.4 GHz with two receivers installed in the prime focus of the 30-meter telescope to obtain maps of the surface error distribution of the 30-meter primary mirror. At a resolution of 0.3m, these 128x128 maps show many of the surface features already seen in the last maps obtained with the Italsat satellite back in September 2000, confirming that the primary mirror is very stable. However, the new maps also show some transient features whose origins are yet under investigation.

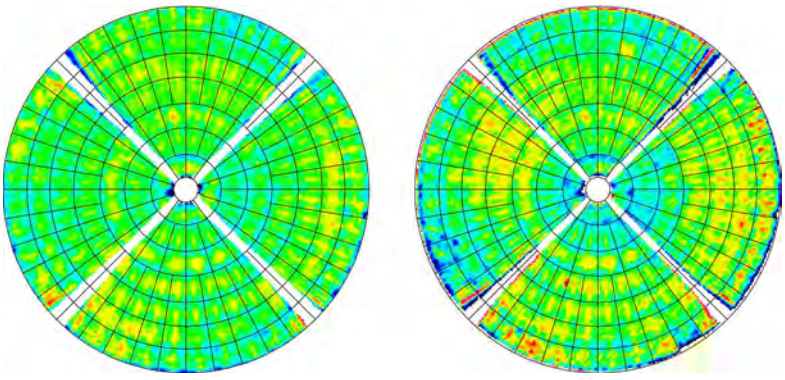

Surface error distribution of the 30-meter primary mirror. Left: Best map taken in September 2000. Right: Best map taken in June 2015. Both maps have been corrected for astigmatism. The map of 2015 is not yet corrected for the feed horn pattern.

ASTRONOMICAL PROJECTS

During the year 2015, a total of 154 projects were observed at the 30-meter telescope. This number includes two Large Programs, 10 Director's time projects, and four VLBI projects. About 17% of these proposals were scheduled in the observing pools, including the continuum pools with the two prototype continuum cameras GISMO and NIKA, which were deinstalled in March 2015. About 14% of the scheduling units, mainly the shorter ones (< 10 hours), were observed remotely. Two thirds of the scheduled projects (66%) were dedicated to Galactic topics, while one third was devoted to nearby galaxies and more distant sources. The vast majority of the scheduled projects used the multiband, dual-polarization heterodyne receiver EMIR (86%). The remaining time was shared between the 1mm 3x3

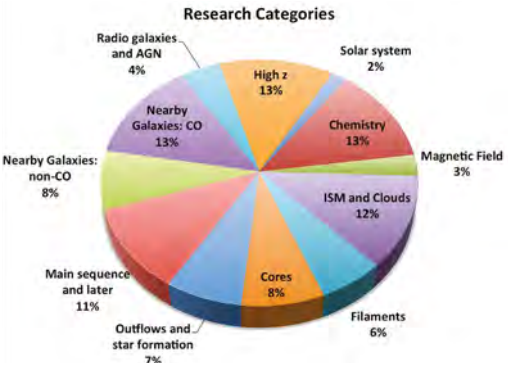

Time distribution of science categories observed in 2015.

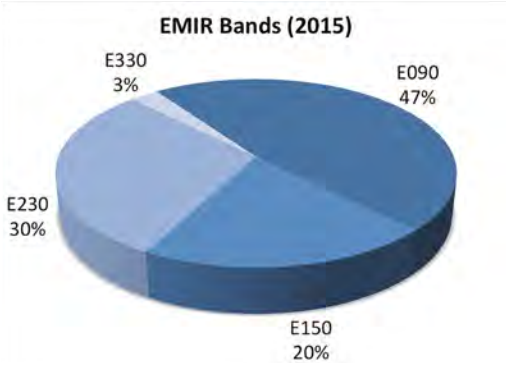

Usage of EMIR bands in 2015.

pixel array receiver HERA (3%), and the two cameras GISMO (3%) and NIKA (8%).

During the scheduling year, 108 astronomers visited the telescope, 18 of which came to support the observing pools. In support of the NIKA pool sessions, an additional group of 16 astronomers and engineers came to the Observatory. Furthermore, as in previous years, two groups of four Master students visited the telescope to observe short projects as part of their training courses, accompanied by one tutor for each group.

The program committee received 33 RadioNet3 TNA-eligible proposals, and recommended 23 for observations at the 30-meter telescope (13 A-grades and 10 B-grades). Among those, 21 could be scheduled at the telescope for a total of 716 hours, and 8 TNA-eligible astronomers were granted travel support to Granada for observing their project.

OBSERVATORY OPERATION

Despite of the strong demands for technical time, which was mostly due to the NIKA2 related work, but also the upgrade of EMIR, the total time spent on observations was high: 64% of the total time were used for observing projects. Weather conditions in 2015 were better than in average years. About 18% of the total time was lost because of adverse meterological conditions, including high wind velocities. The time lost due to unforeseen technical issues was in total less than a full day, 0.4% of the total time. The main reasons were very rare, specific problems with the telescope azimuth drive when scanning at high velocities during holography and with NIKA2. These issues have been investigated in detail to better understand their origin.

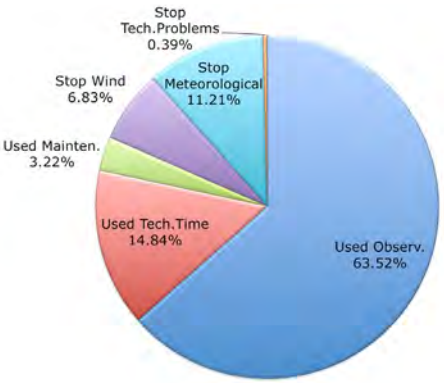

Usage of the total time at the 30-meter telescope.

Main parts of the access road to the observatory were repaired and asphalted in summer 2015. Repaving the upper 2.5 km of the road between Borreguiles and the 30-meter telescope was led by IRAM and was necessary after more than 20 years of operation. The Consejería de Fomento and Cetursa took advantage of the heavy work on the upper part to repave the lower 1.9 km, between Hoya de la Mora and Cruce de Borreguiles, which had been in a poor state. This work much improves the access via road to the observatory for staff, visitors, companies, and equipment. It also allowed a smooth transport of the NIKA2 cryostat by truck to the telescope later in 2015.

In the first half of 2015, the telescope group helped in preparing for the arrival of NIKA2 by adapting the electrical environment, modifying the cranes and air ventilation in the receiver cabin, monitoring the relative alignment of the mounts for the new Nasmyth mirrors M3 and M4, and by commissioning the new cooling system of the two NIKA2 compressors in the telescope pedestal.

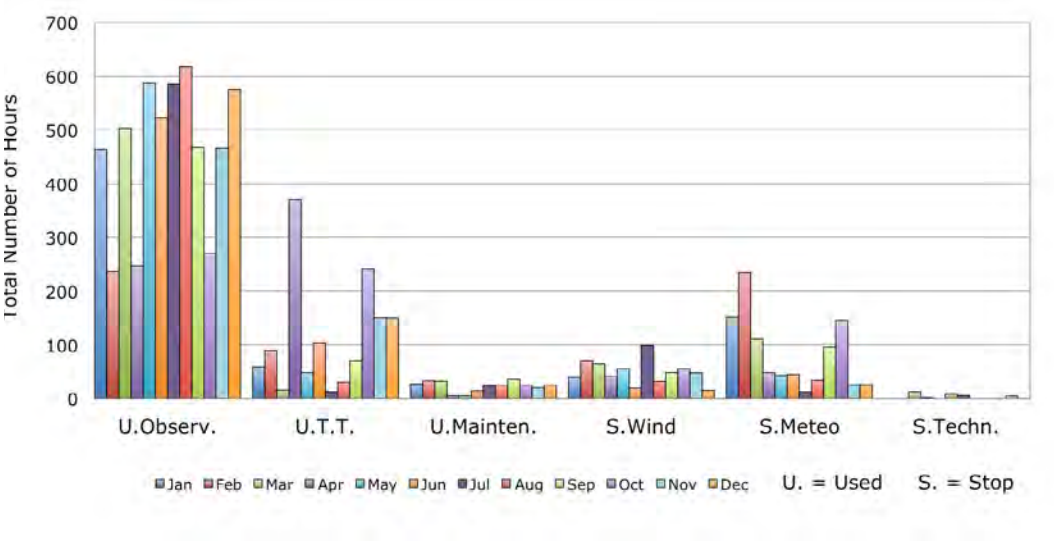

Monthly time distribution of observing time, technical projects (T.T.), maintenance, time lost due to high wind speeds, other adverse meteorological conditions and technical issues.

Work on the upper access road to the 30-meter telescope in August 2015.

FRONTENDS

Most of the recent activity in the frontend group has been focused on the installation of the NIKA2 instrument and the prior preparation of the receiver cabin. Installing the almost 2.5m long cryostat in the cabin required a profound redistribution of all receivers and associated equipment as well as a thorough modification of the optics.

After several years of very successful operation, the prototype cameras GISMO and NIKA were dismounted in March 2015 to allow the installation of the new optics and NIKA2.

OPTICS upgrade in April 2015

One of the most critical parts in the modification of the optics was the replacement of the old Nasmyth mirrors (M3 and M4) and their supporting columns, in use for more than 30 years.

In a first phase and well ahead of the arrival of the NIKA2 cryostat, the much bigger Nasmyth mirrors required by the large field-of-view of the NIKA2 receiver were installed. During three weeks in April 2015 the telescope was stopped to allow dismounting, replacing and aligning all the optical elements in the receiver cabin. In a second and much shorter phase, the two external NIKA2 refocussing mirrors were installed and aligned.

NIKA2 installation in October 2015

Final installation of the cryostat in the cabin went smoothly and as easy as anticipated. The cryostat was lifted to the receiver cabin in three parts and later assembled in-situ. The clever mechanical design of the cryostat allows access to the interior without prior removal from the receiver cabin. This will certainly facilitate the already foreseen upgrades.

Before installation of the NIKA2 receiver some preliminary work had to be done. A bridge crane had to be installed on the receiver cabin ceiling. The crane was later used for laterally shifting the heavy HERA cryostat and associated electronics. A refrigeration system for the helium compressors was installed. The two water-cooled helium compressors used for the NIKA2 pulse tube refrigerators, require a cooling system capable of absorbing the 18 kW of generated heat. The initial system designed by an external company didn't have the required cooling capacity. So, some modifications were required before the system was fully operational. The cabin floor had to be reinforced. The 1.2 tons of weight of the NIKA2 cryostat was estimated to be too high for the existing raised floor in the cabin. Several stainless steel plates plus many extra pedestals were installed in order to increase the maximum load capacity. Apart from the reinforcement of the floor, the area where the cryostat is installed needed special care. The stainless steel structure below this area was modified and a new solid and stable landing plate was prepared for the cryostat and the rotating polarimeter. The area on top of the stairs was prepared for the installation of the NIKA2 acquisition hardware. A thick aluminum pipe was used as a shielding aid for the 40 coaxial cables that brings the signals from the cryostat area to the electronic crates.

Other activities

EMIR bands 1 and 2 (E090 and E150) were upgraded in the late part of the year. The new 2mm mixers correct the low sideband rejection found on some frequencies. For the E090 band all the mixers and the optic block were replaced. The upgraded 3mm band uses an ortho-mode transducer as a polarization splitting element, the observing band has been extended down to 73 GHz.

The constant fight with spurious spectral signals is a never-ending activity. The extreme wide bandwidth of the EMIR receiver makes it prone to interferences. After the upgrade of the 3mm band, a problem with the harmonics of the Gunn oscillator has been detected that will require the installation of a filter, similar to the one already installed in the 2mm band.

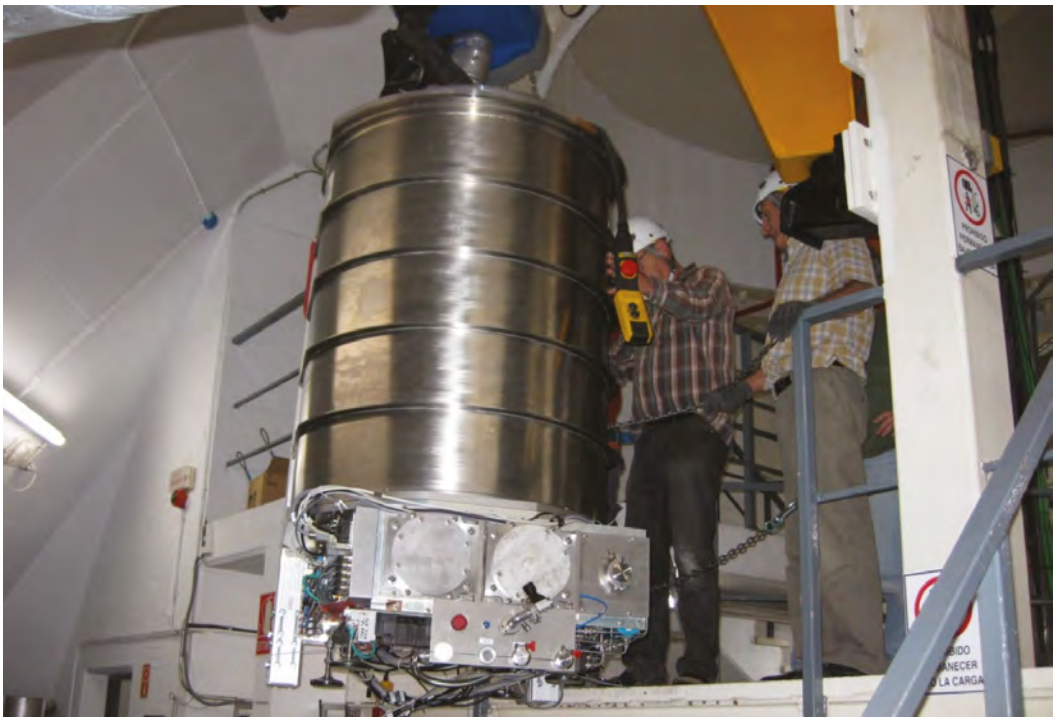

The first part of the NIKA2 cryostat being craned to the receiver cabin.

COMPUTERS & SOFTWARE

A high performance computer has been installed to perform the acquisition of NIKA2 data. The computer runs up to 64 processes in parallel (threads) and comes with 512 GB of main memory and several SSD disks.

The system monitoring software has been replaced by a tool called Icinga which allows for a more efficient and robust monitoring of the computer system.

The computer network has been improved with the acquisition and installation of two new Cisco routers that add better reliability and communicate better with the ISP routers.

In the New Control System (NCS) and its user interface software paKo, several features were added or upgraded. For special purposes, in particular for holography, on-the-fly maps can now have up to 300 subscans. The lower frequency limits for EMIR band E090 were revised to reflect the hardware upgrade. Work is ongoing to improve the new and special features introduced for NIKA2.

SUMMERSCHOOL

The 8th IRAM 30-meter telescope summerschool was held in the week September 11-18, 2015, in Pradollano in the Sierra Nevada. As in previous years, the school was aimed at attracting new astrophysicists to current and future single-dish millimeter and submillimeter facilities. The school was primarily meant for young scientists with little previous experience in millimeter astronomy. It has been limited to 40 students who were selected on the basis of their interests, experience, and references. While most students came from the European Union, we had also several strongly motivated students from the Ukraine, Russia, Turkey, Israel, Japan, USA, Argentina, and Chile. Eleven of the students were supported by the RadioNet3 program.

A series of lectures were held on science topics that have been addressed during the last few years at the 30-meter telescope, from distant galaxies, star-forming clouds in the Milky Way, to comets in the solar system. In addition, two highlight lectures were given on very recent, highly complementary results obtained with the Rosetta mission to comet 67P and on the latests results obtained with the Northern Extended Millimeter Array (NOEMA) showing also the latest news on the ongoing installation of new antennas and receivers at the NOEMA observatory.

At the beginning of the summerschool, four student groups were created. Each group prepared a science case, observed about 8 hours with the 30-meter telescope during two shifts, reduced and interpreted the data, and, at the last day of the school, presented their science case, and a first analysis of the data they took. Each group was guided by one of the lecturers aided by one of the participating IRAM PhD students and postdocs. All groups managed to produce very nice results including a map of a nearby star-forming galaxy at only 11 Mpc distance.

Many positive comments were received from the students via a questionnaire, but also during and after the school. Among the aspects, which could be improved, several students suggested that an interactive tutorial on the GILDAS data reduction software would be very useful.

Participants of the 8th IRAM 30-meter telescope summerschool.

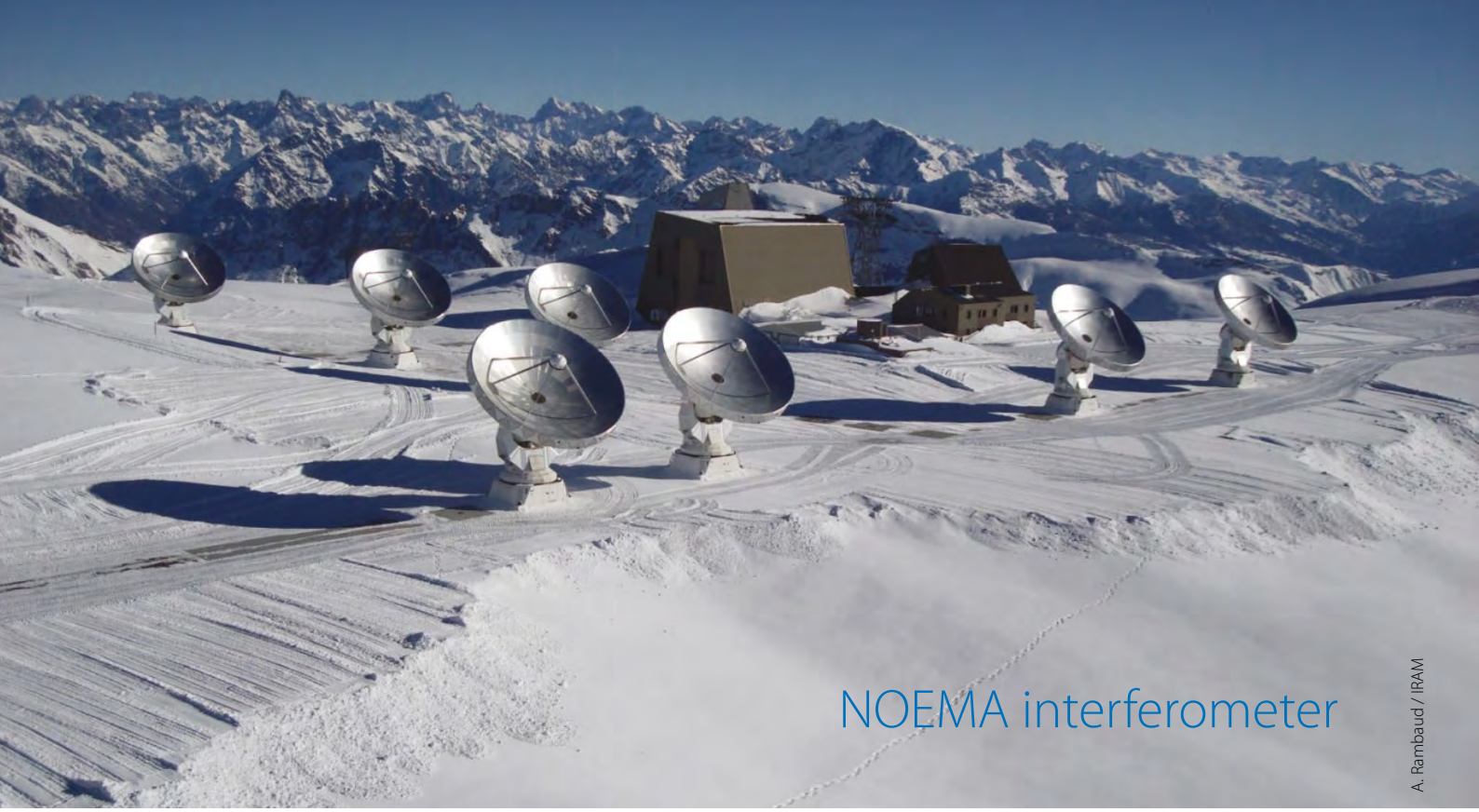

NOEMA interferometer

A. Rambaud / IRAM

An aerial view of the NOEMA site with the seven-antenna array in its most compact configuration. In the background the French Alps on a clear winter day.

Two important events have marked the NOEMA observatory in 2015. The first highlight was the opening of the NOEMA seven-antenna interferometer to the astronomical community. First fringes were observed with antenna 7 towards W3(OH) on Feb 5th, and by early spring 2015 the antenna was already available for regular science observations. The second highlight was the entry into service of the institute's new cable car to the observatory. The cable car was inaugurated on Oct 2nd with the presence of representatives of the contracting companies, the IRAM staff, and numerous officials from the partner organizations, as well as local authorities and representatives.

Work was underway in 2015 to meet the next milestones: (1) the construction and delivery of antenna 8, (2) complete the installation of the 2SB dual polarization receivers for broadband operation (32 GHz), and (3) the construction of PolyFiX, a broadband correlator with 8 GHz frequency coverage in each sideband and polarization. These upgrades were progressing well by the end of the year, and are expected to achieve completion in 2016.

The operation of the NOEMA interferometer in 2015 has been as exciting as in previous years. The interferometer performed according to expectations and continued to operate efficiently with only a few weeks of technical downtime for the commissioning operations of the new antenna, the extensive refurbishment of the correlator room to prepare for the next NOEMA antennas, work to upgrade the observatory computer systems and for the usual antenna maintenance activities. No interferometer downtime was reported for observatory work related to the construction of the next NOEMA antennas and for the integration of the cable car into regular operation. The antennas, receivers and the narrow- and wide-band correlators all worked well throughout the year.

All interferometer observations were performed exclusively in service observing mode. Observations were performed in periods of good to excellent atmospheric phase stability and transparency during most of the wintertime. Observing conditions in spring were reasonably good in terms of atmospheric opacity and stability during April and May, and allowed for useful observations in the high-frequency bands until the mid of April. Good band1 (3mm) and reasonable band2 (2mm) observing conditions were met in the summer months mostly during the second part of the night and typically until around noon. Conditions were good from October till the year's end.

The scheduling of the extended configurations (A and B) was delayed to respond to the constraints of the commissioning and science verification operations of NOEMA antenna 7. The configurations were scheduled from Feb 20 to Apr 09, about four weeks later than planned. Because of the weather conditions during this period and the shortness of the period, the scheduling of projects in the extended configurations could not be optimized. Because of the commissioning of antenna 7 and the limited time that the interferometer spent in A-configuration, several projects requesting the

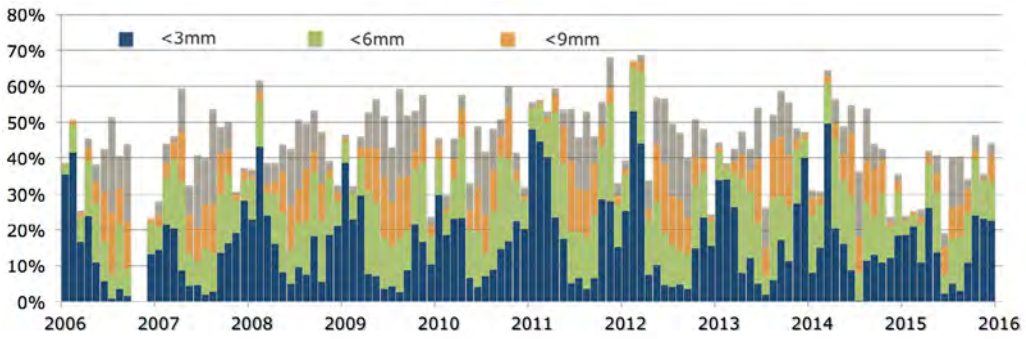

NOEMA observing time and atmospheric water vapor statistics over the last ten years. The overall correlation time accounts for 35% of the total time in 2015. Band 3 (200 – 268 GHz) and band 4 (275 – 373 GHz) programs and observations in the most extended (AB) configurations are for the most part carried out in the winter months when the atmospheric stability and transparency are highest. Science operations were suspended in the autumn of 2006 for the installation of new receivers.

A-configuration could not be completed this year. The A-rated and already started B-rated projects were carried over for observations in the extended configurations in early 2016. In addition to the extended winter configurations, an extended six-antenna A configuration was scheduled for a few days at the end of August that included stations E68, N46 and W27 to exploit the potential of self-calibration for high-resolution and high-dynamic range imaging of a few observing programs in conditions of poor atmospheric phase stability.

The percentage of array-correlation-time invested on science observing programs was on average 35% of the total time, or equivalently, 127 days and nights. Additional 40% have to be accounted for receiver tuning, verifying instrument performance, surface adjustment, antenna maintenance, and on performing the commissioning and science verification of antenna 7 and the new broadband receivers for antenna 1 and 2; the remaining 25% were lost because of precipitation, wind and poor atmospheric phase stability.

The Program Committee (PC) met twice during the year, around four weeks after the deadlines for submission of proposals, and reviewed 225 regular proposals, including 37 TNA eligible proposals, and 9 proposals for observations in the Global 3mm VLBI array (GMVA). In the same year, 12 proposals were received for Director's Discretionary Time (DDT). The program committee recommended 124 of the regular proposals, and recommended the approval of 6 VLBI projects in the frame of the GMVA sessions. In total 262 individual subprojects were accepted plus 10 additional DDT subprojects. Counting the backlog of projects from 2014, science from 106 proposals was scheduled in 2015 at the NOEMA interferometer, including science from 3 Large Programs and 11 DDT proposals. This corresponds to 232 individual projects that received time on the interferometer. All proposals were submitted and evaluated through PMS, the web-based Proposal Management System. Due to the large investment in technical time necessary in the current extension phase of the NOEMA project, Large Programs were not accepted for the interferometer under the Call for Proposals for the winter semester 2015/2016.

The NOEMA observatory continued to provide unique and exciting scientific results in 2015. The weight on galactic research dropped significantly in 2015 because of the narrow-band correlator's inability to handle the signals of more than six antennas. The requested observing time was about the same for high-redshift galaxies, nearby galaxies and young stellar objects. A fairly large amount of observing time was invested in the D-configuration between spring and fall in the detection of line-emission from molecular and atomic transitions in galaxies at high redshift. All the proposals to which time was granted in the course of the year are listed at the end of this annual report.

A technician aligning surface panels in the dish of a NOEMA antenna.

ONGOING WORK AND ACTIVITIES

The integration of antenna 7 into the NOEMA array was the most significant event and was the

most exciting activity of the commissioning and science operations team (NCSO) in 2015. The start of NCSO phase of antenna 7 began on Feb 04, 2015, with the delivery of the antenna to the commissioning team, and officially ended on July 3, 2015. The goals of the NCSO team were to take the new antenna from the stage reached at the end of construction to an instrument that meets the science requirements, and to deliver quantitative information on the antenna performance in terms of sensitivity, image quality and accuracy. The vast majority of the NCSO investigations were aimed at finding those antenna characteristics that were not within the specifications. To achieve this objective, the NCSO team devised specific test procedures, carried out measurements, and processed data to identify and solve problems in close collaboration with the computing, engineering and construction teams. The NCSO team's work organization also relied heavily on the use of Redmine, a project management tool to track technical and operational issues and to report and communicate information. The NCSO activities included single-antenna verifications such as pointing and tracking, surface accuracy measurements and verification of the overall interferometer performance. First images from the commissioning and science verification operations of antenna 7 revealed the power of the new interferometer and helped to identify first areas where work had to be done to improve operational reliability.

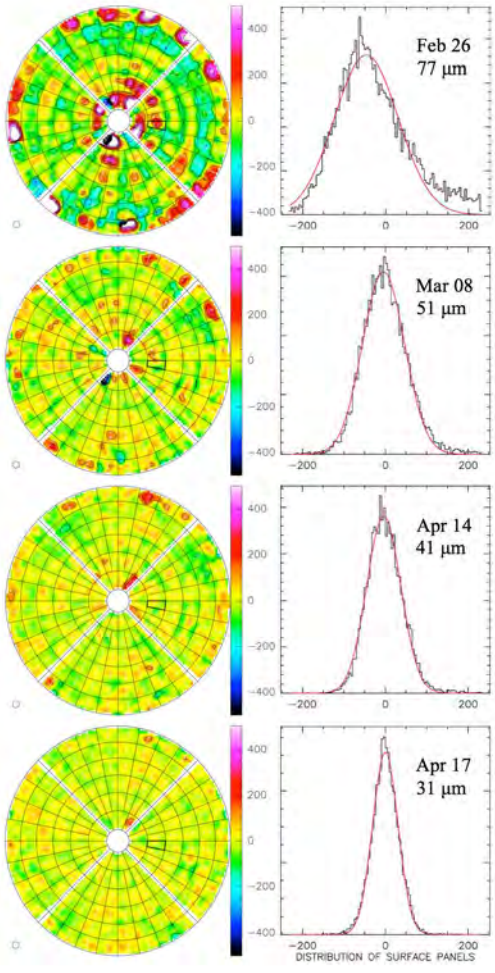

Surface accuracy achieved on antenna 7 since Feb 26, 2015 and after four holography iterations. Left panels: surface panel distribution relative to the ideal paraboloidal surface of the antenna; right: surface RMS.

Coupled to the arrivals of antennas 7 and 8, work was done to adapt and prepare the real-time software of the IF processor and wide-band correlator (WideX) to handle a larger number of antennas. While the WideX correlator was designed to process the signals of up to eight antennas with fixed spectral resolution (2MHz), the narrow-band correlator is limited to processing the signals of up to six antennas but with variable spectral resolution (down to 39 KHz). To provide optimum flexibility for high-spectral resolution studies with the narrow-band correlator, a software upgrade was implemented that allows selecting any subset of six antennas in the array to be connected to the high spectral resolution units.

In the frame of the NOEMA upgrade project, we also report the installation and commissioning of new receivers on antennas 1, 2 and 7. The new receivers are dual sideband mixers designed to operate in orthogonal linear polarization. They cover a nominal bandpass of 8 GHz in each sideband and polarization, and operate in four spectral windows (band 1: 72-116 GHz, band 2: 127-179 GHz, band 3: 200-276 GHz, band 4: 275-373 GHz). Because of tight deadlines and demanding operational plans, it has not been possible to equip antennas 1 and 2 with band 4 mixers in 2015 but the plan is to equip all antennas with the full suite of receivers. To improve the operational reliability of the new receiving systems for astronomical observations, the receiver performance was optimized for fixed frequencies on a grid of 500 MHz steps. The performance of the first three receivers was evaluated over a limited part of the bandpass (4 GHz in two polarisations) through a series of technical verifications with the wideband-correlator (WideX). The three receivers were found to perform better than expected. The full receiver band pass (16 GHz in two polarisations), however, will not be available until the arrival of the new correlator (PolyFiX).

The performance of the first three receivers was evaluated over a limited part of the bandpass (4 GHz) through a series of technical verifications with the wideband-correlator (WideX). The three receivers were found to perform better than expected.

While design work was underway in 2015 to equip the NOEMA antennas with a new generation of sensitive, multi-channel water vapor radiometers for atmospheric phase correction, the construction

of the new radiometers is not expected to complete until 2017. The direct consequence is that antennas 8 and 9 will likely not be equipped from the outset with radiometers to help correct atmospheric fluctuations and provide much improved performance on long baselines and high frequencies. To help mitigate this problem and the problem of non-functional radiometers, an interim radiometer scheme was devised that makes use of nearby antennas as proxies to estimate to first order the atmospheric phase corrections for the antennas without functional radiometers. The interim system was extensively tested during summer 2015 and found to work well.

While much of the focus at the NOEMA observatory has been on the arrival of the new cable car line, on the construction of antenna 8 and on preparing work and materials for the assembly of antennas 9 and 10, much time and efforts have also been put into the regular maintenance program of the seven antennas. More than ever, a sound coordination and integration of the technical departments and external suppliers was required to achieve the necessary level of efficiency in both planning and execution, and a sustainable balance between science production, construction activities and maintenance work. To ensure that antenna maintenance work is made to match the schedule of the different activities, it was necessary to perform part of the less complex maintenance outside the hangar and to extend the maintenance period over a period of 22 weeks. As in previous years, the surface quality of all of the antennas was verified at the end of the maintenance period of each antenna by means of holographic measurements. Surface panels were readjusted when deemed necessary, verified and iteratively improved by holographic means. All in all, the primary surfaces of all seven antennas showed excellent stability and a median accuracy of 36µm RMS.

Orion A-IRC2 spectrum in the 75.2-79.4 GHz range. The new receivers expand the frequency range of band 1 down to 72 GHz.

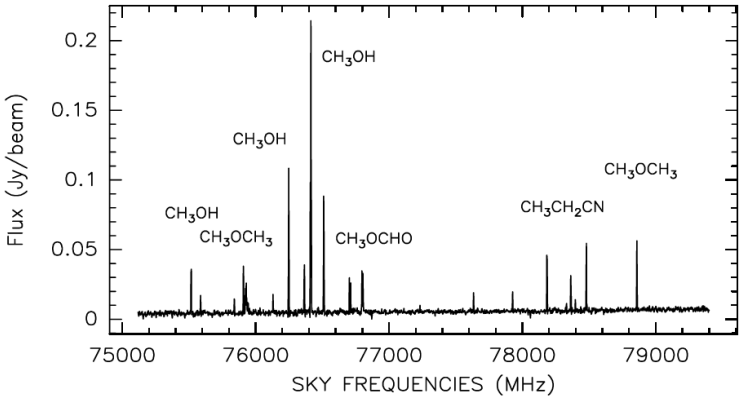

USER SUPPORT

The NOEMA Science Operations Group (SOG) is part of the Astronomy and Science Support Group, a group of astronomers and software engineers with a wide range of expertise and technical knowledge in millimeter wave astronomy and associated techniques. The SOG is staffed with astronomers that regularly act as astronomers on duty (AoD) to optimize the scientific return of the instrument, directly on the site or remotely from Grenoble. The SOG also provides technical support and expertise on the interferometer to investigators and visiting astronomers for questions related to instrumental performance, observing procedures, data reduction and calibration, pipeline-processing and archiving of NOEMA data. The SOG interacts with the scientific software development group for developments related to the long-term future of the interferometer, performs the technical reviewing of the science proposals, collaborates with technical groups to ensure that operational requirements are being met, and keeps documentation up to date. As in 2014, despite manpower constraints and a turnover of two astronomers, the SOG managed to meet the objectives and to overcome organizational and technical development challenges in the NOEMA project.

The IRAM headquarters hosts a regular stream of visiting astronomers from all around the world who stay at the institute for periods between a few days and a few months. While some of the visiting astronomers come to calibrate and analyze data from the NOEMA interferometer, others are part of our Visiting Astronomers Program (VAP). The VAP aims at training research scientists and postgraduate students in interferometry concepts, instrumentation and data reduction, and at strengthening science collaborations. In 2015, IRAM welcomed a researcher from the University of São Paolo/Brazil on his second six-month stay and an INAF researcher from the ARC node in Bologna to prepare and support work for the commissioning of the new NOEMA antennas. Advice and assistance was also given to 28 investigators from Europe, and overseas, visiting IRAM Grenoble for a total of 127 days to reduce and analyze data from the interferometer. Further assistance was provided to experienced astronomers from LAB/Bordeaux, CEA/Saclay, KASI/Daejeon, DPAS/Dalhousie, MPIA/Heidelberg, SNS/Pisa and SAC/Sussex for a total of 42 days to calibrate and analyze NOEMA data remotely from their home institutes. In total 40 science projects received support and advice. The overall level of user support remained

constant over the last two years. IRAM astronomers collaborated on more than 40 projects in which they were directly involved.

DATA ARCHIVE

In a continuing and successful, joined-up effort with the Centre de Données astronomiques de Strasbourg (CDS), data headers of observations carried out with the NOEMA Interferometer are conjointly archived at the CDS, and are available for viewing via the CDS search tools. In 2015, the archive contained coordinates, on-source integration time, frequencies, observing modes, array configurations, project identification codes, etc. for observations carried out in the period from January 1990 to September 2014. The archive is updated at the CDS every 6 months (May and October) and with a delay of 12 months from the end of a scheduling semester in which a project was observed in order to keep some pieces of information confidential until that time.

Access to the science data is initially limited to the principal investigators of the observing programs and to their delegates. While the proprietary period of Large Programs is set to end 18 months after the end of the last scheduling semester in which the program was observed, science data from standard NOEMA observing programs are not subject to a restricted proprietary period. As of Jun 2015, the IRAM Executive Council approved a resolution, effective Dec 01, 2016, that limits the proprietary period of standard NOEMA observing programs to 36 months after the end of the last scheduling semester in which a program was observed.

VLBI NEWS

The 30-meter telescope and NOEMA participated in both Global millimeter VLBI sessions at 3mm (GMVA). The 30-meter telescope observed 97% of the scheduled time from May 14 to 17, while NOEMA suffered from adverse weather conditions and could only observe 33% of this session. On the September 24 campaign, both IRAM facilities observed under good conditions: the 30-meter telescope observed 77% of the time and NOEMA 98%.

The 30-meter telescope participated successfully in a 230 GHz VLBI campaign on March 30, which led to the detection of fringes on 3C273 with the phased Atacama Large Millimeter Array (ALMA). These observations, which achieved an angular resolution of 34 µas, marked the very first VLBI observations of ALMA involving trans-continental baselines. Data from this observation were successfully combined into a single observation processed at MIT-Haystack in the United States and at the Max Planck Institute for Radio Astronomy (MPIfR) in Bonn, Germany. For this campaign, the R2DBE backend was lent at the 30-meter telescope to work together with the four units of Mark6 recorders.

RADIONET TRANSNATIONAL ACCESS (TNA)

The interest from the European community in using the IRAM TNA facilities kept growing in the years 2012 to 2015. The IRAM observatories received more than 1900 observing proposals from more than 1400 unique users originating from 45 countries. In the same period, IRAM counted over 250 TNA proposals submitted by researchers affiliated to scientific institutions from 18 European countries (AT, BE, CH, CZ, DK, FI, GR, HR, HU, IE, IL, IS, IT, NL, PL, PT, SE, UK) and from 2 independent international organizations (ESO, ESA). TNA observing time at the IRAM facilities was granted to 68 TNA eligible proposals for observations with the NOEMA interferometer and to 99 proposals for the IRAM 30-meter telescope. The observing capabilities offered by the two facilities to TNA eligible groups benefitted to more than 200 researchers with a well-balanced distribution between senior scientists (46%) and younger PhD students and post-doctoral researchers (54%). Over the last 4 years, a total of 67 astronomers received financial support through RadioNet3 to either visit the 30-meter telescope to execute their observations, or to visit the IRAM headquarters in Grenoble to reduce their NOEMA interferometer data. Guidance and support was provided to all visitors to ensure the highest quality results on every project.

The synergy of IRAM with ALMA and the Herschel heritage have shown to be of the utmost importance for European scientists. They have been key to astronomers to prepare, complete

and complement observations from these major astronomical facilities, a fact which can be traced by the large number of successful European proposals for ALMA. In the development of synergies, RadioNet3 work program has also been helping to foster interdisciplinary collaborations between European scientists. IRAM has seen various programs aimed at answering key questions in today's astronomical research that were involving theoretical chemists, laboratory chemists, spectroscopic physicists and astronomers from different European countries.

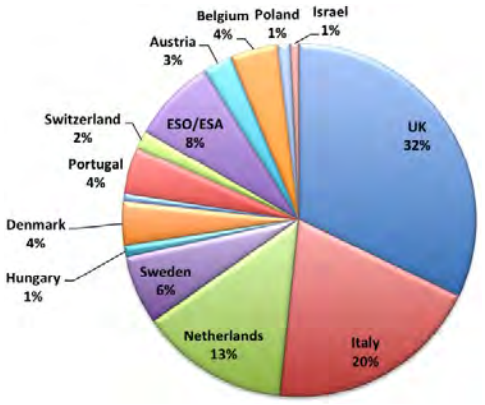

Distribution of RadioNet-eligible Principal Investigators.

ANTENNA MAINTENANCE

The organization of NOEMA antenna construction, maintenance of existing antennas, maintenance and development of existing infrastructure as well as the continuation of normal operation of the observatory made the observatory once more an extremely busy place throughout the year. Coordination of these parallel activities has been a major challenge.

As for the previous years, the maintenance has been carried out during the summer period on a 3 weeks basis per antenna. The antennas were all moved into the hangar during this period of time. However, considering the increasing number of antennas, and in order to improve on the long-term the operational efficiency of the interferometer, a new scheme of maintenance has been tested on antenna 1, with a specific part of its maintenance made outside. While more difficult to organize because of weather conditions, this test highlighted the possibility to set up a scheme where about 2/3 of the maintenance is done with the antenna outside. The remaining maintenance operations that could not be done outside, because of human and material safety reasons, were performed in the hangar. As a consequence, the 2016 maintenance period is foreseen to follow the same pattern with the overall antennas of the interferometer. Even if triggered by the high rate of occupancy of the hall for the assembly of antennas 9 and 10, this scheme of maintenance is likely to be kept even after the construction of NOEMA to minimize the maintenance overheads.

SITE DEVELOPMENT AND MAINTENANCE

Refurbishment & relocation of the HiQ-cable distribution panel

A new High-Quality (HiQ) cable distribution panel was designed and built. The reasons of this evolution were threefold: make an upgrade of the 30-year old HiQ-cable distribution panel located in the basement of the residence building, relocate the distribution panel in the correlator room where operators can act on it faster and more easily, and take into account the increased number of antennas and stations planned for NOEMA.

To complete this operation, a 40-meter long buried waterproof concrete channel was built between the residence building and the correlator room. This structure is now accommodating 81 HiQ-cables, enough to take into account the increasing number of cables for NOEMA and a few spares

The new HiQ-cable distribution panel in the observatory's main building. Every station of the NOEMA array receives reference signals from two HiQ cables, each for one of four receiver bands.

Refurbishment of the technical floor of the correlator room

The number of critical devices stored in the correlator room being very important (correlator, data servers, fiber optics and HiQ-cable distribution panel), it has been decided to clean the underfloor cable distribution system and make it compliant to relevant

regulations. Further work to enhance the quality and cleanliness of this room will be carried out in 2016.

The new snow-cat garage

The construction of this garage (~85 m^2) was necessary because of the heavy occupation of the hall for the assembly of the new antennas. Construction work, which started in 2014, was finished in the late summer 2015. The new garage accommodates a snow-cat, a special lifting platform for the snow-cat with its accessories, and a mini excavator.

The snow-cat garage during construction.

Refurbishment of the 6 tons hoist of the hall

With the assembly of antennas 8, 9 and 10 running partly in parallel, it turned out to be very difficult to store some bulky parts of the antennas for long periods of time. The decision has then been made to refurbish the old 5-ton hoist to bring on the assembly site various parts required for the construction of the antennas. At the same time the hoist was upgraded to carry weights of up to 6 tons to match the maximum weight load of the new cable car.

CABLE CAR

Commissioning of the cable car & beginning of operation

After the winter period, during which LEITNER continued to secure the future sustainable operation of the cable car, and after the appointment of SEETi as cable-car operator, series of tests were carried out on the cable car, in the presence and under the control of the manufacturer, the prime contractor and a department of the STRMTG, the French control agency for ropeways. SEETi received the official operating authorization by the Préfecture des Hautes Alpes on July 30, 2015.

View on the lower station and on the approaching cabin. The cable car connects the lower station near Enclus with the NOEMA observatory at 2560 meters above sea level.

Area around the lower cable car station

The area around the lower cable car station has been rearranged and its access secured to ensure the company's exclusive use of the cable car infrastructure and secure the materials storage area. A fence was built around the overall area with two access gates. Their opening is controlled using an access code or individualized badges. The entire internal area was coated with asphalt resistant to the pressure of the trucks coming regularly to deliver heavy loads for the observatory, like antenna parts and concrete for the construction of the NOEMA baseline extensions. A parking area for 30 vehicles was provided as well as a drop zone for helicopters in case of emergency.

Dismantling of the old cable car

With the operation of the old cable car having been stopped at the beginning of the operation of the new machine, the decision was taken to start dismantling the old cable car infrastructure by removing all the cables and the 2 upper pylons. The dismantling was necessary for safety reasons, in order not to leave the cables of the old cable car unattended.

The new parking area at the lower cable car station.

OTHERS

As for the IM2NP laboratory, which has been carrying out experiments on Single Event Effects (SEE) induced by terrestrial radiation in electronic components, circuits and systems on the NOEMA site for about ten years now, the observatory hosted in 2015 an experiment of the INES Institute (CEA) on the behavior and aging of different technologies of solar cells in harsh weather conditions such as those encountered on the NOEMA site. To achieve this goal, around 40 m^2 of panels were installed on the roof of the observatory's main building and a rack containing all the electronic control system was set up in the attic of the building. This experiment, which is the subject of an agreement between IRAM and INES, is planned to last a minimum of 5 years.

Installation of solar panels for the INES experiment on the observatory main building.

Grenoble headquarters

Frontend Group

2015 was an extremely busy and successful year for the IRAM frontend group. In addition to the usual maintenance tasks for both the NOEMA and Pico Veleta observatories, the group has installed three new receivers on NOEMA antennas, while also upgrading the main Pico Veleta receiver, EMIR, and providing significant support for the installation of the NIKA2 continuum receiver at Pico Veleta. The overall frontend capabilities of the IRAM telescopes thus underwent a major improvement during this year.

NOEMA RECEIVERS

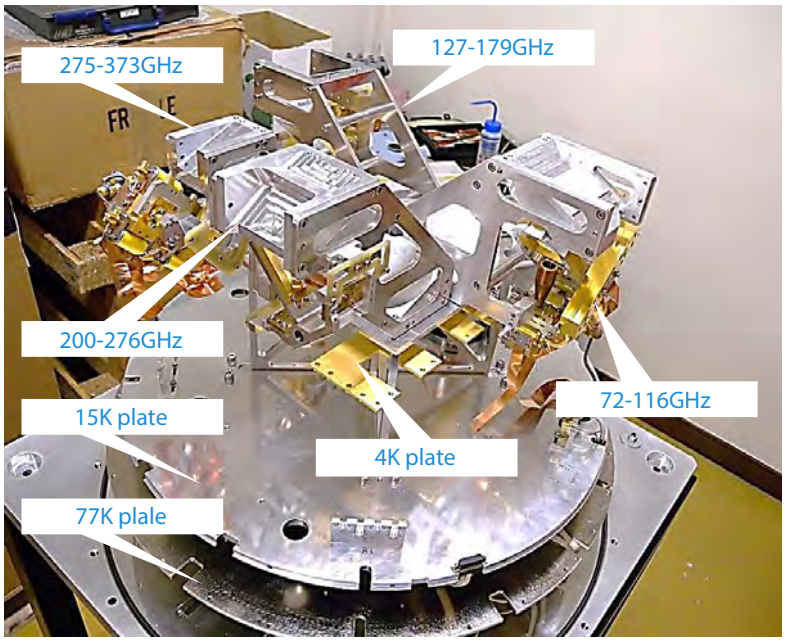

NOEMA receiver during assembling, showing the four optical modules corresponding to the four bands.

After the installation of a new receiver on the NOEMA antenna 7 in December 2014, and its successful commissioning early 2015, the IRAM Frontend group has started a series construction of similar receivers. The performances of the NOEMA receivers are unsurpassed worldwide in the millimeter domain. They are equipped with four bands, covering the 70-371 GHz frequency range. The new generation sideband-separation (2SB) mixers deliver 2x8 GHz IFs and the full dual-polarization system thus delivers a total of 32 GHz per antenna to the correlator.

Two new receivers were constructed and installed on antennas 1 and 2 in November 2015. Again, the commissioning of the receivers showed excellent performances, well within the specifications. These results represent a major achievement for the whole Frontend group after several years of design, prototyping, production, and assembling.

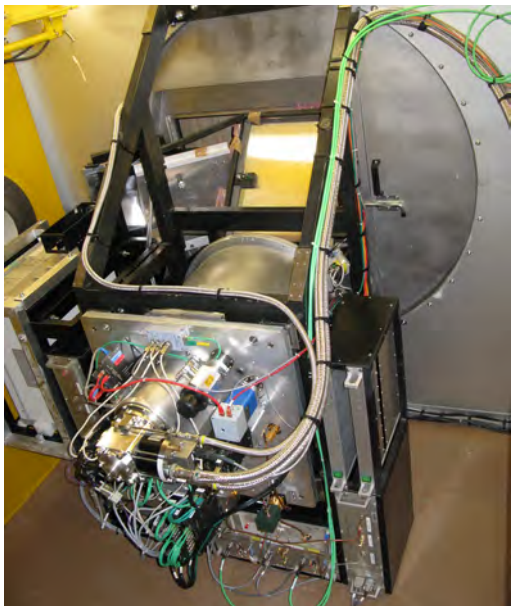

NOEMA receiver during its lift-off into an antenna (left) and after installation in the receiver cabin (right).

The NOEMA receivers include several new, optimized elements, in particular 2SB mixers, optics, IF amplifier chains, optical-fiber-laser racks, control electronics, calibration loads, local oscillators etc. The design of these elements was described in the 2014 IRAM Annual Report.

The deployment of the next receiver, on antenna 8 is scheduled for early 2016. The remaining antennas (3,4,5,6) will be equipped in the course of 2016, so that all NOEMA antennas will have new generation receivers before the end of 2016.

NOEMA LOCAL OSCILLATORS

The Local Oscillator systems on the NOEMA receivers are of two types. The band 1 and band 4 LOs are electronically tunable, YIG-based, while the band 2 and band 3 LOs are based on Gunn oscillators (and actually share the same module, the reference signal been split in two channels before being sent to a frequency doubler or tripler). Following the band 1 LO development, a new band 2 + band 3 electronically tunable LO has been designed and prototyped. It gives excellent results and will be the base of a future upgrade of the NOEMA LO system.

NOEMA WATER VAPOR RADIOMETERS

Water Vapor Radiometers (WVR) operating at 22 GHz have been used on the Plateau de Bure antennas since more than a decade, and have proven to be instrumental in the phase calibration process of the interferometer. For the NOEMA project, a new WVR system has been designed. While still operating on the 22 GHz water vapor line, it will provide 14 channels (instead of 3), with sensitivity and stability significantly improved. The receiver is designed with an 18-26 GHz RF frontend followed by a 4-12 GHz IF filter-bank, which combines band–pass filters and an integrated 16-splitter (14 detectors + 2 monitoring channels).

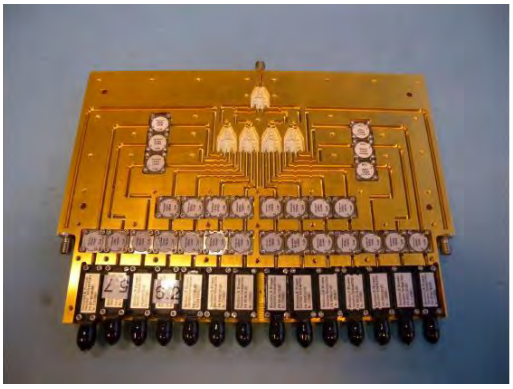

Filter bank bottom part for the NOEMA 18-26 GHz WVR.

EMIR UPGRADE

The EMIR receiver has been installed in 2009 on the Pico Veleta antenna. Since then, it went already through two major upgrades, in 2011 and 2013. In November 2015, EMIR was again upgraded. This major intervention took place only a couple of weeks apart from the installation of the NOEMA receivers on antennas 1 and 2, and only a couple of months after the installation of NIKA2 at the 30-meter

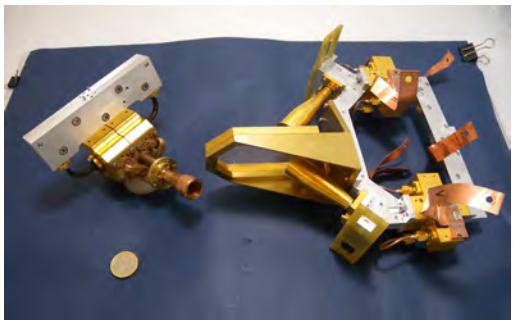

New (left) and old (right) EMIR Band 1 (3 mm) modules. The use of an OMT instead of a grid allows the module to be much more compact, with one single horn and adjacent mixer blocks.

telescope, making this period of time one of the busiest ever for the IRAM receiver groups.

On EMIR, the full 3 mm module was swapped. The new system includes 2SB NOEMA-like mixers, providing 2x8 GHz bandwidth in each polarization, and covering the 70-116 GHz window, and a new optical module, including an OMT, that was designed and validated for the 67-116 GHz window. This is the very first time an OMT is installed on an IRAM telescope to achieve the splitting of the two polarization signals. The new EMIR 3 mm band can now be operated down to 70.3 GHz, the lower limit being actually set by the local oscillator. This opens the 70-80 GHz frequency range, which contains several critical deuterated molecular lines, for astronomical observations.

This EMIR upgrade opens the possibility to cover the full 67-116 GHz window with one single band, using SIS mixer technologies; this corresponds to the ALMA Band 2 + Band 3 covered simultaneously.

EMIR 2 mm mixers were also exchanged in November. In fact, between 2009 and 2015, all EMIR bands were upgraded, so that the current instrument has now the same performances than the NOEMA receivers. IRAM intends to continue in the future to regularly, and as rapidly as possible, upgrade EMIR in order to keep this receiver equipped with state-of-the-art systems.

ALMA BAND 7

In 2015, IRAM has delivered to ESO the last spare parts and mixers for the ALMA Band 7, and has concluded its contractual obligations towards the ALMA project. The Band 7 maintenance is now under ALMA responsibility. Two IRAM staff members have travelled to Chile at the end of the year, to help for the maintenance of a few cartridges and to ensure that the local staff is formed to these tasks.

DUAL-BAND RECEIVER

IRAM has designed a complete dual-band (2 mm + 1.3 mm) receiver for the Max-Planck-Institute for Solar System Research in Göttingen, Germany. This receiver will be used as radiometer for atmospheric sounding, and will be installed at the Zugspitze scientific station in the German Alps. The receiver is based on NOEMA developments, in particular the Band 2 and Band 3 2SB mixers. The assembling of the receiver has made significant progress in 2015, and the completion is scheduled for mid-2016.

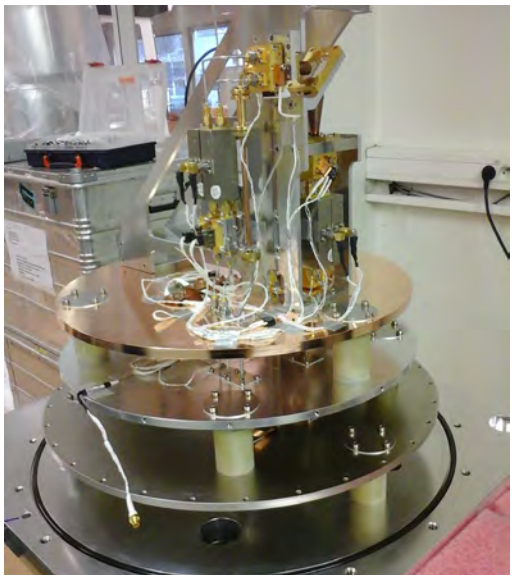

Dual-Band receiver during construction (left) and during the first tests (right).

Superconducting Devices Group

On a technological level, the activities of the SIS group have focused around three main themes: fabrication of SIS junction devices, KID production and development, and development of other microwave components and new technologies.

SIS DEVICES

During the year, production of SIS devices for the three frequency bands of NOEMA has been the main activity. The cessation of activity of our subcontractor that provided the final wafer-lapping stage of the production chain forced IRAM to find a new company that is able to reliably lap 2" wafers. In the meantime, in-house expertise was developed to lap down smaller devices. This enabled an even more efficient allocation of resources in the development stage of the fabrication parameters.

Besides NOEMA, the group started production of SIS junctions for broadband receivers in the 330-420 GHz band at the Smithsonian Astrophysical Observatory (SAO). This collaboration with the SAO will continue in 2016. First feedback on the produced junctions shows that they have a remarkably high Q of 28, demonstrating the state of the art of IRAM's SIS production facilities.

KID DEVICES

With respect to Kinetic Inductance Detectors, the group continued work on designing and prototyping aluminum KID arrays for NIKA2. Inhomogeneity of the aluminum film thickness has been identified as the major challenge for large arrays that are closely packed in readout frequency. Several avenues for tackling this challenge, both in array design and in better material control, have been and are still being investigated.

Besides development directly related to NIKA2, the group has been continuing the development of sub-stoichiometric titanium nitride films, as an alternative material for KIDs. The advantage of this material lies in its tunable critical temperature, allowing for lower-frequency applications (below the bandgap of aluminum). The group has been able to improve the homogeneity of the TiN films to better than 75% over a 2" wafer, and was able to produce arrays of 100 distinguishable pixels.

OTHER DEVICES AND PROCESS DEVELOPMENT

Activities to produce normal-metal microwave elements for use in the detector integration (IF couplers, resistors) continued. Besides that, a research internship allowed IRAM to launch the development of beam lead technology. These thick beam leads will finally allow an easier packaging of the microwave elements and reduce parasitic inductances. This development is very promising and will be continued in 2016.

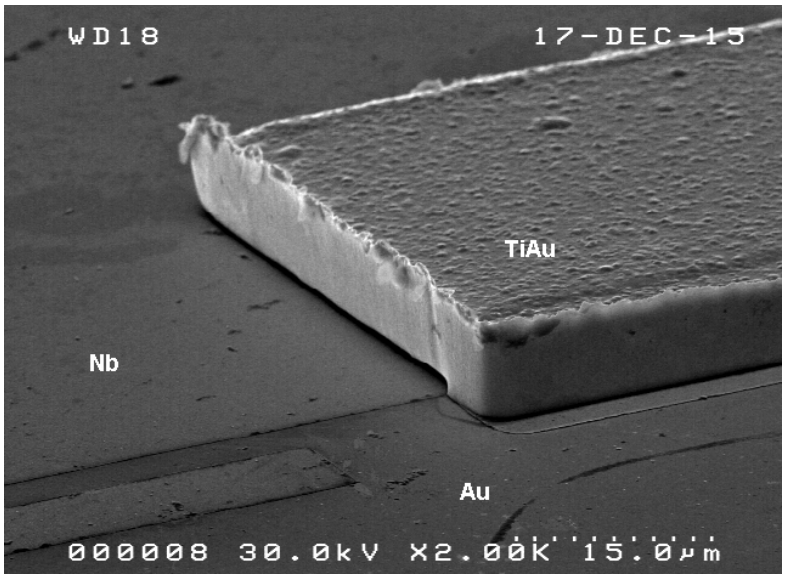

First successful test of a gold plated beam lead structure produced in the IRAM cleanroom.

Backend Group

DEVELOPMENT OF THE NEXT CORRELATOR FOR NOEMA: POLYFIX

The future correlator system, dubbed PolyFiX, will be composed of 4 cabinets. Each of them will process an 8 GHz receiver sideband thanks to an analog signal processing module called the IF processor, which in turn feeds a pair of digital correlation units capable of digitizing a 0-4GHz instantaneous bandwidth and of processing the 66 baselines of the 12-antenna NOEMA array.

Analog IF Processor

Each of the 4-12 GHz IF bandwidths delivered by the NOEMA receivers must be down converted into two equal DC-4GHz basebands in order to accommodate the analog bandwidth of the correlator digitizers.

A simple scheme using a common LO for both basebands was previously prototyped and successfully tested.

This single downconversion scheme allows for very few spurious lines that can be easily flagged as they appear at fixed, known frequencies in the 4GHz baseband.

After going through several design iterations, four complete IF processor units have been built to process the total bandwidth delivered by the NOEMA receivers (32GHz = 2× 8GHz sidebands ×2 polarisations). Each unit is able to process one sideband and supports up to 12 antennas.

Thanks to a compact design, a complete unit is housed in a single 19" rack, its monitoring and control electronic being included.

This will allow for an efficient and smart integration into the future PolyFiX cabinets.

Digital correlator

The PolyFiX correlator development has continued both in terms of hardware and gateware designs.

Digitizer Board Prototype Beginning of 2015, the Digitizer board has been build based on the DiFER (Digital Front End Rover) experimental board that previously validated the use of the e2v high-speed ADC prototype chip EV5AS210 for NOEMA.

The PolyFiX Digitizer board includes a wideband signal conditioning stage, the high-speed 5-Bit ADC, an 8GHz PLL to clock the ADC and an ALTERA Arria V GX FPGA.

Preliminary electrical tests have started and some basic gateware has been written to check electrical interfaces between the FPGA and its peripherals.

Left: View of the PolyFix Digitizer Board Prototype, right : Close view of a NOEMA IF Processor Unit.

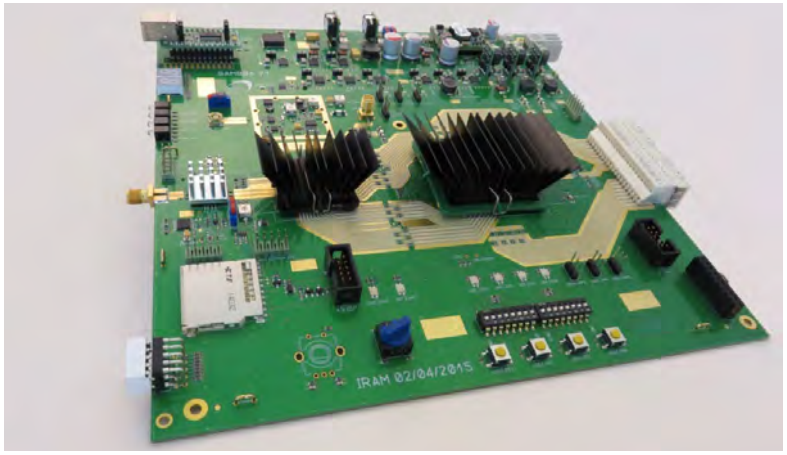

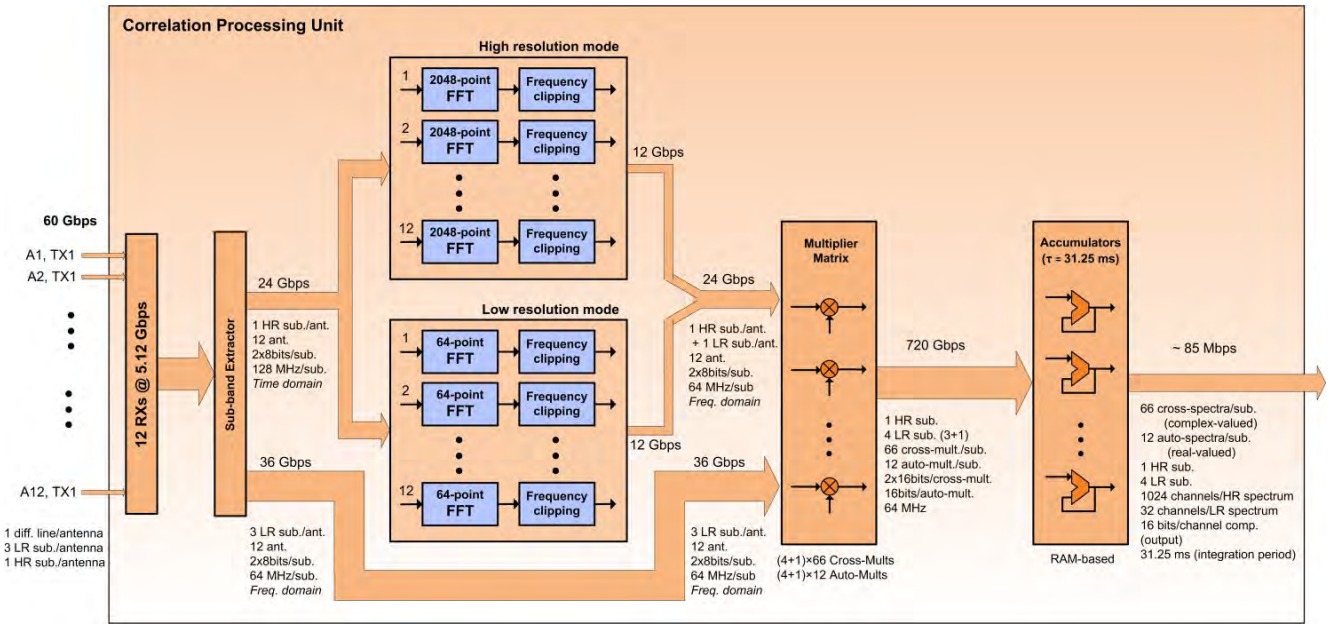

Block Diagram showing the signal processing to be implemented.

Correlator Board Prototype The Correlator board prototype, dubbed "Combo" with respect to its functionality to combine the antenna signals all together, has gone through an extensive phase of gateware development throughout 2015. The digital signal processing depicted in the figure hereabove will be achieved using only one FPGA.

This FPGA will support the baseline processing for 12 antennas over a subset of 4 subbands of 64MHz each (3 with low resolution and 1 with both high and low resolution). It will compute simultaneously the spectral power densities of the signals of each antenna.

As a consequence, multiple constraints were to be faced: Trade-off between the FPGA fabric distributed memory and block memory (On-Chip RAM granularity), management of a mix of time domain and frequency domain data, and an array of 330 cross-spectra and 60 spectra to be synthesized.

A by-product of this complexity is an increase in time needed for designing and testing. Nevertheless, a significant portion of the gateware blocks has already been designed and each VHDL module was individually tested through functional simulations.

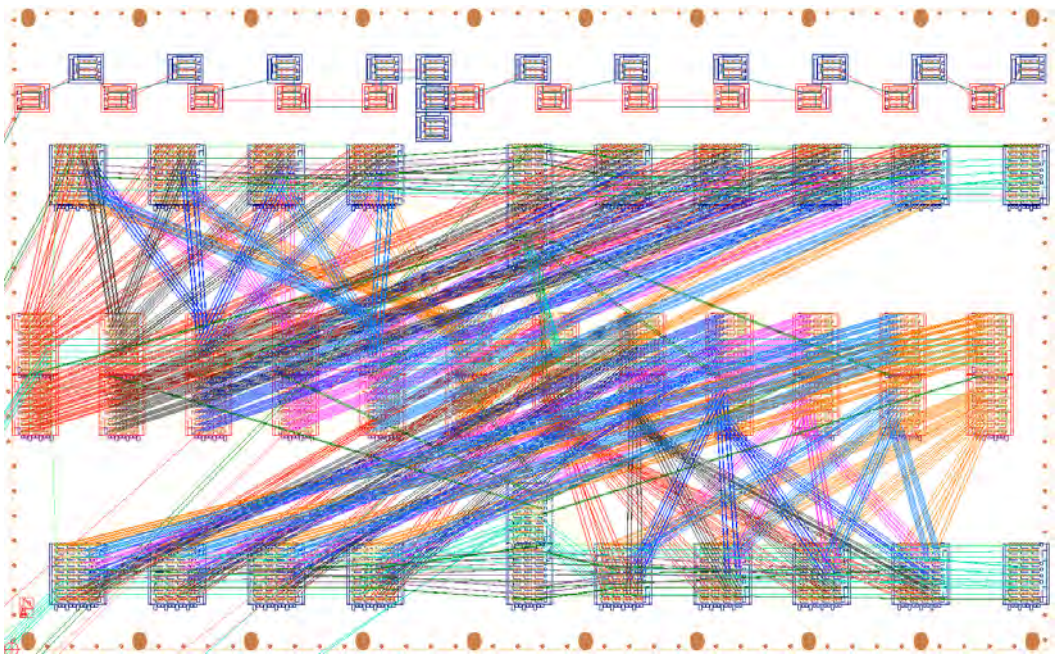

View of the PolyFix midplane prototype showing the high density of the connections (384 high-speed serial links).

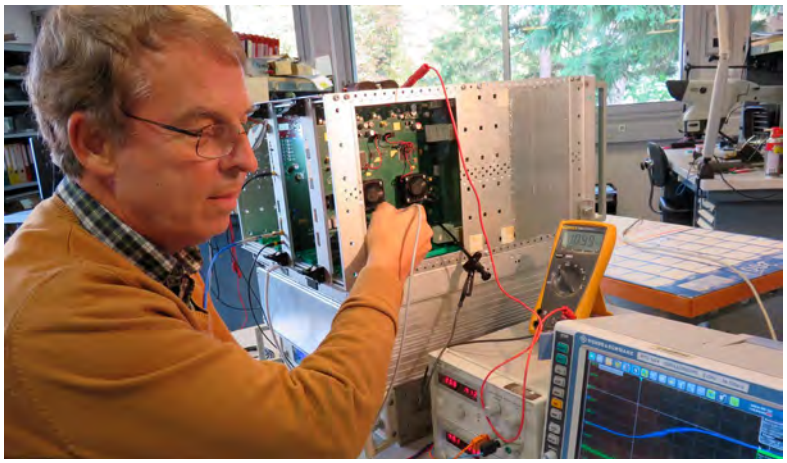

Backend group engineer testing the PolyFix correlator unit prototype.

PolyFix Midplane Board and Correlator Unit Prototype By mid-2015, the first prototype of the midplane board has been realized. This 18-layer board provides a high bandwidth link (5Gbps) from every digitizer slot to every correlator slot so that the 66 baselines can be produced in each of the correlator FPGA over 256MHz (1/16th of the baseband full spectrum). It provides also connections to the readout board for the correlator data dump and for the system monitoring and control.

The delivery of this central board has triggered the assembly of the prototype rack, which will accommodate the 12 digitizer and 8 correlator boards and the readout board.

Several tests were carried out that showed no major mechanical or electrical issues. They are expected to continue in 2016, notably to verify the signal integrity over the whole set of 384 high-speed serial links, before entering the production phase of this key system component.

LO1 CONTROL & TRANSPORT SYSTEM: LO1REF NEW BATCH

In each antenna, the first LO is derived from a 15GHz reference signal generated by the LO1Ref, a tunable YIG oscillator. With the growing number of NOEMA antennas, more LO1Ref spare modules are needed. It has therefore been decided to start the fabrication of a new batch of LO1ref modules to make sure astronomical operations will not be interrupted by the maintenance of these modules.

The main sub-assemblies composing the LO1Ref modules have been fabricated.

Due to the very long lead time of some specific parts, final assembly and test of these new modules are scheduled to complete by the 3rd quarter of 2016.

View of the new batch of LO1Ref modules during assembly. On the left: a set of YIG voltage-controlled oscillators.

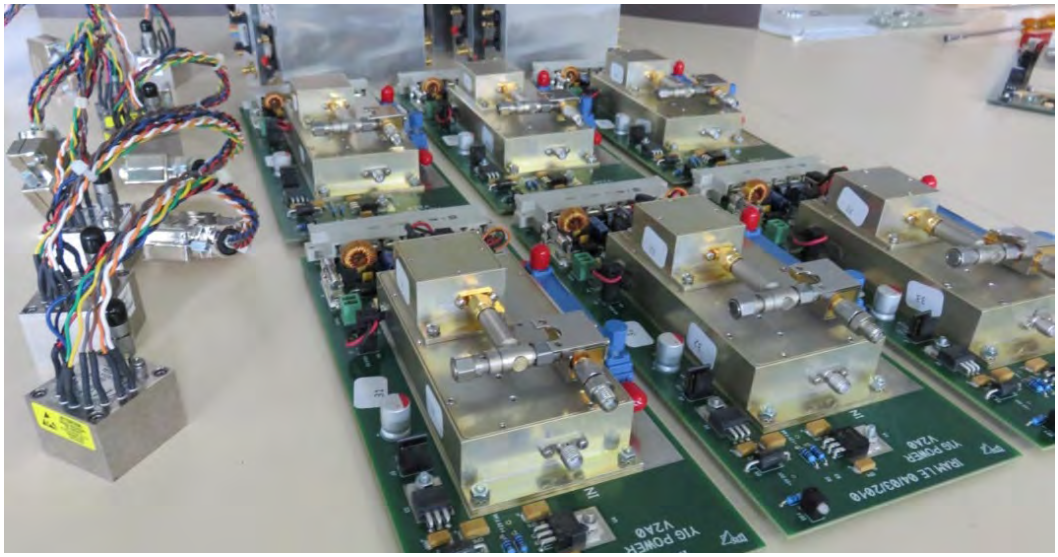

Mechanical Group

DRAWING OFFICE

The mechanical group's drawing office worked on numerous mechanical designs in close collaboration with the other IRAM groups and also for external laboratories. While the group's main activity in 2015 was focused on NOEMA, the group has also been tasked with the following work items:

- Design, manufacturing and installation of new support frame structures for the M3 and M4 mirrors in the cabin of the IRAM 30-meter telescope
- Design and start of manufacturing of a set of mixers/couplers for a multi-beam band 3 receiver with 7 pixels
- Design, manufacturing and assembly of a complete Dual Band Receiver for the Max-Planck Institute for Solar System Research (MPISSR)

New M3 and M4 support frame structures for the IRAM 30-meter telescope cabin

Due to the installation of new equipment inside the cabin, the main goal of this project was to relocate the fixation of the M3 and M4 support frames from the floor to the roof of the receiver cabin.

By integrating the new design, more space became available in the receiver cabin to integrate new receivers like the dual-band continuum camera NIKA2.

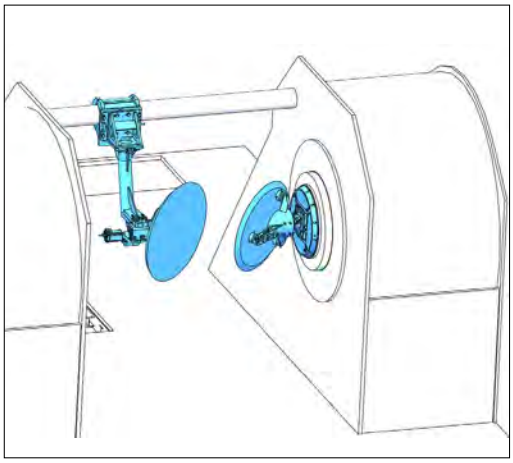

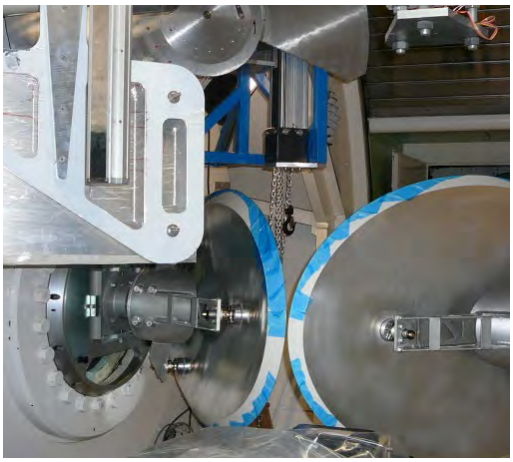

CAD picture and real photo of the new M3 and M4 support structures.

Mixers / couplers for a multi-beam band 3 receiver with 7 pixels

The design and manufacturing of new mixers/couplers has been a new challenge for the mechanical lab. This new type of coupler is composed of 7 small couplers all joined together. The main difficulty is related to the fabrication of this piece of hardware by keeping the same manufacturing accuracy between each waveguide and each coupler; this means keeping the distance between two waveguides within a tolerance of +/- 0,005 mm. In close collaboration with engineers of the IRAM Frontend Group and external partners, the Mechanical Group succeeded in designing a prototype. The production of the prototype was launched at the end of 2015.

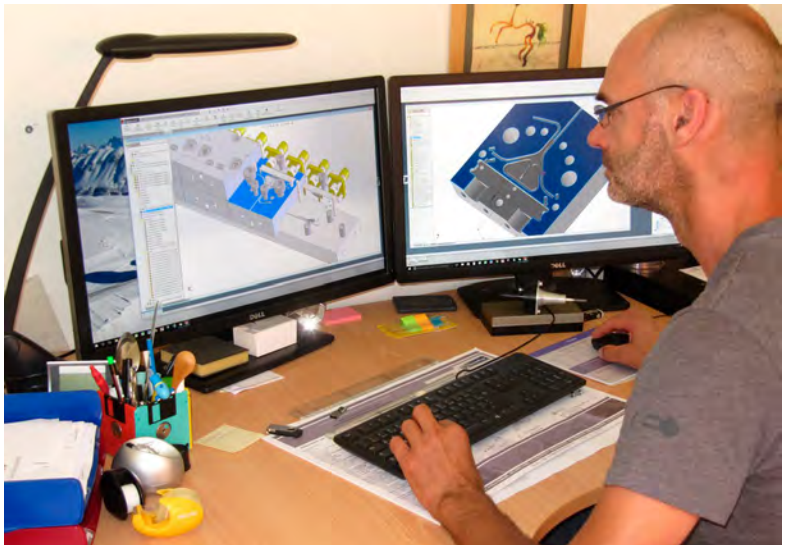

Technical designer working on a multi-beam receiver for band 3.

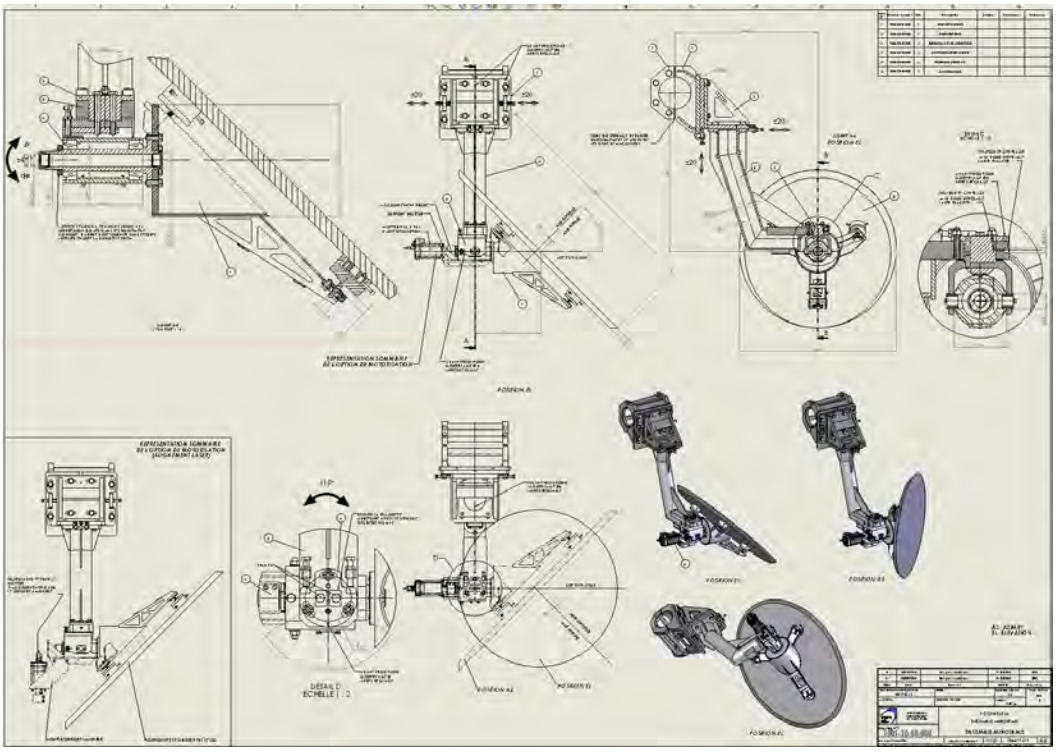

Mechanical drawings of the M3 mirror support structure for the cabin of the 30-meter telescope.

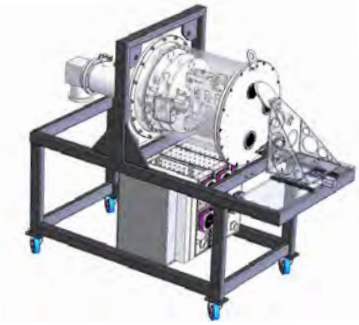

3D CAD view of the complete Dual Band Receiver that includes the cryostat, supporting frame, racks of electronics, receiver equipment inside the dewar and calibration device.

Dual band receiver

IRAM has been asked to design and manufacture a complete dual band front end for an external partner, based on the NOEMA band 2 and 3 receivers. This has been achieved over a relatively short timescale within the mechanical team drawing office, thanks to the expertise acquired over the years and particularly on the NOEMA project.

MECHANICAL WORKSHOP

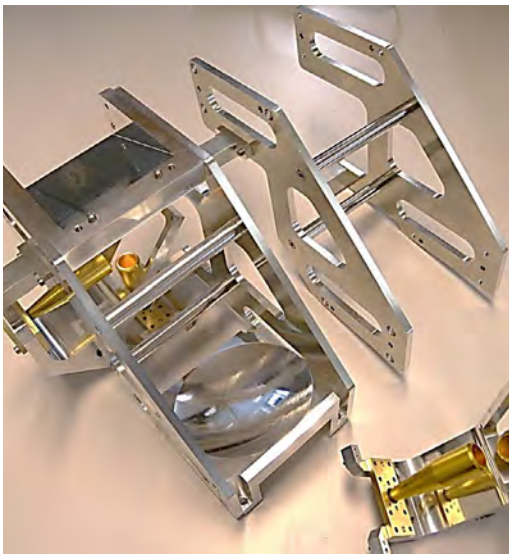

Support frames and optical components for the NOEMA receivers.

The workload of the mechanical workshop was extremely high throughout the year 2015. The main task was the manufacturing of microwave components for all 12 receivers for the NOEMA antennas. In total, the workshop produced 30 mixers for each of the bands 1, 2 and 3, tens of optical mirrors with their support frames for bands 1 and 2, and tens of horns.

In parallel the mechanical workshop worked for many other projects like the Dual Band receiver, 7-pixel mixers, specific optical windows for the NIKA2 project, and many prototype parts for the mechanical lab and all the IRAM labs.

NOEMA – CONSTRUCTION OF ANTENNAS

Antenna 7 has been totally assembled and delivered for commissioning in February 2015. The construction of the first NOEMA antenna took little more time than expected due to delays of outsourced work and due to the need to streamline and coordinate construction work in view of the next antennas. As described in the IRAM Annual Report 2014, reduction of the primary dish mass without impact on antenna performance was one of the most important objectives for the new NOEMA antennas. After a series of validation tests on antenna 7, it was concluded that the objective of balancing the primary dish without adding extra weights was reached. According to first estimates, the weight of the primary dish including the counter-weights was reduced by more than 2 tons.

In an effort to accelerate assembly work on antennas 8, 9 and 10, a detailed analysis of the construction of antenna 7 was made that showed that the construction of the future antennas could be better coordinated and integrated. In this way, work on the construction of antenna 8 could start on time (November 2014) with the objective of performing first tests in view of the astronomical commissioning around the mid of April 2016.

The antenna construction plan, at the end of 2015, involved the following milestones:

Antenna 8 ready for commissioning	Mid-April 2016
Start construction of antenna 9	October 2015
Antenna 9 ready for commissioning	March 2017
Start construction of Antenna 10	June 2016
Antenna 10 ready for commissioning	October 2017

As of December 2015, the NOEMA project was reporting the following:

- First astronomical commissioning of antenna 8 set to April 13, 2016
- Construction of antenna 9 proceeding according to plan

NOEMA antenna 7 by night. Light in the antenna backup structure is shining through the panels of the primary mirror.

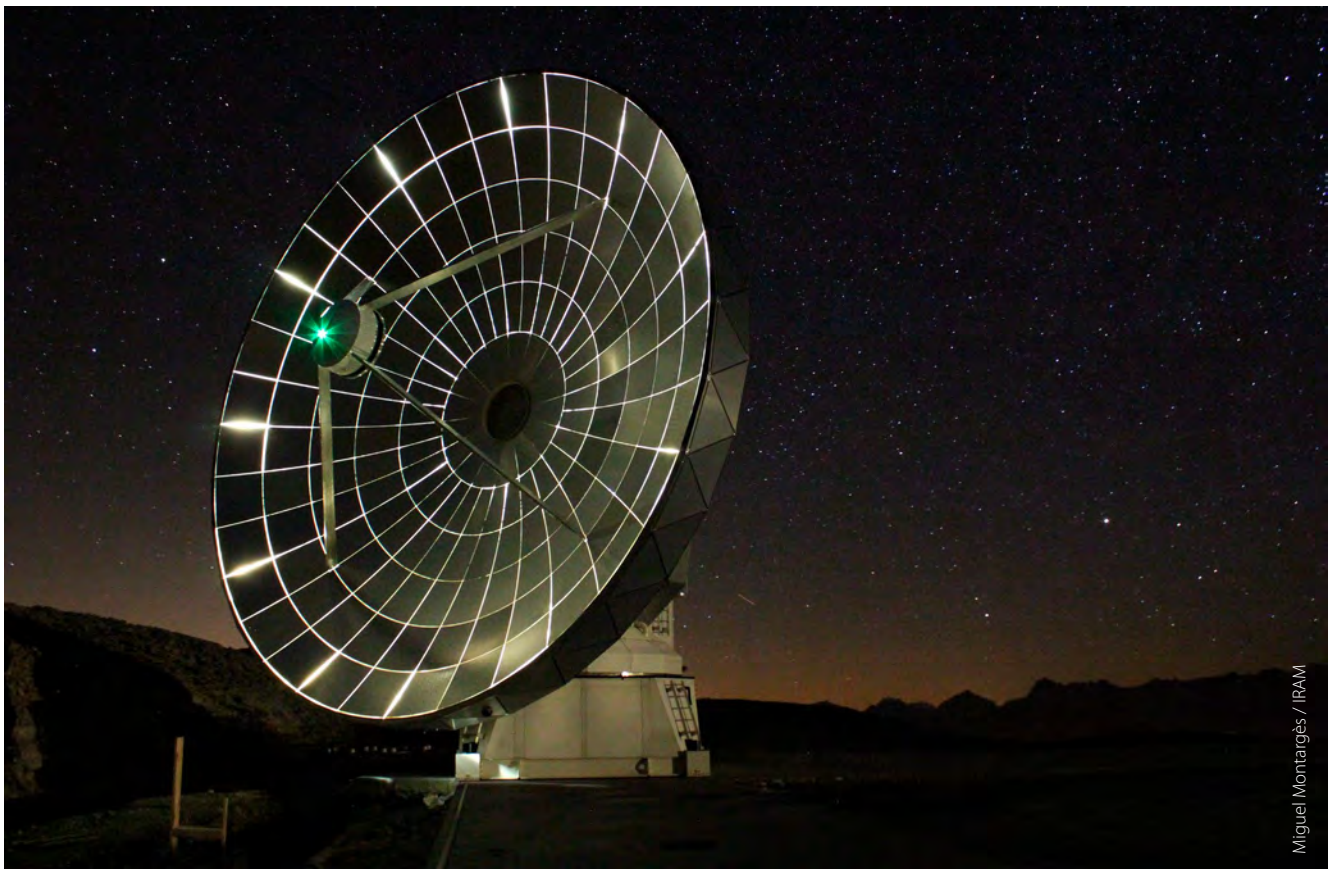

Computer Group

UPGRADES

After upgrading its storage servers in 2014, the Computer Group was forced to upgrade its backup infrastructure in 2015. The new backup system is based on a 16-bays QNAP server populated with 4TB hard disks. The device is located in the cellar of the IRAM headquarters, far away from the computer room to protect data against severe occurrences like a fire. For the moment only 50 TB have been provisioned, but the system can easily be extended with expansion racks. The backup process runs every Friday night through a dedicated 10 Gbps fiber optic network and takes 6 hours to complete.

In June 2015, there was a 9-day scheduled shutdown of the NOEMA computer room to protect sensitive devices against dust generated by drilling holes into the concrete walls for the new HiQ-cable distribution panel. To avoid a loss of control of the interferometer, an optical bypass was set up for a recovery system in the control room, so that the operators were able to drive the antennas as usual. The opportunity was also seized to reorganize the cable paths under the floor of the correlator room.

The Computer Group has proceeded to an evaluation of Microsoft Windows 10 during the summer months. Unlike with Windows 8, the first impressions were so positive that it was decided to set up a pilot test with a dozen of volunteers. At the end of the year, no particular compatibility problems have been encountered and users really like the new graphical interface. Furthermore, as the upgrade was going to be free of charge until July 2016, a massive migration to Windows 10 was scheduled for the first quarter of 2016.

During fall, the NOEMA observatory has been physically connected to the SuperDevoluy ski resort with fiber optics. This was a major milestone in improving the IRAM network infrastructure. At the end of 2015, the Computer Group was waiting for the commissioning of the network by the telecommunication company.

NOEMA

The Computer Group has designed an EtherCAT interface for the receiver vacuum gauge reader. The interface is based on an EtherCAT piggyback board from Beckhoff Automation GmbH and an IRAM analog intermediate board. This interface allows the upgrade of the receiver fieldbus without replacing the existing vacuum gauge readers.

Weekly meeting of the IRAM Grenoble Computer Group staff members.

Dual Band Receiver Software

The NOEMA receiver control software was adapted for the Dual Band Receiver, built by IRAM for the Max-Planck Institute for Solar System Research (MPISSR). The software runs on a DELL PowerEdge R220 with a Dell Remote Access Controller. With such a management controller, the computer, including the device firmware, and the software can be maintained remotely.

Science Software

The main goal of the science software activities at IRAM is to support the preparation, the acquisition and the reduction of data both at the 30-meter telescope and NOEMA. This includes the delivery of 1) software to the community for proposing and setting-up observations, 2) software to the IRAM staff for use in the online acquisition system, and 3) offline software to end users for final reduction of their data. The IRAM GILDAS software is also freely available to and used by other radio telescopes, like APEX, Herschel/HIFI, SOFIA/upGREAT, and YEBES/40m. Specific efforts are also done to image and deconvolve ALMA data inside GILDAS.

On the single-dish side, NIKA2 the dual color continuum camera was installed in the autumn of 2015 at the 30-meter telescope for commissioning. The first step to ensure the data processing for this instrument was to produce online FITS formatted files that consistently contain the binary streams from both the camera and the telescope movements. This implied defining a new version of the IRAM FITS format, called IMBFITS. Special software was then developed to qualify the NIKA2 performance. A number of issues were identified among which problems of synchronization with the telescope, instrument stability, and in the optics of NIKA2. While easy ones were solved rapidly, others are still in the process of being fixed.

Support was provided for third-party telescopes in the frame of CLASS, the GILDAS software for the reduction and analysis of spectroscopic data. First, following a request from the Herschel community, CNES funded an IRAM program to support the archival science data format of the HIFI instrument. This deliverable, which was made in collaboration with the Herschel Science Center, ESAC in Madrid and IRAP in Toulouse, was handed to the community in March 2015. Secondly, the USER section, which was resurrected in 2013 to respond to the needs of the SOFIA observatory, was generalized in 2015 to deliver the possibility to store 2D arrays. Thirdly, work was done to ease the import of wideband position-position-frequency cubes like ALMA data cubes in CLASS to enable their quick analysis: the LMV command was generalized to be able to directly read ALMA FITS data cubes, and the FILE IN command was enhanced to support the direct reading of a cube to avoid the data duplication implied by the LMV command. The support for third-party telescopes in CLASS required new threads of development directly useful for the data reduction and analysis of the 30-meter telescope data. While only the RADIO projection of sky coordinates was accessible, CLASS now supports many different projection systems, among which the gnomonic, orthographic, azimuthal, stereographic, lambert, aitoff and radio systems.

A new concept was also introduced in the CLASS data format, namely the concept of associated arrays to store, for instance, flag arrays. One of the foreseen applications will be the possibility to store arrays of system, receiver and calibration temperatures as a function of frequency, a requirement to support extremely wideband spectra. Moreover, many minor user requests were answered as, for instance, the possibility to have a direct access to the modeled brightness temperatures when fitting lines. All these developments implied a pause during the first 6 months of 2015 in the development of MRTCAL, the calibration software that will progressively replace MIRA. This time was used to automatically collect 30-meter telescope data that MRTCAL could not calibrate. Subsequent detailed examinations have shown that this happens mostly when the data were not fully conforming to the IMBFITS standard because of problems in the online data acquisition. This led the MRTCAL developers to relax data conformance checks from errors to warnings when it was possible to obtain calibrated data without compromising the robustness of the calibration. Finally, work was needed to produce holographic maps of the surface of the 30-meter telescope from observations of the 39.4 GHz beacon of the ESA Alphasat communication satellite launched in July 2013.

On the interferometric side, much work continued to be directed towards the NOEMA project. Antenna 7 got its first interferometric light in April 2015. This led to an intense campaign of online software integration and tests to support different combinations of pre-existing and new hardware. As part of this effort, a new monitoring section was added to the interferometric data format in order to streamline the debugging process. New hardware on antenna 7 includes, among others, a new mechanism to drive the subreflector and a new set of receivers at 3, 2, and 1 mm. It was also decided to tune the receivers on a fixed local oscillator tuning grid with a frequency spacing of 500 MHz as this turns out to provide repeatable tuning and optimized receiver performance. This implied work on ASTRO to allow end-users to easily

select the most appropriate tuning frequency while avoiding system-related frequency interferences. Moreover, while the WIDEX correlator was already able to process up to 8 antennas simultaneously, the possibility to plug any 6 among the 7 antennas to the narrow band correlator was implemented. This ensures that the high resolution spectroscopy mode will be able to use 6 antennas during the antenna maintenance period in the summer 2015 and 2016, improving the interferometer overall efficiency for Galactic science during the transition period up to the advent of PolyFiX, NOEMA's future wide-band high-spectral resolution correlator. Finally, the monitoring pipelines in use at the observatory were adapted to the arrival of the new NOEMA antennas.

The upcoming arrival of PolyFiX implies a large amount of preparatory work. First, a common nomenclature for the new frontend/backend system was agreed upon to ensure good communication between developers and consistency throughout software developments. Secondly, the control of the processor of the intermediate frequency band through an EtherCat bus was developed and interfaced to a graphical user interface. A test version of the software to work with the correlator hardware/firmware was also developed to help the backend group in shaping their developments. Finally, one of the main challenges of NOEMA is to cope with the large increase of the data rate (up to 180 MB/s). In sideband-separating mixers (2SB), the lower and upper sidebands (LSB and USB) are both signal bands. The Walsh phase switching scheme of the NOEMA interferometer enables to separate the image and the signal sidebands. While it largely improves the rejection of the image band in the signal band compared to a single-dish telescope, it also produces a separated image band for each sideband (LSB and USB) mostly dominated by noise. Writing the image band thus uselessly doubles the data rate. CLIC, the calibration software of NOEMA, was therefore adapted to only write the signal band, instead of both the signal and image band. This reduces the size of the datasets, and thus of the NOEMA archive, by a factor of two. It still is possible to write both the signal and image sideband on demand in order to be able to precisely measure the receiver rejection, an important parameter to calibrate the visibilities amplitude.

While the tuning of the calibration algorithms is extremely instrument specific, imaging and deconvolution of interferometric data is mostly independent of the acquisition instrument. Hence, the advent of broadband spectra (8 GHz per polarization) at high spectral resolution in ALMA triggered a series of changes in MAPPING, the GILDAS imaging and deconvolution software. In particular, the group continued in 2015 to refurbish the way the software deals 1) with the Doppler corrections due to the Earth's daily and yearly movements and 2) with the variation of the dirty beam (and other quantities) with the frequency. New functionalities were also introduced as the possibility to subtract a baseline of order 0 or 1 through each visibility before imaging. Another example is the possibility to self-calibrate the data in phase. This work, made in collaboration with the Observatoire de Bordeaux, lays out the path to the unprecedented wide bandwidth, high spectral resolution of the NOEMA project when the new correlator will become available.

All software developments are based on the common GILDAS services, e.g., a set of common low-level libraries, collectively named GILDAS kernel, which take care of the scripting and plotting capabilities of GILDAS. The codes were adapted to support new compilers as the Apple LLMV C++ compiler or new version of compilers as ifort 14. The possibility to automatically detect 1) memory overflows (i.e., illegal access beyond array boundaries) and 2) memory leaks using peculiar options of the GFORTRAN compiler are now regularly used to improve the robustness of new codes. Parallelization using OpenMP were first introduced in MAPPING deconvolution commands to benefit from the presence of multi-cores processor in any desktop today.

Finally, work to extend PMS, IRAM's Proposal Management System, with a Setup Management System started in 2015. The goal is to simplify the production of observing procedures for NOEMA. In the same area, the time estimators for both observatories were adapted to handle the latest hardware changes.

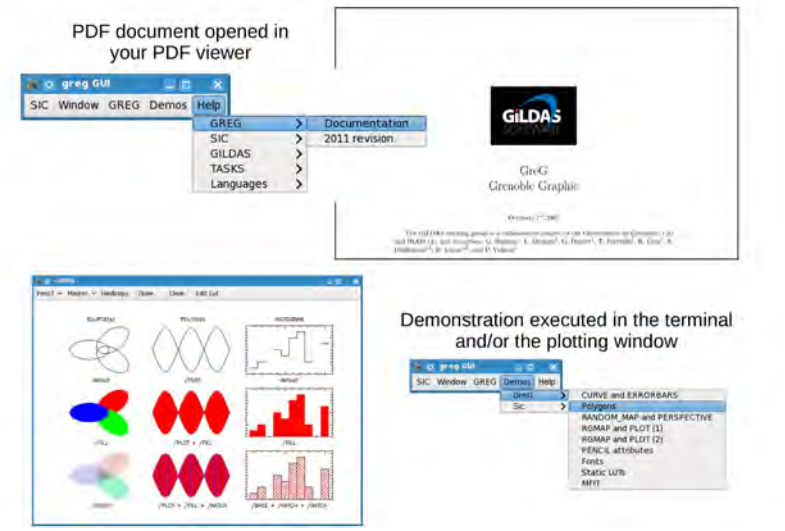

GILDAS widgets provide help to users about specific tasks and objects. Various resources like the GILDAS web page, documentations, IRAM software memos, on-line command help and demonstration procedures are now directly accessible.

IRAM ARC node

KYODO

IRAM is a node of the European ALMA Regional Center (ARC), the structure responsible for the ALMA science operations in Europe. The nodes are in charge of providing user support to the community. IRAM's involvement in the ARC is part of a long-term, global involvement in the design, construction, and operation of ALMA. One of the main goals of the IRAM ARC node is to provide to the astronomical community a common support for the IRAM and ALMA facilities, hence maximizing the scientific synergies between the observatories.

ALMA USER SUPPORT

The ARC node staff acts as "Contact Scientists" for the accepted ALMA projects, providing help and expertise to check and validate the Scheduling Blocks (SB) that are created from the initial proposals. The IRAM ARC node supports projects from the French, German, and Spanish communities, which represent more than 35% of all accepted and filler projects in Europe. In 2015, projects from ALMA Cycle 2 and Cycle 3 were considered. However, because of the limited manpower available at IRAM and the large number of projects (including backup projects) for which Scheduling Blocks have to be created, it was unfortunately not possible for IRAM to support all requests, and a number of PIs were therefore requested to contact another ARC node in Europe.

Another major service provided by the IRAM ARC node is the face-to-face support for data reduction: users can obtain direct help for the data reduction, in a way similar to the support provided for the NOEMA projects. Travel funding is available for users affiliated to the IRAM funding agencies. In 2015, more than 20 projects were supported during face-to-face visits.

Data fillers to transfer calibrated data between the CASA and GILDAS were further developed, allowing the data to be imaged in both software environments. Imaging ALMA data in GILDAS has proven to be quite efficient and useful for comparison with IRAM data or specific processing (e.g. adding short-spacings from the 30-meter telescope).

TELESCOPE CALIBRATION SOFTWARE

IRAM is responsible for the development and maintenance of one of the key software for the real-time operations of ALMA, the Telescope Calibration (TelCal) software. TelCal is performing all real-time calibrations necessary to operate the array. Just like in 2014, the TelCal group participated to the ALMA long-baselines campaign during fall 2015, as several of the TelCal processing tools (in particular, the atmospheric phase correction) were instrumental to allow the longest baselines to be used.

MAIN ADMINISTRATIVE ACTIONS

As last year, the administration's work environment has been significantly improved by upgrading the IT system. The implementation of the new IT system has been key to maintaining quality accounting. French and Spanish accounting employees now share a common database that provides the administration with a real time management of IRAM's financial information.

The staff administration has moved to the new legal standard for social declarations (DSN). This work item has requested an important human involvement and also an important upgrade of the IT system. This item is scheduled to be finished in 2016.

As special highlight in 2015, the administration was heavily involved in the selection of a private company to operate and maintain the NOEMA observatory cable car. The whole selection process and the negotiations of the contract have offered the opportunity to work on a very accurate topic in partnership with legal advisors and auditors.

FINANCIAL RESULTS

As last year, IRAM benefits from a well-balanced financial situation. Long-term investments are covered with long-term financial resources that secure the development of both NOEMA and the 30-meter telescope.

Income Budget in k€	Actual 2015
Contributions from Associates	17,592
Other Income including budgetary reports	13,904
Total Income Budget	31,496

Expenditure Budget in k€	Actual 2015
Operation	13,114
Investment	8,940
Total Expenditure Budget	22,054

HUMAN RESOURCES

IRAM employed 114 FTE in 2015, 94 in France and 20 in Spain.

A special action has been undertaken to support employment of disabled persons in cooperation with a dedicated public local structure. This scheme may evolve into a long-term partnership with an ESAT (Etablissements et Services d'Aide par le Travail) in 2016.

SAFETY

Emergency Response Plan of the NOEMA Observatory

The safety at the NOEMA Observatory being a top priority, IRAM has been collaborating in 2015 with the Hautes-Alpes mountain rescue services to develop specific Safety Plans for First aid and Fire rescue. Nowadays the rescue services have not only at their disposal new specific safety equipment at the observatory but they have also technical plans to arrive faster. Last but not least, two helicopter "Drop Zones" were prepared for emergency situations, one on the eastern track of the interferometer and one close to the hangar.

New Digital Radio Relay

The analog radio relay was replaced with a new system based on digital technology to improve the radio signal coverage at the NOEMA Observatory. The new system allows the staff to receive technical and safety alerts from the Observatory monitoring system. Furthermore, a phone interface was installed that allows the staff to connect their handheld transceivers to the phone network.

In the event of a failure of the NOEMA radio relay signal, the handheld transceivers can connect to the external relay of the Hautes-Alpes mountain rescue services and communicate in case of emergency.

Fire detection safety rules compliant to European regulations

Further to decree n°2002-460 of April 4th, 2002, concerning the general protection of people against the dangers of ionizing radiation, all the ionization smoke detectors have to be removed and replaced before 2020. Therefore, 141 detectors were replaced with optical smoke detectors at the observatory in 2015.

Night lights of the city of Granada outlining the silhouette of the 30-metre telescope on Pico Veleta (Sierra Nevada).

IRAM STAFF LIST

Group	NAME Surname	Position
	IRAM Headquarters, Grenoble, France	
DIRECTION	SCHUSTER Karl-Friedrich	Director
	GUETH Frédéric	Deputy Director
	DELLA BOSCA Paolo	
	GUELIN Michel	
	ZACHER Karin	
ADMINISTRATION FRANCE	DELAUNAY Isabelle	Head of Administration
	BACHET Claude	
	COHEN BOULAKIA Sandrine	
	DAMPNE Maryline	
	FERREIRA Dina	
	INDIGO Brigitte	
	MAIRE Béatrice	
	MANFREDI Marilyne	
	MARCOUX Stéphane	
	PALARIC Laurent	
	SIMONE Jeannine	
	ZERROUKHI Akila	
ASTRONOMY & SCIENCE SUPPORT GROUP	NERI Roberto	Head of the Astronomy & Science Support Group
	BARDEAU Sébastien	
	BERJAUD Catherine	
	BEAKLINI Pedro Paolo*	
	BOISSIER Jérémie	
	BREMER Michael	
	BROGUIERE Dominique	
	CASTRO CARRIZO Arancha	
	CHAPILLON Edwige	
	DOWNES Wilfriede	
	DRUARD Clément	
	DUMAS Gaëlle	
	HERRERA CONTRERAS Cinthya	
	KRIPS Melanie	
	LEFEVRE Charlène	
	KÖNIG Sabine	
	MARTIN RUIZ Sergio	
	MIGNANO Arturo*	
	MONTARGES Miguel	
	PETY Jérôme	
	PIETU Vincent	
	REYNIER Emmanuel	
	ROCHE Jean-Christophe	
	RODRIGUEZ MARTINEZ Monica*	
	ROMERO Charles	
	VAN DER LAAN Tessel	
	WINTERS Jan-Martin	
	ZYLKA Robert	
FRONTEND GROUP	NAVARRINI Alessandro	Head of the Frontend Group
	ADANE Amar	
	BERTON Marylène	
	BORTOLOTTI Yves	
	CHENU Jean-Yves	
	FONTANA Anne-Laure	
	GARNIER Olivier	
	LECLERCQ Samuel	
	MAHIEU Sylvain	
	MAIER Doris	
	MATTIOCCO François	
	MOUTOTE Quentin	
	PARIOLEAU Magali	
	PERRIN Guillaume	
	PISSARD Bruno	
	REVERDY Julien	
	SERRES Patrice	
BACKEND GROUP	GENTAZ Olivier	Head of the Backend Group
	BALDINO Maryse	
	CHAVATTE Philippe	
	GARCIA GARCIA Roberto	
	GEOFFROY Daniel	
	MAYVIAL Jean-Yves	
MECHANICAL GROUP	LEFRANC Bastien	Head of the Mechanical Group
	COPE Florence	
	COUTANSON Laurent	
	DANNEEL Jean-Marc	
	JUBARD Vincent	
	LAZARO Gaëtan	
	ORECCHIA Jean-Louis	

Group	NAME Surname	Position
COMPUTER GROUP	BLANCHET Sébastien	Head of the Computer Group
	CHALAIN Julien	
	DUMONTROTY Patrick	
	REYGAZA Mickaël	
SUPERCONDUCTING DEVICES GROUP	DRIESSEN Eduard	Head of the Superconducting Devices Group
	BARBIER Arnaud	
	BILLON-PIERRON Dominique	
	COIFFARD Grégoire	
	HALLEGUEN Sylvie	
	HAMELIN Catherine	
NOEMA, Plateau de Bure, France		
NOEMA, PLATEAU DE BURE	GAUTIER Bertrand	Station Manager
	AZPEITIA Jean-Jacques	
	CASALI Julien	
	CAYOL Alain	
	CHAUDET Patrick	
	CONVERS Bruno	
	DAN Michel	
	DI LEONE SANTULLO Cécile	
	GROSZ Alain	
	KINTZ Philippe	
	LAPEYRE Laurent	
	LEONARDON Sophie	
	MASNADA Lilian	
	MOURIER Yvan	
	RAMBAUD André	
	SALGADO Emmanuel	
IRAM 30-meter telescope, Granada, Spain		
IRAM 30-METER TELESCOPE, GRANADA	KRAMER Carsten	Station Manager
	PENALVER Juan	Deputy Station Manager
	BILLOT Nicolas	
	BRUNSWIG Walter	Head of the Computer Group
	DAMOUR Frederic	
	ESPANA Gloria	
	FRANZIN Esther	
	GALVEZ Gregorio	
	GARCIA José	
	GARCIA Pablo	
	GONZALEZ Manuel	
	HERMELO Israel	
	JOHN David	
	LARA Maria	
	LOBATO Enrique	
	LOBATO Javier	Head of Administration
	MARKA Claudia	
	MELLADO Pablo	
	MENDEZ Isabel	
	MORENO Maria	
	MUNOZ GONZALEZ Miguel	
	NAVARRO Santiago	Head of the Receiver Group
	PAUBERT Gabriel	
	PEULA Victor	
	RUIZ Carmen	
	RUIZ Ignacio	
	RUIZ Manuel	
	SANCHEZ Salvador	
	SANCHEZ Rosa	
	SANTAREN Juan Luis	
	SANTIAGO Joaquin	
	SERRANO David	
	SIEVERS Albrecht	
	UNGERECHTS Hans	

* Visiting Astronomer

Telescope schedules

30-METER TELESCOPE

Ident.	Title of investigations	Authors
188-12	Star formation efficiencies and X_{CO} in intermediate mass galaxies	Saintonge, Tacconi, Kramer, Schiminovich, Buchbender, Catinella, Cortese, Genzel, Gracia-Carpio, Giovanelli, Haynes, Heckman, Lutz, Moran, Schuster, Sternberg, Wang
128-14	Search for H_2S on Uranus and Neptune	Moreno, Lellouch
129-14	A potential detection of glycine in a Solar-System Precursor	Jimenez-Serra, Testi, Caselli, Marcelino, Billot, Viti, Bachiller, Vastel, Lefloch
130-14	Formation of complex organic molecules: abundance of protonated formaldehyde	Bacmann, Faure, Garcia-Garcia
131-14	A search for the CO-H_2 van der Waals complex, a sensitive indicator for low temperatures	Potapov, Graf, Schlemmer, Schilke, Sanchez-Monge
133-14	Protonation and isomerization in cold dark clouds	Lattanzi, Caselli, Bizzocchi
134-14	Probing deuteration models in warm dense gas regions	Trevino-Morales, Sanchez-Monge, Fuente, Rodriguez, Roueff, Kramer, Rodriguez-Rico, Gonzalez-Garcia
135-14	Deuteration and chemical complexity induced by efficient ice evaporation in Barnard 5	Taquet, Charnley, Wirstrom, Persson
137-14	On the effects of UV radiation and X-rays on the chemistry in the Sgr B2 molecular cloud complex	Armijos Abendano, Requena-Torres, Martin-Pintado, Martin Ruiz, Riquelme
138-14	Deuterium Astration in the Galactic Center	Pillai, Riquelme
139-14	Polarimetric Monitoring of the Encounter of Cloud G2 with SgrA*	Agudo, Thum, Molina, Casadio, Wiesemeyer, L. Gomez, Sievers
140-14	Giant molecular loops in the Galactic center: The 5.5 complex.	Riquelme, Torii, Enokiya, Menten, Fukui, Gusten, Usui
142-14	Observing Molecular Ions with IRAM to Probe Cosmic Rays Accelerated at the Forward Shock of the Supernova Remnant W49B	Lopez, Bolatto, Battersby
145-14	The Anatomy of the Orion B Giant Molecular Cloud	Pety, Guzman Veloso, Gratier, Tremblin, Bardeau, Goicoechea, Gerin, Le Petit, Liszt, Lucas, Oberg, Peretto, Sievers, Roueff
146-14	Completing the unbiased spectral survey of NGC 7023, a mild-UV illuminated PDR	Pilleri, Fuente, Gerin, Joblin, Pety, Goicoechea, Berne, Gonzalez-Garcia, Valdivia
150-14	Probing the detailed connection between dense gas and star formation in the Aquila molecular cloud complex	Andre, Konyves, Shimajiri, Bontemps, Braine, Schneider, Maury, Ladjelate
152-14	Dynamical and chemical evolution of the globally collapsing DR21 ridge	Bontemps, Schneider, Fechtenbaum, Andre, Braine, Csengeri
153-14	Filamentary structure, infall convergent flow and massive star formation	Lu, Zhang, Jimenez-Serra, Liu
154-14	Environmental Dependence of Kinematic Structure in Cold Interstellar Filaments	Wang, Testi, Caselli, Zhang, Liu, Jimenez-Serra, Walmsley, Burkert, Ginsburg, van der Tak, Dale, Ho
155-14	Perseus B5: Structure Formation from the Filament to the Coherent Core, to Star Forming Condensations	Hope Chen, Pineda, Goodman, Hacar, Alves, Offner
156-14	Kinematics and Structure of the High Density Gas within Filaments in the Taurus Molecular Cloud	Punanova, Caselli, Pon
158-14	Unbiased spectral survey of CygX-N63 a unique pre-hot core source	Bontemps, Fechtenbaum, Csengeri, Lefloch, Herpin, Duarte Cabral, Schneider, Wakelam
161-14	Constraining the mass and dust properties of the most massive starless clumps in the Galaxy	Traficante, Billot, Fuller, Peretto, Molinari
162-14	Establishing the nature of a new class of young massive stars	Cesaroni, Sanchez-Monge, Beltran, Molinari, Olmi
163-14	The protosolar nebula heritage: Nitrogen fractionation in ices	Hily-Blant, Daniel, Faure, Pineau des Forets, de Souza Magalhaes, Noel-Rist
164-14	An Unbiased Chemical Survey of Low-Mass Protostars in Perseus	Oya, Sakai, Lopez-Sepulcre, Watanabe, Yamamoto
167-14	Characterizing the turbulence and protostellar outflows in the L1251B protocluster	Maury, Corbel
168-14	Master2 Internship from Grenoble University: Herbig-Haro jets in Star-Forming Regions	Lefloch
169-14	A Recalibration of Molecular Abundances	Rice, Jorgensen, Maret, Hily-Blant, Faure, Bergin, Wampfler
171-14	HD32509, a unique system in transition between primordial and debris disks.	Moor, Abraham, Csengeri, Kospal, Juhasz
172-14	A deep search for (primordial?) CO gas in hybrid disks	Pericaud, Di Folco, Dutrey, Guilloteau, Pietu

Ident.	Title of investigations	Authors
173-14	Probing the Circumstellar Environment of Y Gem - A candidate for Binarity and Active Accretion	Sahai, Sanchez-Contreras, Patel
174-14	Intensity variation of the thermal SiO emission in IRC+10420.	Quintana-Lacaci, Cernicharo, Bujarrabal, Castro-Carrizo, Agundez, Sanchez-Contreras
175-14	A Line Survey of the Supergiant O-rich star VY CMa. IV	Quintana-Lacaci, Teyssier, Cernicharo, Sanchez-Contreras, Alcolea, Marcelino, Velilla Prieto, Bujarrabal
177-14	Molecular complexity in the Red Supergiant Betelgeuse	Herpin, Lebre, Auriere, Josselin, Petit, Philippe, Alizee, Sanchez-Contreras, Velilla Prieto
178-14	Nitrogen Isotopic Enrichment in IC443 G: Investigating Supernova Ejecta Mixing into Molecular Clouds	adande, Charnley, Cordiner
180-14	On the extended dust emission around evolved stars	Billot, Bujarrabal, Sanchez-Contreras, Castro-Carrizo, Alcolea, Desert, Ponthieu
181-14	Measuring the large scale dust-to-gas mass ratio in IRC+10216	Agundez, Cernicharo, Joblin, Demyk, Berne, Guelin, Velilla Prieto, Etxaluze, Leclercq
182-14	Testing the anion time-dependent chemistry in IRC+10216: radical and anion short spacing observations	Guelin, Cernicharo, Agundez, Winters
183-14	Nuclear ashes in the oldest known 'nova' CK Vul	Kaminski, Menten, Tylenda, Patel, Hajduk
184-14	Millimeter Observations of the Galactic Centre Magnetar J1745-2900	Torne, Eatough, Karuppusamy, Kramer, Paubert
185-14	CN N=2-1 Zeeman Observations of Massive Star Forming Cores	Falgarone, Crutcher, Troland, Hily-Blant
188-14	Exploring molecular gas in low stellar mass galaxies	Martin Ruiz, Bothwell, Wagg, Maiolino, Aravena, Moller, Cicone, Riechers
189-14	Physical condition of molecular clouds in M31	Dumas, Martin Ruiz, Aladro, Ceccarelli, Lefloch, Hily-Blant, Lopez-Sepulcre
190-14	Completing the 30-meter Observations of the Key Local Galaxy Reference Sample	Schruba, Walter, Leroy, Sandstrom, Kramer, Usero, Hughes, Zschaechner
192-14	Searching for evidence of cooling in group-dominant ellipticals.	Leslie Hamer, Salome, Combes, O'Sullivan, Babul, Raychaudhury
194-14	Molecular Gas in MASSIVE Galaxies	Greene, Davis, Ma, Blakeslee
195-14	Search for intra-cluster molecular gas in star-forming tails of the Coma cluster ram pressure stripped galaxies	Jachym, Sun, Kenney, Cortese, Combes, Yagi, Yoshida, Palous, Roediger
196-14	Toward a complete census of gas in low-*z* post-merger galaxies	Sargent, Ellison, Coppin, Saintonge, Scudder, Violino
197-14	Cross-calibrating dust- and CO-based gas mass measurements from intermediate to the largest gas reservoirs in the nearby universe	Wuyts, Rosario, Lutz, Tacconi, Genzel, Schreiber Forster
198-14	A direct measurement of the dust destruction timescale in passive galaxies	Michalowski, Hjorth, Zavala, Hughes, Gall
199-14	The dust SED of dwarf galaxies: NGC4449	Hermelo
200-14	Constraining the millimeter dust excess emission in Herschel dwarf galaxies with NIKA	Albrecht, Madden, Remy-Ruyer, Bertoldi
202-14	Reactive ions in M 82	Alonso-Albi, Fuente, Garcia-Burillo, Trevino-Morales, Ginard, Usero, Gerin
203-14	Comparison of Chemical Compositions between Two Regions in NGC 3627	Watanabe, Sakai, Nishimura, Kuno, Yamamoto
206-14	The EMIR Nearby Galaxy Dense Gas Survey	Bigiel, Leroy, Usero, Walter, Cormier, Schuster, Garcia-Burillo, Kramer, Pety, Sandstrom, Schinnerer, Hughes, Kepley, Bolatto, Schruba, Dumas, Zschaechner
207-14	Tracing dense gas in subsolar metallicity galaxies	Braine, Andre, Bontemps, Schneider, Kramer, Shimajiri
208-14	The evolution of dense gas in extragalactic starbursts. A multi-line survey of CH_3CCH	Aladro, Martin Ruiz, Viti, Harada, Riquelme, Kelly
209-14	Dense Molecular Gas in the Wind of NGC 253	Bolatto, Walter, Leroy, Zschaechner, Warren
210-14	Cool Gas Physics in Abell 1068	Oonk, Frayer, Edge
211-14	HCN and HCO^+ emission in NGC 1275	Salome, Salome, Combes, Sun, Wang
212-14	The Extreme ISM of Luminous Local AGN	Davies, Gracia-Carpio, Sternberg, Burtscher, Lin, Rosario
214-14	MAPI: Monitoring AGN with Polarimetry at the IRAM-30-m	Agudo, Thum, Molina, Casadio, L. Gomez, Marscher, Jorstad, Wiesemeyer
215-14	Spectral survey at 1 and 3 mm towards new absorption line systems in radio-loud quasars	Martin Ruiz, Leon, Impellizzeri, Combes, Vila-vilaro, Villard, Guillermin
217-14	The atomic and dense molecular gas in the brightest gravitationally lensed galaxies from the Planck all-sky survey	Nesvadba, Yang, Canameras, Omont, Dole, Scott, Lagache, Beelen, Flores-Cacho, Chary, Le Floc'h, MacKenzie, Konig, Boone, Dicken, Frye, Krips, Malhotra, Soucail, Yan
219-14	Spectroscopic redshifts of bright sources within high-*z* proto-cluster candidates discovered with Planck and Herschel	Dole, Krips, Lagache, Beelen, Giard, Scott, Konig, Nesvadba, Frye, Le Floc'h, Chary, Kneissl, Flores-Cacho, Dicken, Martinache, Guery, Pointecouteau, Bethermin, Soucail, Pierini, Macias-Perez
220-14	Redshift and SED determination for serendipitous Planck-selected submillimeter galaxies.	Blain, Jones, Bridge

Ident.	Title of investigations	Authors
221-14	Searching for the bright reverse shock emission in gamma-ray bursts	Castro-Tirado, Kramer, Hermelo, Bremer, Winters, Gorosabel, Perez-Ramirez, Tello
222-14	Kinetic Sunyaev-Zel'Dovich mapping towards MACS J0717.5+3745 (NIKA GT)	Comis, Adam, Adane, Ade, Andre, Beelen, Belier, Benoit, Bideaud, Billot, Bourrion, Calvo, Catalano, Coiffard, D'Addabbo, Desert, Doyle, Goupy, Kramer, Leclercq, Macias-Perez, Martino, Mauskopf, Mroczkowski, Mayet, Monfardini, Pajot, Pascale, Pointecouteau, Ponthieu, Reveret, Ritacco, Rodriguez, Savini, Schuster, Sievers, Tucker, Zylka
223-14	High-resolution SZ Confirmation of the Most Massive High-*z* Clusters in the Universe	Mroczkowski, Benford, Clarke, Kovacs, Staguhn, Young
224-14	High-resolution SZE Observations of Galaxy Cluster Mergers with GISMO	Young, Mroczkowski, Knowles, Moodley, Intema, Sievers, Hughes, Benford, Staguhn, Kovacs, Hilton, Reese
227-14	Study of a SPIRE Dropout: Candidate Very High Redshift Dusty Galaxy	Beelen, Clements, Perez-Fournon, Bussmann, Riechers, Omont, Michalowski, van der Werf, Dannerbauer, Gonzalez-Nuevo, Temi, Oteo, Dunne
228-14	Unveiling the average dusty star forming galaxies in the early Universe	Schaerer, Boone, Richard, Kneib, Clement, Egami, Dessauges-Zavadsky, Rawle, Combes, Pello, Smail, Edge, Staguhn, Lutz, Weiss, Ivison, Perez-Gonzalez
229-14	Dust emission in Ultra-Luminous Quasars at z>5	Wang, Fan, Wu, Wang, Walter, Yang, Ho, McGreer, Kim, Zuo, Jiang
230-14	The deepest blind survey ever done simultaneously at 1.2 and 2 mm: a pathfinder for NIKA2 cosmological surveys (NIKA GT)	Lagache, Beelen, Ponthieu, Bethermin, Daddi, LIU, Aussel, Boone, Desert, Eales, Elbaz, Macias-Perez, Omont, Pascale, Adam, Adane, Ade, Belier, Benoit, Bideaud, Billot, Bourrion, Calvo, Catalano, Coiffard, D'Addabbo, Dole, Doyle, Goupy, Kramer, Leclercq, Martino, Mauskopf, Mayet, Monfardini, Pajot, Reveret, Rodriguez, Savini, Schuster, Sievers, Tucker, Zylka
232-14	COSMO Part III: The synergetic GISMO survey in the COSMOS field	Staguhn, Karim, Schinnerer, Smolcic, Bertoldi, Aravena, Smail, Benford, Kovacs, Swinbank, Dwek, Su, Sargent, Riechers, Weiss, Magnelli
233-14	Towards BH imaging in Active Galactic Nuclei	Krichbaum, Roy, Rottmann, Sanchez, Bremer, Doeleman, Fish, Zensus, Gusten, Menten, Falcke
237-14	Infall Signatures in the Youngest Protostars	Stutz, Tobin, Henning, Myers, Wilson, di Francesco, Megeath, Watson, Stanke, Wyrowski, Linz
D02-14	N_2H^+ and N_2D^+ in Iras16293E	Pagani, Lefevre, Belloche
D03-14	OTF 30-meter maps for short ALMA spacing observations at 3 and 1mm	Cernicharo
D04-14	Molecular inventory and isotopic ratios in comet C/2014Q2 (Lovejoy)	Biver, Bockelee-Morvan, Boissier, Colom, Debout, Lis, Milam, Moreno, Crovisier
D05-14	A complete and deep HERA map of M33	Braine, Schuster
D06-14	A combined 1.3 and 3mm VLBI study of jet genesis in M87	Krichbaum, Lu, Bremer, Gomez
D07-14	Radioactive ^{26}AlF in the remnant of an ancient stellar merger	Kaminski, Menten, Tylenda, Patel
001-15	Ground truth for the composition of comet 67P, the Rosetta target	Biver, Bockelee-Morvan, Crovisier, Boissier, Lellouch, Paubert, Erard, Snodgrass
003-15	Sulfur depletion in dark clouds	Hily-Blant, Bonfand
004-15	Looking for the sulfur reservoir in IRAS 16293-2422	Majumdar, Gratier, Wakelam, Caux
005-15	The spatial distribution of complex organic molecules in prestellar cores	Bacmann, Faure, Garcia-Garcia
006-15	Mapping ionic species in the photon-dominated region (PDR) Mon R2	Trevino-Morales, Fuente, Pilleri, Kramer, Roueff, Gerin, Ossenkopf, Goicoechea, Rizzo, Pety, Cernicharo, Garcia-Burillo
007-15	Probing the formation of complex molecules around the ultracompact HII region Mon R2	Trevino-Morales, Fuente, Goicoechea, Cernicharo, Sanchez-Monge, Kramer, Pilleri, Pety
008-15	Probing deuteration models in warm dense regions	Trevino-Morales, Sanchez-Monge, Fuente, Rodriguez, Roueff, Rodriguez-Rico, Kramer
009-15	Deuterium Fraction in the Ophiuchus Molecular Cloud	Punanova, Caselli, Pon, Friesen, Pineda
010-15	Deuterated methanol and CO distribution in the starless core L1544	Bizzocchi, Caselli, Lattanzi, Michela Giuliano
011-15	Deuterium Astration in the Galactic Center	Riquelme, Pillai, Requena-Torres, Albertsson, Kauffmann
012-15	The role of environment and of cloud depth in the formation of small hydrocarbons	Cuadrado, Goicoechea, Cernicharo, Fuente, Joblin, Pilleri
013-15	CCH in diffuse interstellar clouds as a probe of carbon-chain chemistry	Schmidt, Kaminski
015-15	Mapping Rosette with 32 GHz Bandwidth	Kauffmann, Goldsmith, Menten, Wyrowski, Yamamoto, Watanabe, Weiss, Wiesemeyer
016-15	Large-scale morphology, chemistry, and kinematics of Sgr B2 starburst (II)	Goicoechea, Etxaluze, Cernicharo, Tercero
019-15	Polarimetric Monitoring of the Encounter of Cloud G2 with SgrA*	Agudo, Thum, Molina, Casadio, Wiesemeyer, L. Gomez, Sievers, Sohn
020-15	Mapping the Bones of the Milky Way	Battersby, Goodman, Sanchez-Monge, Schilke, Zucker, Pillai, Goldsmith, McGehee, Bally, Ragan, Burkhart, Arce, Pineda, Dame, Imara, Carpenter, Smith, LIS, Jackson, Lopez

Ident.	Title of investigations	Authors
021-15	Short spacings to complete the ALMA SV data of Orion KL	Tercero, Cernicharo, Lopez, Brouillet, Despois, Baudry, Castro-Carrizo
022-15	Infering the UV radiation field around molecular clouds using ground-based observations	Leschinski, Hacar, Alves, Forbrich, Teixeira
024-15	W28: an ideal target to study the interaction of cosmic rays and ISM	Vaupre, Hily-Blant, Dubus, Montmerle, Padovani, Gabici, Bennacer, Ceccarelli, Dumas
025-15	The Cosmic-Ray Flux in Dense Cores	Indriolo, Bergin
026-15	A star forming region triggered by microquasar jets	Mirabel, Maury
027-15	Triggered Star Formation Around the Infrared Bubble N10	Gama, Lefloch, Lepine, Mendoza
028-15	On the thermal state of a dense layer enclosing a HII region	Gong, Henkel, Li, Wyrowski, Mao, Urquhart
029-15	Testing the "fray-and-fragment" scenario of core formation	Tafalla, Hacar
030-15	Characterizing the Filamentary Molecular Structure of Orion A	Suri, Sanchez-Monge, Schilke, Carpenter, Bally, Johnstone, Mairs, Klessen, Schmiedeke, Pineda, Kauffmann, Goldsmith, Pillai, Glover, Smith, Nakamura
032-15	Probing the detailed connection between dense gas and star formation in the Aquila molecular cloud complex	Andre, Konyves, Shimajiri, Bontemps, Braine, Schneider, Maury, Ladjelate
033-15	Probing the evolution of a large sample of prestellar cores in the Aquila cloud	Konyves, Andre, Shimajiri, Ladjelate
034-15	Dynamical and chemical evolution of the globally collapsing DR21 ridge	Bontemps, Schneider, Fechtenbaum, Andre, Braine, Csengeri, Simon
035-15	Infall and outflow in a filamentary hub (II)	Fuente, Trevino-Morales, Cernicharo, Didelon, Kramer, Motte, Pilleri, Rayner, Sanchez-Monge, Schneider, Tremblin
038-15	Establishing the nature of a new class of young massive stars	Cesaroni, Sanchez-Monge, Beltran, Molinari, Olmi
039-15	HEFE Deep: Interpreting Line Profiles in L1641	Nagy, Megeath, Billot, Stutz, Wyrowski, Stanke, Fischer, Heitsch, Smith, Safron, Osorio Gutierrez, Menten, Tobin, Furlan, Abreu-Vicente
040-15	Gas properties toward prestellar cores associated with dust grain growth	Ristorcelli, Demyk, Billot, Paladini, Hughes, Juvela, Montillaud, Pelkonen, Montier, Bernard, Ysard, paradis, Meny, Rivera-Ingraham, koehler, Lefevre, Tibbs, Pagani
041-15	Testing the possibility of carbon fractionation in HCN	de Souza Magalhaes, Hily-Blant, Daniel, Faure
042-15	Measuring the $^{14}N/^{15}N$ ratio in massive dense cores	Fontani, Caselli, Ceccarelli, Bizzocchi, Daniel, Hily-Blant
043-15	Chemical signatures of episodic luminosity outbursts in embedded protostars	Taquet, Van Dishoeck, Persson, Wirstrom, Visser
044-15	CN N=2-1 Zeeman Observations of Massive Star Forming Cores	Falgarone, Crutcher, Troland, Hily-Blant
045-15	Mapping the kinematics of the dense gas in a magnetized prestellar core	Alves, Juarez, Girart, Caselli, Pon, Franco, Frau
046-15	Confirming the coupling of gas and magnetic field in the Pipe nebula cores	Juarez, Girart, Frau, Beltran, Franco, Alves, Morata, Caselli
047-15	High Density Polarization in Perseus B1-E	Sadavoy, Houde, di Francesco, Bastien, Basu, Bailey, Clemens, Hezareh, Albert, Wiesemeyer
048-15	Identifying circumstellar disk tracers in the (almost) massive YSO AFGL490	Marka
049-15	The molecular content of hybrid disks: HD141569A as a case study	Pericaud, Di Folco, Dutrey, Guilloteau, Augereau, Pietu
050-15	A pilot search for radio recombination line emission from emerging ionized winds in pre-Planetary Nebulae	Sanchez Contreras, Baez-Rubio, Alcolea, Martin-Pintado, Bujarrabal
051-15	Unveiling the contribution of UV photo-chemistry in proto-planetary nebulae	Pilleri, Cernicharo, Joblin, Sanchez Contreras, Demyk, Cox, Quintana-Lacaci
052-15	Probing NH_3 Formation in Oxygen-rich Circumstellar Envelopes	Wong, Menten, Kaminski, Wyrowski
054-15	A search for molecular emission in classical novae: towards a test of explosive nucleosynthesis	Kaminski, Menten
055-15	OTF 30-meter maps for short ALMA spacing observations at 3 mm	Cernicharo, Castro-Carrizo, Agundez, Quintana-Lacaci, Velilla Prieto, Guelin, Gottlieb, Joblin
056-15	Time variability monitoring of molecular emission in IRC+10216	Cernicharo, Teyssier, Quintana-Lacaci, Agundez, Guelin, Velilla Prieto, Neufeld, Garcia-Lario, Marka
058-15	Molecular Gas in a Very Low-Metallicity Galaxy	Imara, Leroy, Bigiel, Dame, Cormier
059-15	Molecular depletion times and the CO-to-H_2 conversion factor in metal-poor galaxies	Hunt, Garcia-Burillo, Combes, Bianchi, Casasola, Caselli, De Lucia, Galli, Granato, Henkel, Magrini, Menten, Monaco, Silva, Weiss
060-15	Mapping M 82 outflow in CS, CN and N_2H^+	Alonso-Albi, Fuente, Garcia-Burillo, Gerin, Usero, Ginard, Trevino-Morales
061-15	The Distribution of the Bulk Molecular Medium in NGC 4254	Jimenez Donaire, Bigiel, Usero, Leroy, Cormier
062-15	A direct measurement of the dust destruction timescale in passive galaxies	Michalowski, Hjorth, Zavala, Gall
063-15	Exploring scaling relations between gas and dust across cosmic time	Magdis, Rigopoulou, Daddi, Elbaz, Bethermin, Combes, Perez-Fournon, Alonso-Herrero, Hatziminaoglou
064-15	Detection of Molecular Gas and its Excitation in local Lyman Alpha Emitters	Oteo, Puschnig, Hayes, Ostlin, Cannon, Schaerer, Freeland

Ident.	Title of investigations	Authors
065-15	Molecular Gas in Local Analogs for High-Redshift Galaxies	Bian, Wang, Kewley, Groves
067-15	Do the most massive galaxies lack cold gas?	Davis, Greene, Ma, Blakeslee
068-15	Molecular oxygen in NGC 6240 and VII Zw31	Wang, Li, Zhang, Goldsmith, Shi, Zhang, Fang
069-15	Hydrogen millimeter recombination lines as a SFR indicator	Badescu, Bertoldi, Karim, Magnelli, Yang
071-15	Characterising the dense gas in the HerCULES sample	Weiss, Greve, Zhang, Xilouris, Leonidaki, Tunnard, van der Werf, Walter, Gao, Aalto
072-15	^{13}CO observation of a post-starburst galaxy SDSS J103757.35+461440.2	Chen, JIN, Chen, Braine, Gao, Gu
075-15	Probing The Accretion Disk of NGC 7469 with Simultaneous 3 mm and X-Ray Monitoring	Behar, D. Baldi, Billot, Feruglio, Horesh, Laor, Kaastra, Mehdipour, Paubert
076-15	MAPI: Monitoring AGN with Polarimetry at the IRAM-30-m	Agudo, Thum, Molina, Casadio, L. Gomez, Marscher, Jorstad, Wiesemeyer
077-15	CO redshifts for serendipitous Planck-selected submillimeter galaxies.	Blain, Jones, Bridge
078-15	Completing the CO Redshift Search for the Herschel Lensing Survey (HLS) Bright Sources	Egami, Dessauges-Zavadsky, Rawle, Clement, Richard, Kneib, Combes, Boone, Perez-Gonzalez, Schaerer, Altieri
079-15	Molecular gas in lensed high-*z* ULIRGs with submillimeter H_2O emission	Yang, Beelen, Omont, van der Werf, Ivison, Gavazzi, Neri, Krips, Gonzalez-Alfonso, Gao, Oteo
080-15	Blind Redshifts for Ultra-red, Bright Herschel Galaxies	Dannerbauer, Perez-Fournon, Ivison, Eales, Bakx, Marques-Chaves, Martinez-Navajas, Riechers, Clements, Oteo, Valiante, Omont, Asboth, Wardlow, Conley
D01-15	Measuring dust temperature in a edge-on disk through absorption of CO line emission	Guilloteau, Dutrey, Pietu, Chapillon, Difolco, Henning, Semenov, Grosso
D02-15	Molecular fingerprints of an unbiased sample of Galactic MSF clumps: Completing the sample	Menten, Wyrowski
D03-15	Redshift scan of new strongly-magnified submm galaxies.	Burgarella, Goto, Sakamoto, Momose, Mazyed, Marquez
D04-15	First detection of PO towards a star-forming region	Rivilla, Fontani, Martin-Pintado, Beltran, Cesaroni, Casell

NOEMA INTERFEROMETER

Ident	Title of Investigations	Authors
X--3	Resolving the star-forming clumps in a lensed L* galaxy at z~1.6	Dessauges-Zavadsky, Combes, Krips, Schaerer, Zamojski, Richard, Cava, Boone, Kneib, Egami, Omont, Rawle, van der Werf
X--7	HD141569: disk dissipation caught in action - DDT Request ^{12}CO 2-1	Dutrey, Pericaud, Di Folco, Guilloteau, Pietu, Augereau
X053	PHIBSS2: molecular gas at the peak epoch of galaxy formation	Combes, Garcia-Burillo, Neri, Tacconi, Genzel, Contini, Bolatto, Lilly, Boone, Bouche, Bournaud, Burkert, Carollo, Colina, Cooper, Cox, Feruglio, Freundlich, Schreiber, Juneau, Kovac, Lippa, Lutz, Naab, Omont, Renzini, Saintonge, Salome, Sternberg, Walter, Weiner, Weiss, Wuyts
X070	HD141569: disk dissipation caught in action	Pericaud, Di Folco, Dutrey, Pietu, Guilloteau, Augereau
X0CC	A Detailed Investigation of the ISM in the Most Distant Starburst Galaxy	Riechers, Perez-Fournon, Omont, Neri, Bradford, Clements, Cooray, Wardlow, Cox, Krips, Dowell, Ivison, Kamenetzky, Conley, Vieira, Bock, Oliver
D14AE	Spectroscopic confirmation of a novel, possibly fundamental stage of structure formation at z~2.5	David Elbaz, Tao Wang, Emanuele Daddi, Xinwen Shu, Daizhong Liu, Chiara Feruglio, Sergio Martin Ruiz, Qinghua Tan, Francesco Valentino, Raphael Gobat
D14AF	Complex Organic Molecules in the protocluster OMC2-FIR4	Cecilia Ceccarelli, Paola Caselli, Claudio Codella, Francesco Fontani, Bertrand Lefloch, Luca Bizzocchi
S14AX	Mapping the gaseous and dusty envelope of Betelgeuse	Miguel Montarges, Pierre Kervella, Arancha Castro-Carrizo, Jan Martin Winters, Valentin Bujarrabal, Guy Perrin, Leen Decin, Anita M. S. Richards, Eamon O'Gorman, Thibaut Le Bertre, Xavier Haubois, Stephen Ridgway, Graham Harper, Iain McDonald, Andrea Chiavassa, Sylvestre Lacour
S14BD	The dense gas fraction of inefficiently star-forming gas	Eva Schinnerer, Annie Hughes, Sharon E. Meidt, Miguel Querejeta, Dario Colombo, Santiago Garcia-Burillo, Clare Dobbs, Todd Thompson
S14BE	High Resolution Imaging of Dense Gas in the Outer Spiral Arm of M51	Hao Chen, Jonathan Braine, Yu Gao
S14BR	Hydrogen millimeter recombination lines as a SFR indicator	Toma Badescu, Frank Bertoldi, Yujin Yang, Alexander Karim, Benjamin Magnelli, Kaustuv Basu
S14BX	Strong Differential Lensing in a Distant Wet-Dry Merger: Gas Properties	Dominik A. Riechers

Ident	Title of Investigations	Authors
L14AB	Fragmentation and disk formation during high-mass star formation	Henrik Beuther, Thomas Henning, Hendrik Linz, Siyi Feng, Katharine Johnston, Rolf Kuiper, Sarah Ragan, Dmitry Semenov, Frederic Gueth, Jan Martin Winters, Karl M. Menten, James Urquhart, Timea Csengeri, Pamela Klaassen, Joseph C. Mottram, Peter Schilke, Melvin Hoare, Luke Maud, Stuart Lumsden, Maria Teresa Beltran, Riccardo Cesaroni, Malcolm Walmsley, Alvaro Sanchez-Monge, Qizhou Zhang, Cornelis Dullemond, Frederique Motte, Philippe Andre, Gary Fuller, Nicolas Peretto, Roberto Galvan-Madrid, S. Longmore, Sylvain Bontemps, Th. Peters, Aina Palau, R. Pudritz, Hans Zinnecker
E14AG	[CII] and dust in a new luminous quasar at z=6.53	Fabian Walter, Bram Venemans, Eduardo Banados, Roberto Decarli
E14AH	Nucleus and inner coma of new comet C/2014 Q2 (Lovejoy)	Jeremie Boissier, Nicolas Biver, Dominique Bockelee-Morvan, Raphael Moreno, Jacques Crovisier, Stefanie Milam, Pierre Colom, Vincent Debout, Laurent Jorda, Philippe Lamy, Olivier Groussin
E14AI	[CII] and dust emission in a massive star forming galaxy at z = 7.730	Pascal Oesch, Daniel Schaerer, Fabian Walter, Frederic Boone, Roberto Decarli
E14AL	A giant molecular outflow in the z=2.85 QSO1549	Scott Chapman, Frank Bertoldi, Chuck Steidel, Ian Smail, Arif Babul, James Geach
E14AM	First evidence of quenching by star formation efficiency suppression in z=0.56 bulge rich spirals	Emanuele Daddi, Fadia Salmi, Frederic Bournaud, Daizhong Liu, Georgios Magdis, Mark T. Sargent, Matthieu Bethermin, Marie Martig, Francesco Valentino, Paola Dimauro, Marc Huertas-Company, David Elbaz, Mark Dickinson, Stephanie Juneau, Sergio Martin Ruiz
I15AA	Dense gas in the central kpc of the Medusa merger	Sabine Koenig, Susanne Aalto, Sebastien Muller, John Gallagher, Rob Beswick, Eva Jutte
W14AA	The L1157-B1 astrochemical laboratory: testing the origin of DCN	Francesco Fontani, Claudio Codella, Cecilia Ceccarelli, Bertrand Lefloch, Serena Viti, Milena Benedettini, Gemma Busquet
W14AB	Dynamics and chemistry in the earliest phase of high-mass star formation	Siyi Feng, Henrik Beuther, Thomas Henning, Sarah Ragan, Hendrik Linz, Qizhou Zhang, Rowan Smith
W14AF	Molecule Formation in Protostellar Jets : a study of CepE	Bertrand Lefloch, Antoine Gusdorf, Claudio Codella, Cecilia Ceccarelli
W14AI	Tracing for the first time a prestellar core towards a distant high-mass star forming region	Charlotte Vastel, Jerome Pety, Maryvonne Gerin, Bhaswati Mookerjea
W14AP	Probing the birth of low mass stars: confirmation of the detection of a FHSC in Barnard 1b	Maryvonne Gerin, Asuncion Fuente, Jose Cernicharo, Jerome Pety, Evelyne Roueff, Benoit Commercon, Francois Levrier, Darek Lis, Nuria Marcelino
W14AY	SO in young stellar objects: outflows, binary streamers or accretion shocks?	Stephane Guilloteau, Edwige Chapillon, Vincent Pietu, Anne Dutrey, Laura Reboussin, Ya-Wen Tang, Nicolas Grosso, Valentine Wakelam, Frederic Gueth
W14BB	Class I methanol masers: shock tracers in deeply embedded sources	Silvia Leurini, Timea Csengeri, Karl M. Menten, Friedrich Wyrowski, Frederic Gueth
W14BQ	Behind the wall: planet formation in a giant "dead zone" around GG Tau A?	Anne Dutrey, Emmanuel Di Folco, Vincent Pietu, Frederic Gueth, Edwige Chapillon, Stephane Guilloteau, Ya-Wen Tang, Jeffrey Bary, Jean-Marc Hure, Michal Simon, Arnaud Pierens, Herve Beust, Franck Hersant, Yann Boehler
W14BT	Additional compact-configuration observations of 13CO emission in 89 Her	Valentin Bujarrabal, Arancha Castro-Carrizo, Hans Van Winckel, Javier Alcolea
W14BU	The remarkable disk orbiting AC Her	Valentin Bujarrabal, Arancha Castro-Carrizo, Hans Van Winckel, Javier Alcolea
W14BZ	Mapping the gas conditions in IC342	Monica Rodriguez, Stefanie Muehle, Susanne Aalto, Francesco Costagliola, Antonio Alberdi Odriozola, Miguel Angel Perez-Torres
W14CB	Resolving the nuclear cold molecular gas in nearby Seyfert galaxies	Almudena Alonso-Herrero, Santiago Garcia-Burillo, Cristina Ramos Almeida, Luis Colina, Jose Miguel Rodriguez Espinosa, Eleonora Sani, Rachel Mason, Chris Packham, Nancy Levenson, Pat Roche, Dimitra Rigopoulou, Masatoshi Imanishi, Pilar Esquej
W14CD	Anatomy of a Spiral Arm: from Molecular Gas to Stars	Eva Schinnerer, David S. Meier, S. Meidt, Santiago Garcia-Burillo, Frank Bigiel, Antonio Usero, Jerome Pety, Gaelle Dumas, Annie Hughes, Miguel Querejeta
W14CG	Molecular Gas and Induced Star Formation in the Interacting Galaxy NGC 2276	Annie Hughes, Eva Schinnerer, Miguel Querejeta, Jerome Pety, Gaelle Dumas, Santiago Garcia-Burillo, Clare Dobbs, S. Meidt, Florent Renaud
W14CH	Resolving the molecular outflow in the buried QSO IRAS F08572+3915	Annemieke Janssen, Eckhard Sturm, Roberto Maiolino, Eduardo Gonzalez-Alfonso, Richard Davies, Sylvain Veilleux, Enrico Piconcelli, Fabrizio Fiore, Santiago Garcia-Burillo, Susanne Aalto, Claudia Cicone, David Rupke, Jacqueline Fischer, Javier Gracia-Carpio, Chiara Feruglio, Linda Tacconi, Dieter Lutz, Alessandra Contursi
W14DB	The ultra-massive black hole in NGC 1277 probed via CO kinematics: follow-up observations	Julia Scharwachter, Francoise Combes, Philippe Salome, Melanie Krips, Ming Sun
W14DD	Do all ULIRGs have vibrationally excited HCN?	Susanne Aalto, Sergio Martin Ruiz, Kazushi Sakamoto, Eduardo Gonzalez-Alfonso, Sebastien Muller, Francesco Costagliola, Santiago Garcia-Burillo, Elisabeth Mills, Paul van der Werf, Christian Henkel

Ident	Title of Investigations	Authors
W14DG	Hiding in Plain Sight - self-absorbed, low power AGN in massive galaxies	Alastair Edge, Michael Hogan, Philippe Salome, Francoise Combes, Helen Russell, Keith Grainge
W14DS	Evolution of CO and Star Formation as Probed by Herschel-Selected Pure Starbursts at z~1.5	Emanuele Daddi, Daizhong Liu, J. Silverman, Giulia Rodighiero, Frederic Bournaud, Dieter Lutz, Mark T. Sargent, Georgios Magdis, Matthieu Bethermin, Yu Gao, Stephanie Juneau, Daichi Kashino
W14DV	Probing the Molecular Gas Reservoir of Extreme [CII] Emitters at z~1.8	Carl Ferkinhoff, Gordon Stacey, Thomas Nikola, Drew Brisbin, Fabian Walter
W14DY	A gas-rich `dark' galaxy at the peak of galaxy assembly	Roberto Decarli, Fabian Walter, Chris L. Carilli, Dominik A. Riechers, Roberto Neri
W14EQ	High-resolution CO in the HyLIRG maximal disk, H1700.850.1	Frank Bertoldi, Scott Chapman
W14ES	Zooming in onto star formation in the brightest gravitationally lensed galaxies from the Planck all-sky survey	Nicole Nesvadba, R. Canameras, Herve Dole, Douglas Scott, Guilaine Lagache, Alexandre Beelen, I. Flores-Cacho, Ranga-Ram Chary, Emeric Le Floc'h, T. MacKenzie, Sabine Koenig, Frederic Boone, Dan Dicken, Brenda Frye, Melanie Krips, Sangeeta Malhotra, G. Soucail, Lin Yan, Chentao Yang
W14FG	Millimeter-wave imaging of Planck-detected point sources	Andrew Blain, Carrie Bridge, Suzy Jones
W14FH	Dynamical Structure of the Star-Forming Interstellar Medium in a Newly-Discovered (Unlensed) Starburst at z=5.3	Dominik A. Riechers, Jacqueline Hodge, Fabian Walter, Emanuele Daddi, Roberto Neri, Chris L. Carilli
W14FP	The Youngest Dust Forming Galaxy in the Universe?	Johannes Staguhn, Eli Dwek, Richard G. Arendt, Jorge Gonzalez, Fabian Walter, Ting Su, Sune Toft, Thomas R. Greve, Michal J. Michalowski
D15AB	Constraining the Millimetre Properties of the Broad-Band SED During the Fading of the 2015 Outburst of V404 Cyg	Alexandra Tetarenko, Gregory Sivakoff
D15AC	A direct view into the planet formation process: the circumplanetary disk of DH Tau B	Francois Menard, Claudio Caceres
S15AD	Chemical characterization of the outflows from the very young protostellar objects B1b-S and B1b-N	Maryvonne Gerin, Asuncion Fuente, Jerome Pety, Jose Cernicharo, Darek Lis, Nuria Marcelino, Evelyne Roueff, Benoit Commercon, Henry Wootten, Andrea Ciardi, Fabien Daniel
S15AF	Nature of ultra-low-mass Herschel cores in Ophiuchus and Taurus	Philippe Andre, Bilal Ladjelate, Pedro Palmeirim, Vera Konyves, Alexander Menshchikov
S15AL	Universality of filament formation? The massive case in DR21	Sylvain Bontemps, Nicola Schneider, Jonathan Braine, Timea Csengeri, Frederique Motte, Philippe Andre, Pierre Gratier
S15AN	Tracing for the first time a prestellar core towards a distant high-mass star forming region	Charlotte Vastel, Jerome Pety, Maryvonne Gerin, Bhaswati Mookerjea
S15AR	Origin of the Highest Velocity Protostellar Outflow	David Wilner, Christopher De Pree, Lars E. Kristensen
S15AT	Improving and tracing the structure of AB Aur molecular disk in SO and CS emission	Susana Pacheco Vazquez, Asuncion Fuente, Jose Cernicharo, Rafael Bachiller, Roberto Neri, Marcelino Agundez, Javier R. Goicoechea, Tomas Alonso-Albi
S15AU	Particle growth in protoplanetary disks across the stellar/substellar transition	Gerrit van der Plas, Francois Menard, Jennifer Patience, Paul Harvey
S15AV	A closer look at the lifeline of GG Tau Aa: excitation condition and shock tracers	Edwige Chapillon, Anne Dutrey, Vincent Pietu, Stephane Guilloteau, Frederic Gueth, Ya-Wen Tang, Emmanuel Di Folco
S15BA	Rotating and expanding gas in post-AGB nebulae	Valentin Bujarrabal, Arancha Castro-Carrizo, Javier Alcolea, Hans Van Winckel
S15BK	Molecular gas in the Medusa's dusty tail	Sabine Koenig, Susanne Aalto, Sebastien Muller, John Gallagher, Rob Beswick, Eva Jutte
S15BL	Molecular gas in a multi-phase ram pressure stripped gas tail	Pavel Jachym, Ming Sun, Jeffrey Kenney, Luca Cortese, Francoise Combes, Masafumi Yagi, Michitoshi Yoshida, Jan Palous, Elke Roediger
S15BN	Mapping the structure and kinematics of the CO luminous galaxy NGC 940	Stephen Leslie Hamer, Philippe Salome, Francoise Combes, Somak Raychaudhury, Ewan O'Sullivan, Arif Babul
S15BO	CS (and Iron) in the cold core of the Perseus Cluster	Dennis Downes, Roberto Neri
S15BP	Gas in MASSIVE Galaxies: Dynamical IMF measurements with molecular gas	Timothy Davis, Jenny Greene, Chung-Pei Ma, John Blakeslee
S15BS	CO Outflows from Star Formation-Dominated ULIRGs	Fabian Walter, Adam Leroy, Axel Weiss, Roberto Decarli, Laura Zschaechner
S15BX	A Deep CO Observation of the Powerful AGN in the MS0735 Cluster	Adrian Vantyghem, Brian McNamara, Helen Russell, Alastair Edge, Michael Hogan, Francoise Combes, Philippe Salome
S15BZ	Do the fundamental constants change with time?	Nissim Kanekar, Karl M. Menten
S15CA	Exploring H_2O 183 GHz megamaser at high redshift	Alain Omont, Chentao Yang, Eduardo Gonzalez-Alfonso, Nissim Kanekar, Alexandre Beelen, Roberto Neri, Simon Dye, R. Gavazzi, Rob Ivison, Hugo Messias, Paul van der Werf, Andrew Baker
S15CC	Tracing the formation of cluster galaxy populations: the gas content and dynamics of ultraluminous starbursts in a z=1.62 cluster	Ian Smail, Mark Swinbank, Chian-Chou Chen
S15CE	Studying the CO Excitation of Extreme [CII] Emitters at z~1.8	Carl Ferkinhoff, Fabian Walter, Gordon Stacey, Thomas Nikola
S15CF	Measuring CO excitation in a CO(1-0)-selected sample at z~2.4	Roberto Decarli, Dominik A. Riechers, Fabian Walter, Chelsea Sharon, Riccardo Pavesi

Ident	Title of Investigations	Authors
S15CH	Dense gas in the brightest lensed galaxies of the Planck all-sky survey	Raoul Canameras, Nicole Nesvadba, Melanie Krips, Sabine Koenig, Alexandre Beelen, Douglas Scott, Ranga-Ram Chary, Lin Yan, Sangeeta Malhotra, Brenda Frye, Chentao Yang, Alain Omont, Dan Dicken
S15CN	A survey for CO(3-2) in H1549+19, the most overdense protocluster known at z>2	Frank Bertoldi, Scott Chapman, Chuck Steidel, Andrew Blain, Ian Smail, Rob Ivison, James Geach
S15CO	Molecular gas contents of galaxies in a forming massive cluster at z=2.503	Tao Wang, David Elbaz, Emanuele Daddi, Daizhong Liu, Sergio Martin Ruiz
S15CV	Probing the Excitation of H_2O Emission in Lensed Herschel Galaxies	Alain Omont, Chentao Yang, Roberto Neri, Alexandre Beelen, Paul van der Werf, Eduardo Gonzalez-Alfonso, Melanie Krips, Rob Ivison, R. Shane Bussmann, R. Gavazzi, Yu Gao, Matthew Lehnert, Helmut Dannerbauer
S15CW	First detection of high speed molecular gas at high redshift	Chiara Feruglio, Enrico Piconcelli, Simona Gallerani, Fabrizio Fiore, Andrea Ferrara, Luca Zappacosta, Roberto Maiolino, Roberto Neri, Giustina Vietri, Claudia Cicone, Nicola Menci, Cristian Vignali
S15CX	Fuel and consumption of a massive rotating disk galaxy 1.3Gyr after the Big Bang	Alexander Karim, Chris L. Carilli, Vernesa Smolcic, Dominik A. Riechers, Benjamin Magnelli, Eva Schinnerer, Kartik Sheth, Frank Bertoldi, Manuel Aravena, A. Koekemoer, E. van Kampen, Johannes Staguhn, Mark T. Sargent, Sune Toft, Ian Smail, Mark Swinbank, Elaine Grubmann
S15CY	Interstellar Medium Excitation in a New Sample of z>5 Dusty Starbursts	Dominik A. Riechers, Ismael Perez-Fournon, Roberto Neri, Alex Conley, Alain Omont
S15CZ	The first 850micron drop-out source, a lensed normal dusty galaxy at the epoch of reionization?	Frederic Boone, Daniel Schaerer, Johannes Staguhn, Johan Richard, Jean-Paul Kneib, Eiichi Egami, Tim Rawle, Ian Smail, Chian-Chou Chen, Alastair Edge, Axel Weiss, Miroslava Dessauges-Zavadsky, Francoise Combes, Benjamin Clement, Roser Pello, Pablo G. Perez-Gonzalez, Dieter Lutz, Rob Ivison, Bruno Altieri
S15DA	The interstellar medium of a [CII]-bright QSO host galaxy at z=6.5	Roberto Decarli, Eduardo Banados, Fabian Walter, Bram Venemans
S15DB	Pinpointing the positions of the z > 3 bright submillimeter galaxies in the northern SCUBA-2 CLS fields	Fabian Walter, Rob Ivison, Carl Ferkinhoff, Roberto Decarli, Paul van der Werf, Ian Smail, James Dunlop, Scott Chapman, Mark Swinbank, Chian-Chou Chen, James Simpson, James Geach, Kristen Coppin, Marco Spaans, Alexander Karim, Duncan Farrah, Michal J. Michalowski
S15DE	Constraining the Jet Properties of Transient Black Hole X-ray Binaries	Alexandra Tetarenko, Gregory Sivakoff, Dipankar Maitra, Sera Markoff, Simone Migliari, James Miller-Jones, Dave Russell, Thomas Russell, Craig Sarazin, Anthony Rushton, Michael Rupen
L15AA	Seeds Of Life in Space	Cecilia Ceccarelli, Paola Caselli, Francesco Fontani, Claudio Codella, Bertrand Lefloch, Charlotte Vastel, Jaime Pineda, Andy Pon, Pierre Hily-Blant, Roberto Neri, Luca Bizzocchi, Izaskun Jimenez-Serra, Felipe Alves, Rafael Bachiller, Sandrine Bottinelli, Emmanuel Caux, Gaelle Dumas, Robert Lucas, Linda Podio, Anna Punanova, Nami Sakai, Satoshi Yamamoto, Serena Viti, Anton Vasyunin, Francois Dulieu, Alexandre Faure, Silvia Spezzano, Laurent Wiesenfeld, Nadia Balucani, Ali Jaber, Albert Rimola, Ian Sims, Patrice Theule, Piero Ugliengo, Ana Chacon-Tanarro, Rumpa Choudhury, Vianney Taquet
E15AD	The birth of the giant: Pristine gas accretion and host galaxy assembly in a QSO at z~6.6	Roberto Decarli, Fabian Walter, Bram Venemans, Eduardo Banados, Emanuele Paolo Farina
W15AA	Mapping the dynamics and thermal structure of Venus upper atmosphere	Arianna Piccialli, Raphael Moreno, Emmanuel Lellouch, Thierry Fouchet, Arielle Moullet, Thibault Cavalie
W15AE	Kinematics and a search for hierarchical structures within the B213-10 dense core	Anna Punanova, Jaime Pineda, Paola Caselli, Andy Pon
W15AH	Detecting the signature of nitrogen fractionation in ices	Victor de Souza Magalhaes, Alexandre Faure, Pierre Hily-Blant, Fabien Daniel
W15AI	Tracing Organic Nitrogen in Star Formation: Mapping HCN abundance in a Class I protostar	Thomas Rice, Edwin A. Bergin, Jes Jorgensen
W15AT	Disentangling outflows in massive star forming regions	Veronica Allen, Floris van der Tak, Riccardo Cesaroni, Maria Teresa Beltran, Alvaro Sanchez-Monge
W15AX	Imaging the water snowline in protostars with HCO^+	Ewine F. Van Dishoeck, Jes Jorgensen, Ruud Visser, Magnus Persson, Edwin A. Bergin, Daniel Harsono
W15BD	NOEMA imaging of a Young Solar System Analogue	Jean-Francois Lestrade, Sasha Hinkley, Grant Kennedy, Elisabeth Matthews, Wilner David, Jonathan P. Williams, Mark C. Wyatt, Brendan Bowler, Dimitri Mawet, Karl Stapelfeldt, D. Padgett
W15BL	The gaseous circumstellar environment of the red supergiant Mu Cep	Miguel Montarges, Arancha Castro-Carrizo, Valentin Bujarrabal, Jan Martin Winters, Pierre Kervella, Leen Decin, Andrea Chiavassa, Guy Perrin, Stephen Ridgway, Thibaut Le Bertre, Graham Harper, Iain McDonald, Xavier Haubois
W15BN	Imaging radioactive ^{26}AlF in the remnant of a stellar merger	Tomasz Kaminski, Karl M. Menten, Nimesh Patel, Romuald Tylenda, Jan Martin Winters
W15BR	Tracing Cloud Formation in a Spiral Arm	Erik Rosolowsky, Jonathan Braine, Eric Koch, Dario Colombo, Pierre Gratier, Frank Bertoldi, Sylvain Bontemps, Mederic Boquien, Christof Buchbender, D. Calzetti, Francoise Combes, Clare Dobbs, Santiago Garcia-Burillo, Carsten Kramer, Nicola Schneider, Paul van der Werf, Manolis Xilouris

Ident	Title of Investigations	Authors
W15CV	Molecular gas kinematics in H2-bright quenched elliptical galaxies	Quentin Salome, Philippe Salome, Pierre Guillard, Matthew Lehnert
W15DA	Constraining the cold accretion onto the most massive Black Holes	Philippe Salome, Michael Hogan, Alastair Edge, Brian McNamara, Stephen Hamer, Francoise Combes, Helen Russell, A.C. Fabian, Grant R. Tremblay
W15DB	NGC5044 - an extremely self-absorbed, low power AGN	Alastair Edge, Michael Hogan, Brian McNamara, Helen Russell, Philippe Salome, Francoise Combes, Keith Grainge
W15DI	Quenching via suppression of the efficiency of star formation in bulge rich spirals at z=0.5-1.5	Emanuele Daddi, Daizhong Liu, Fadia Salmi, Chiara Mancini, Sergio Martin Ruiz, Mark T. Sargent, Frederic Bournaud, Georgios Magdis, Matthieu Bethermin, Marie Martig, Francesco Valentino, Paola Dimauro, Marc Huertas-Company, Stephanie Juneau, David Elbaz, Mark Dickinson
W15DW	Tracing the molecular gas in strongly lensed starburst galaxies at z~2.5 using CI	Thomas R. Greve, Richard Tunnard, Thomas Bisbas, Serena Viti, Jeff Wagg, Stella Offner, Karen Olsen
W15DY	Probing Buried Nuclei Through Vibrationally-Excited HCN in Distant Dusty Starbursts	Dominik A. Riechers, Susanne Aalto, Roberto Neri, Eduardo Gonzalez-Alfonso
W15DZ	An exceptional intensively star forming proto-cluster candidate at z=2.36 selected from Planck	Herve Dole, Emanuele Daddi, Clement Martinache, Melanie Krips, Guilaine Lagache, Alexandre Beelen, Martin Giard, Douglas Scott, Sabine Koenig, Brenda Frye, Emeric Le Floc'h, Ranga-Ram Chary, Ruediger Kneissl, Etienne Pointecouteau, Bruno Altieri, Alessandro Rettura, Matthieu Bethermin, George Helou, Jean-Loup Puget, Lin Yan, Juan Macias-Perez, David Guery, Chentao Yang
W15EB	CI in the cold molecular halo of a z=2.6 radio galaxy	Bjorn Emonts, Montserrat Villar-Martin, Matthew Lehnert, Helmut Dannerbauer, Padelis Papadopoulos, Carlos De Breuck, Thomas Bisbas, Santiago Garcia-Burillo, R. Norris, Gustaaf van Moorsel, Luis Colina, Santiago Arribas
W15EF	1mm follow-up of Herschel-selected z>3 galaxies: resolving the multiplicity and securing the SEDs in the early Universe	Daizhong Liu, Emanuele Daddi, Georgios Magdis, Mark Dickinson, Hanae Inami, Qinghua Tan, Yu Gao, Mark T. Sargent, Matthieu Bethermin, Maurilio Pannella, Fabian Walter, Tao Wang, Xinwen Shu
W15EQ	H_2O^+ and OH^+ in high-z ULIRGs: diagnostic of their starburst, AGN and chemistry	Chentao Yang, Alain Omont, Eduardo Gonzalez-Alfonso, Paul van der Werf, Alexandre Beelen, Roberto Neri, R. Shane Bussmann, Pierre Cox, Ismael Perez-Fournon, Michel Guelin, Roberto Gavazzi, Yu Gao, Rob Ivison, Melanie Krips, Dominik A. Riechers
W15ET	Pinpointing the location of ultra-red submm galaxies at z>4	Melanie Krips, Ivan Oteo, Rob Ivison
W15FD	The ISM in QSOs at the epoch of reionization	Roberto Decarli, Fabian Walter, Bram Venemans, Eduardo Banados, Emanuele Paolo Farina, Dominik A. Riechers
GMVA-15A-MA002	Revealing the polarized fine structure of AGN Relativistic Jets with the GMVA	Antonio Alberdi Odriozola, Eduardo Ros, Thomas Krichbaum, Miguel Angel Perez-Torres, Juan-Maria Marcaide, Ivan Marti-Vidal, Jose Carlos Guirado
GMVA-15A-BL219	Imaging the biconical jet of M87 on scales of 3-100 Schwarzschild radii	Rusen Lu, Thomas Krichbaum, Sheperd Doeleman, Gopal Narajanan, Craig R. Walker, Jose L. Gomez, Keiichi Asada, Masanori Nakamura, Michael Bremer, Pablo de Vicente, Michael Lindqvist, Jonathan Leon-Tavares, Gisela Ortiz, Monika Moscibrodzka, Cornelia Mueller
GMVA-15B-098	SiO maser missed emission in AGB CSEs: extended component or weak maser clumps?	Alain Baudry, Francisco Colomer, Valentin Bujarrabal, Antonio Diaz, J. F. Desmurs, Javier Alcolea, Pablo de Vicente

Publications

The list of publications, conferences and workshop papers as well as thesis based upon data obtained using the IRAM instruments are provided in the following two tables. The first table gives the list of publications from the users' community, the second table gives the list of publications with the IRAM staff members, including technical publications.

USERS' COMMUNITY

2004	Cold gas in group-dominant elliptical galaxies	O'Sullivan E., Combes F., Hamer S., Salomé P., Babul A., Raychaudhury S.	2015, A&A 573, A111
2005	Fragmentation and kinematics of dense molecular cores in the filamentary infrared-dark cloud G011.11-0.12	Ragan S. E., Henning T., Beuther H., Linz H., Zahorecz S.	2015, A&A 573, A119
2006	Fast molecular jet from L1157-mm	Tafalla M., Bachiller R., Lefloch B., Rodríguez-Fernández N., Codella C., López-Sepulcre A., Podio L.	2015, A&A 573, L2
2007	New constraints on dust emission and UV attenuation of z = 6.5-7.5 galaxies from millimeter observations	Schaerer D., Boone F., Zamojski M., Staguhn J., Dessauges-Zavadsky M., Finkelstein S., Combes F.	2015, A&A 574, A19
2008	Jet-induced star formation in 3C 285 and Minkowski's Object	Salomé Q., Salomé P., Combes F.	2015, A&A 574, A34
2009	Molecular gas and nuclear activity in early-type galaxies: any link with radio loudness?	Baldi R. D., Giroletti M., Capetti A., Giovannini G., Casasola V., Pérez-Torres M. A., Kuno N.	2015, A&A 574, A65
2010	Brightness temperature constraints from interferometric visibilities	Lobanov A.	2015, A&A 574, A84
2011	Chains of dense cores in the Taurus L1495/B213 complex	Tafalla M., Hacar A.	2015, A&A 574, A104
2012	Polarization measurement analysis. I. Impact of the full covariance matrix on polarization fraction and angle measurements	Montier L., Plaszczynski S., Levrier F., Tristram M., Alina D., Ristorcelli I., Bernard J.-P.	2015, A&A 574, A135
2013	First detection of CF^+ towards a high-mass protostar	Fechtenbaum S., Bontemps S., Schneider N., Csengeri T., Duarte-Cabral A., Herpin F., Lefloch B.	2015, A&A 574, L4
2014	Can we trace very cold dust from its emission alone?	Pagani L., Lefèvre C., Juvela M., Pelkonen V.-M., Schuller F.	2015, A&A 574, L5
2015	Detection of a large fraction of atomic gas not associated with star-forming material in M17 SW*	Pérez-Beaupuits J. P., Stutzki J., Ossenkopf V., Spaans M., Güsten R., Wiesemeyer H.	2015, A&A 575, A9
2016	The chemistry and spatial distribution of small hydrocarbons in UV-irradiated molecular clouds: the Orion Bar PDR	Cuadrado S., Goicoechea J. R., Pilleri P., Cernicharo J., Fuente A., Joblin C.	2015, A&A 575, A82
2017	New N-bearing species towards OH 231.8+4.2. HNCO, HNCS, HC_3N, and NO	Velilla Prieto L., Sánchez Contreras C., Cernicharo J., Agúndez M., Quintana-Lacaci G., Alcolea J., Bujarrabal V., Herpin F., Menten K. M., Wyrowski F.	2015, A&A 575, A84
2018	Deuteration and evolution in the massive star formation process. The role of surface chemistry	Fontani F., Busquet G., Palau A., Caselli P., Sánchez-Monge Á., Tan J. C., Audard M.	2015, A&A 575, A87
2019	Detection of glycolaldehyde toward the solar-type protostar NGC 1333 IRAS2A	Coutens A., Persson M. V., Jørgensen J. K., Wampfler S. F., Lykke J. M.	2015, A&A 576, A5
2020	Complex organic molecules in organic-poor massive young stellar objects	Fayolle E. C., Öberg K. I., Garrod R. T., van Dishoeck E. F., Bisschop S. E.	2015, A&A 576, A45
2021	MAMBO image of the debris disk around ε Eridani: robustness of the azimuthal structure	Lestrade J.-F., Thilliez E.	2015, A&A 576, A72
2022	Physical properties of z>4 submillimeter galaxies in the COSMOS field	Smolčić V., Karim A., Miettinen O., Novak M., Magnelli B., Riechers D. A., Schinnerer E., Capak P., Bondi M., Ciliegi P., Aravena M., Bertoldi F., Bourke S., Banfield J., Carilli C. L., Civano F., Ilbert O., Intema H. T., Le Fèvre O., Finoguenov A., Hallinan G., Klöckner H.-R., Koekemoer A., Laigle C., Masters D., McCracken H. J., Mooley K., Murphy E., Navarette F., Salvato M., Sargent M., Sheth K., Toft S., Zamorani G.	2015, A&A 576, A127

2023	Antifreeze in the hot core of Orion. First detection of ethylene glycol in Orion-KL	Brouillet N., Despois D., Lu X.-H., Baudry A., Cernicharo J., Bockelée-Morvan D., Crovisier J., Biver N.	2015, A&A 576, A129
2024	Sulphur-bearing molecules in diffuse molecular clouds: new results from SOFIA/GREAT and the IRAM 30 m telescope	Neufeld D. A., Godard B., Gerin M., Pineau des Forêts G., Bernier C., Falgarone E., Graf U. U., Güsten R., Herbst E., Lesaffre P., Schilke P., Sonnentrucker P., Wiesemeyer H.	2015, A&A 577, A49
2025	Molecular gas content in strongly lensed z ~ 1.5-3 star-forming galaxies with low infrared luminosities	Dessauges-Zavadsky M., Zamojski M., Schaerer D., Combes F., Egami E., Swinbank A. M., Richard J., Sklias P., Rawle T. D., Rex M., Kneib J.-P., Boone F., Blain A.	2015, A&A 577, A50
2026	Molecular ions in the O-rich evolved star OH231.8+4.2: HCO^+, $H^{13}CO^+$ and first detection of SO^+, N_2H^+, and H_3O^+	Sánchez Contreras C., Velilla Prieto L., Agúndez M., Cernicharo J., Quintana-Lacaci G., Bujarrabal V., Alcolea J., Goicoechea J. R., Herpin F., Menten K. M., Wyrowski F.	2015, A&A 577, A52
2027	Laboratory millimeter wave spectrum and astronomical search for vinyl acetate	Kolesniková L., Peña I., Alonso J. L., Cernicharo J., Tercero B., Kleiner I.	2015, A&A 577, A91
2028	The resolved star-formation relation in nearby active galactic nuclei	Casasola V., Hunt L., Combes F., García-Burillo S.	2015, A&A 577, A135
2029	Mapping CS in starburst galaxies: Disentangling and characterising dense gas	Kelly G., Viti S., Bayet E., Aladro R., Yates J.	2015, A&A 578, A70
2030	Connection between inner jet kinematics and broadband flux variability in the BL Lacertae object S5 0716+714	Rani B., Krichbaum T. P., Marscher A. P., Hodgson J. A., Fuhrmann L., Angelakis E., Britzen S., Zensus J. A.	2015, A&A 578, A123
2031	Chemical evolution in the early phases of massive star formation. II. Deuteration	Gerner T., Shirley Y. L., Beuther H., Semenov D., Linz H., Albertsson T., Henning T.	2015, A&A 579, A80
2032	Fine-structure line deficit in S 140	Ossenkopf V., Koumpia E., Okada Y., Mookerjea B., van der Tak F. F. S., Simon R., Pütz P., Güsten R.	2015, A&A 580, A83
2033	Smoke in the Pipe Nebula: dust emission and grain growth in the starless core FeSt 1-457	Forbrich J., Lada C. J., Lombardi M., Román-Zúñiga C., Alves J.	2015, A&A 580, A114
2034	Infrared dark clouds on the far side of the Galaxy	Giannetti A., Wyrowski F., Leurini S., Urquhart J., Csengeri T., Menten K. M., Bronfman L., van der Tak F. F. S.	2015, A&A 580, L7
2035	Resolving the chemical substructure of Orion-KL	Feng S., Beuther H., Henning T., Semenov D., Palau A., Mills E. A. C.	2015, A&A 581, A71
2036	Hierarchical fragmentation and collapse signatures in a high-mass starless region	Beuther H., Henning T., Linz H., Feng S., Ragan S. E., Smith R. J., Bihr S., Sakai T., Kuiper R.	2015, A&A 581, A119
2037	Star and jet multiplicity in the high-mass star forming region IRAS 05137+3919	Cesaroni R., Massi F., Arcidiacono C., Beltrán M. T., Persi P., Tapia M., Molinari S., Testi L., Busoni L., Riccardi A., Boutsia K., Bisogni S., McCarthy D., Kulesa C.	2015, A&A 581, A124
2038	Ram pressure stripping in the Virgo Cluster	Verdugo C., Combes F., Dasyra K., Salomé P., Braine J.	2015, A&A 582, A6
2039	Restarting radio activity and dust emission in radio-loud broad absorption line quasars	Bruni G., Mack K.-H., Montenegro-Montes F. M., Brienza M., González-Serrano J. I.	2015, A&A 582, A9
2040	Tentative detection of ethylene glycol toward W51/e2 and G34.3+0.2 ***	Lykke J. M., Favre C., Bergin E. A., Jørgensen J. K.	2015, A&A 582, A64
2041	Optical and radio variability of BL Lacertae	Gaur H., Gupta A. C., Bachev R., Strigachev A., Semkov E., Wiita P. J., Volvach A. E., Gu M. F., Agarwal A., Agudo I., Aller M. F., Aller H. D., Kurtanidze O. M., Kurtanidze S. O., Lähteenmäki A., Peneva S., Nikolashvili M. G., Sigua L. A., Tornikoski M., Volvach L. N.	2015, A&A 582, A103
2042	Searching for trans ethyl methyl ether in Orion KL*	Tercero B., Cernicharo J., López A., Brouillet N., Kolesniková L., Motiyenko R. A., Margulès L., Alonso J. L., Guillemin J.-C.	2015, A&A 582, L1
2043	Hyperfine structure of the cyanomethyl radical (CH_2CN) in the L1544 prestellar core	Vastel C., Yamamoto S., Lefloch B., Bachiller R.	2015, A&A 582, L3
2044	Disentangling the excitation conditions of the dense gas in M17 SW	Pérez-Beaupuits J. P., Güsten R., Spaans M., Ossenkopf V., Menten K. M., Requena-Torres M. A., Wiesemeyer H., Stutzki J., Guevara C., Simon R.	2015, A&A 583, A107
2045	Molecular depletion times and the CO-to-H_2 conversion factor in metal-poor galaxies	Hunt L. K., García-Burillo S., Casasola V., Caselli P., Combes F., Henkel C., Lundgren A., Maiolino R., Menten K. M., Testi L., Weiss A.	2015, A&A 583, A114
2046	Filament fragmentation in high-mass star formation	Beuther H., Ragan S. E., Johnston K., Henning T., Hacar A., Kainulainen J. T.	2015, A&A 584, A67
2047	Excitation Conditions in the Multi-component Submillimeter Galaxy SMM J00266+1708	Sharon C. E., Baker A. J., Harris A. I., Tacconi L. J., Lutz D., Longmore S. N.	2015, ApJ 798, 133

2048	The Kiloparsec-scale Star Formation Law at Redshift 4: Widespread, Highly Efficient Star Formation in the Dust-obscured Starburst Galaxy GN20	Hodge J. A., Riechers D., Decarli R., Walter F., Carilli C. L., Daddi E., Dannerbauer H.	2015, ApJ 798, L18
2049	Dust Continuum Emission as a Tracer of Gas Mass in Galaxies	Groves B. A., Schinnerer E., Leroy A., Galametz M., Walter F., Bolatto A., Hunt L., Dale D., Calzetti D., Croxall K., Kennicutt R., Jr.	2015, ApJ 799, 96
2050	High-lying OH Absorption, [C II] Deficits, and Extreme L_{FIR}/M_{H2} Ratios in Galaxies	González-Alfonso E., Fischer J., Sturm E., Graciá-Carpio J., Veilleux S., Meléndez M., Lutz D., Poglitsch A., Aalto S., Falstad N., Spoon H. W. W., Farrah D., Blasco A., Henkel C., Contursi A., Verma A., Spaans M., Smith H. A., Ashby M. L. N., Hailey-Dunsheath S., García-Burillo S., Martín-Pintado J., van der Werf P., Meijerink R., Genzel R.	2015, ApJ 800, 69
2051	Discovery of Large Molecular Gas Reservoirs in Post-starburst Galaxies	French K. D., Yang Y., Zabludoff A., Narayanan D., Shirley Y., Walter F., Smith J.-D., Tremonti C. A.	2015, ApJ 801, 1
2052	Spectroscopic Confirmation of an Ultra Massive and Compact Galaxy at z = 3.35: a Detailed Look at an Early Progenitor of Local Giant Ellipticals	Marsan Z. C., Marchesini D., Brammer G. B., Stefanon M., Muzzin A., Fernández-Soto A., Geier S., Hainline K. N., Intema H., Karim A., Labbé I., Toft S., van Dokkum P. G.	2015, ApJ 801, 133
2053	Methanol in the Starless Core, Taurus Molecular Cloud-1	Soma T., Sakai N., Watanabe Y., Yamamoto S.	2015, ApJ 802, 74
2054	Assessing Molecular Outflows and Turbulence in the Protostellar Cluster Serpens South	Plunkett A. L., Arce H. G., Corder S. A., Dunham M. M., Garay G., Mardones D.	2015, ApJ 803, 22
2055	The Weak Carbon Monoxide Emission in an Extremely Metal-poor Galaxy, Sextans A	Shi Y., Wang J., Zhang Z.-Y., Gao Y., Armus L., Helou G., Gu Q., Stierwalt S.	2015, ApJ 804, L11
2056	An Unbiased 1.3 mm Emission Line Survey of the Protoplanetary Disk Orbiting LkCa 15	Punzi K. M., Hily-Blant P., Kastner J. H., Sacco G. G., Forveille T.	2015, ApJ 805, 147
2057	Bright [C II] 158 μm Emission in a Quasar Host Galaxy at z = 6.54	Bañados E., Decarli R., Walter F., Venemans B. P., Farina E. P., Fan X.	2015, ApJ 805, L8
2058	The Kinematic and Chemical Properties of a Potential Core-forming Clump: Perseus B1-E	Sadavoy S. I., Shirley Y., Di Francesco J., Henning T., Currie M. J., André P., Pezzuto S.	2015, ApJ 806, 38
2059	Abundance Anomaly of the ^{13}C Isotopic Species of c-C_3H_2 in the Low-mass Star Formation Region L1527	Yoshida K., Sakai N., Tokudome T., López-Sepulcre A., Watanabe Y., Takano S., Lefloch B., Ceccarelli C., Bachiller R., Caux E., Vastel C., Yamamoto S.	2015, ApJ 807, 66
2060	HNC in Protoplanetary Disks	Graninger D., Öberg K. I., Qi C., Kastner J.	2015, ApJ 807, L15
2061	Scaling Relations of the Properties for CO Resolved Structures in Nearby Spiral Galaxies	Rebolledo D., Wong T., Xue R., Leroy A., Koda J., Donovan Meyer J.	2015, ApJ 808, 99
2062	Resolving the Merging Planck Cluster PLCK G147.3-16.6 with GISMO	Mroczkowski T., Kovács A., Bulbul E., Staguhn J., Benford D. J., Clarke T. E., van Weeren R. J., Intema H. T., Randall S.	2015, ApJ 808, L6
2063	First Measurements of ^{15}N Fractionation in N_2H^+ toward High-mass Star-forming Cores	Fontani F., Caselli P., Palau A., Bizzocchi L., Ceccarelli C.	2015, ApJ 808, L46
2064	The Disk-outflow System in the S255IR Area of High-mass Star Formation	Zinchenko I., Liu S.-Y., Su Y.-N., Salii S. V., Sobolev A. M., Zemlyanukha P., Beuther H., Ojha D. K., Samal M. R., Wang Y.	2015, ApJ 810, 10
2065	Spatially Resolved Dense Molecular Gas and Star Formation Rate in M51	Chen H., Gao Y., Braine J., Gu Q.	2015, ApJ 810, 140
2066	Faint CO Line Wings in Four Star-forming (Ultra)luminous Infrared Galaxies	Leroy A. K., Walter F., Decarli R., Bolatto A., Zschaechner L., Weiss A.	2015, ApJ 811, 15
2067	Submillimeter Observations of CLASH 2882 and the Evolution of Dust in this Galaxy	Dwek E., Staguhn J., Arendt R. G., Kovács A., Decarli R., Egami E., MichaŃowski M. J., Rawle T. D., Toft S., Walter F.	2015, ApJ 813, 119
2068	Excitation Mechanisms for HCN (1-0) and HCO^+ (1-0) in Galaxies from the Great Observatories All-sky LIRG Survey	Privon G. C., Herrero-Illana R., Evans A. S., Iwasawa K., Perez-Torres M. A., Armus L., Díaz-Santos T., Murphy E. J., Stierwalt S., Aalto S., Mazzarella J. M., Barcos-Muñoz L., Borish H. J., Inami H., Kim D.-C., Treister E., Surace J. A., Lord S., Conway J., Frayer D. T., Alberdi A.	2015, ApJ 814, 39
2069	Discovery of Molecular Gas around HD 131835 in an APEX Molecular Line Survey of Bright Debris Disks	Moór A., Henning T., Juhász A., Ábrahám P., Balog Z., Kóspál Á., Pascucci I., Szabó G. M., Vavrek R., Curé M., Csengeri T., Grady C., Güsten R., Kiss C.	2015, ApJ 814, 42
2070	Isotopic Ratios of $^{18}O/^{17}O$ in the Galactic Central Region	Zhang J. S., Sun L. L., Riquelme D., Henkel C., Lu D. R., Zhang Y., Wang J. Z., Wang M., Li J.	2015, ApJS 219, 28
2071	The density structure of the L1157 molecular outflow	Gómez-Ruiz A. I., Codella C., Lefloch B., Benedettini M., Busquet G., Ceccarelli C., Nisini B., Podio L., Viti S.	2015, MNRAS 446, 3346

2072	The evolution of the cold interstellar medium in galaxies following a starburst	Rowlands K., Wild V., Nesvadba N., Sibthorpe B., Mortier A., Lehnert M., da Cunha E.	2015, MNRAS 448, 258
2073	Tracing cool molecular gas and star formation on ~ 100 pc scales within a z ~ 2.3 galaxy	Thomson A. P., Ivison R. J., Owen F. N., Danielson A. L. R., Swinbank A. M., Smail I.	2015, MNRAS 448, 1874
2074	Characterizing extragalactic anomalous microwave emission in NGC 6946 with CARMA	Hensley B., Murphy E., Staguhn J.	2015, MNRAS 449, 809
2075	Shedding light on the formation of the pre-biotic molecule formamide with ASAI	López-Sepulcre A., Jaber A. A., Mendoza E., Lefloch B., Ceccarelli C., Vastel C., Bachiller R., Cernicharo J., Codella C., Kahane C., Kama M., Tafalla M.	2015, MNRAS 449, 2438
2076	Molecular and atomic gas in dust lane early-type galaxies - I. Low star formation efficiencies in minor merger remnants	Davis T. A., Rowlands K., Allison J. R., Shabala S. S., Ting Y.-S., Lagos C. d. P., Kaviraj S., Bourne N., Dunne L., Eales S., Ivison R. J., Maddox S., Smith D. J. B., Smith M. W. L., Temi P.	2015, MNRAS 449, 3503
2077	Synchrotron spectral index and interstellar medium densities of star-forming galaxies	Basu A., Beck R., Schmidt P., Roy S.	2015, MNRAS 449, 3879
2078	Astrochemistry at work in the L1157-B1 shock: acetaldehyde formation	Codella C., Fontani F., Ceccarelli C., Podio L., Viti S., Bachiller R., Benedettini M., Lefloch B.	2015, MNRAS 449, L11
2079	A blind CO detection of a distant red galaxy in the HS1700+64 protocluster	Chapman S. C., Bertoldi F., Smail I., Blain A. W., Geach J. E., Gurwell M., Ivison R. J., Petitpas G. R., Reddy N., Steidel C. C.	2015, MNRAS 449, L68
2080	The JCMT Gould Belt Survey: first results from the SCUBA-2 observations of the Ophiuchus molecular cloud and a virial analysis of its prestellar core population	Pattle K., Ward-Thompson D., Kirk J. M., White G. J., Drabek-Maunder E., Buckle J., Beaulieu S. F., Berry D. S., Broekhoven-Fiene H., Currie M. J., Fich M., Hatchell J., Kirk H., Jenness T., Johnstone D., Mottram J. C., Nutter D., Pineda J. E., Quinn C., Salji C., Tisi S., Walker-Smith S., Francesco J. D., Hogerheijde M. R., André P., Bastien P., Bresnahan D., Butner H., Chen M., Chrysostomou A., Coude S., Davis C. J., Duarte-Cabral A., Fiege J., Friberg P., Friesen R., Fuller G. A., Graves S., Greaves J., Gregson J., Griffin M. J., Holland W., Joncas G., Knee L. B. G., Könyves V., Mairs S., Marsh K., Matthews B. C., Moriarty-Schieven G., Rawlings J., Richer J., Robertson D., Rosolowsky E., Rumble D., Sadavoy S., Spinoglio L., Thomas H., Tothill N., Viti S., Wouterloot J., Yates J., Zhu M.	2015, MNRAS 450, 1094
2081	The variation in molecular gas depletion time among nearby galaxies - II. The impact of galaxy internal structures	Huang M.-L., Kauffmann G.	2015, MNRAS 450, 1375
2082	Multiwavelength behaviour of the blazar OJ 248 from radio to γ-rays	Carnerero M. I., Raiteri C. M., Villata M., Acosta-Pulido J. A., D'Ammando F., Smith P. S., Larionov V. M., Agudo I., Arévalo M. J., Arkharov A. A., Bach U., Bachev R., Benítez E., Blinov D. A., Bozhilov V., Buemi C. S., Bueno Bueno A., Carosati D., Casadio C., Chen W. P., Damljanovic G., Paola A. D., Efimova N. V., Ehgamberdiev S. A., Giroletti M., Gómez J. L., González-Morales P. A., Grinon-Marin A. B., Grishina T. S., Gurwell M. A., Hiriart D., Hsiao H. Y., Ibryamov S., Jorstad S. G., Joshi M., Kopatskaya E. N., Kurtanidze O. M., Kurtanidze S. O., Lähteenmäki A., Larionova E. G., Larionova L. V., Lázaro C., Leto P., Lin C. S., Lin H. C., Manilla-Robles A. I., Marscher A. P., McHardy I. M., Metodieva Y., Mirzaqulov D. O., Mokrushina A. A., Molina S. N., Morozova D. A., Nikolashvili M. G., Orienti M., Ovcharov E., Panwar N., Pastor Yabar A., Puerto Giménez I., Ramakrishnan V., Richter G. M., Rossini M., Sigua L. A., Strigachev A., Taylor B., Tornikoski M., Trigilio C., Troitskaya Y. V., Troitsky I. S., Umana G., Valcheva A., Velasco S., Vince O., Wehrle A. E., Wiesemeyer H.	2015, MNRAS 450, 2677
2083	Hyperfine transitions of ^{13}CN from pre-protostellar sources	Flower D. R., Hily-Blant P.	2015, MNRAS 452, 19
2084	Highly perturbed molecular gas in infalling cluster galaxies: the case of CGCG97-079	Scott T. C., Usero A., Brinks E., Bravo-Alfaro H., Cortese L., Boselli A., Argudo-Fernández M.	2015, MNRAS 453, 328
2085	A millimetre-wave redshift search for the unlensed HyLIRG, HS1700.850.1	Chapman S. C., Bertoldi F., Smail I., Steidel C. C., Blain A. W., Geach J. E., Gurwell M., Ivison R. J., Petitpas G. R., Reddy N.	2015, MNRAS 453, 951
2086	High radio-frequency properties and variability of brightest cluster galaxies	Hogan M. T., Edge A. C., Geach J. E., Grainge K. J. B., Hlavacek-Larrondo J., Hovatta T., Karim A., McNamara B. R., Rumsey C., Russell H. R., Salomé P., Aller H. D., Aller M. F., Benford D. J., Fabian A. C., Readhead A. C. S., Sadler E. M., Saunders R. D. E.	2015, MNRAS 453, 1223
2087	A molecular scan in the Hubble Deep Field North	Decarli R., Walter F., Carilli C., Riechers D.	2015, IAUS 309, 265
2088	Spatially Extended and High-Velocity Dispersion Molecular Component in Spiral Galaxies: Single-Dish Versus Interferometric Observations	Caldú-Primo A., Schruba A., Walter F., Leroy A., Bolatto A. D., Vogel S.	2015, AJ 149, 76
2089	AGN feedback and jet-induced star formation	Salomé Q., Salomé P., Combes F., Hamer S.	2015, sf2a conf. 441
2090	Water and complex organic molecules in the warm inner regions of solar-type protostars	Coutens A., Jørgensen J. K., Persson M. V., Lykke J. M., Taquet V., van Dishoeck E. F., Vastel C., Wampfler S. F.	2015, sf2a conf. 437

2091	Follow-Up Observations Toward Planck Cold Clumps with Ground-Based Radio Telescopes	Liu T., Wu Y., Mardones D., Kim K.-T., Menten K. M., Tatematsu K., Cunningham M., Juvela M., Zhang Q., Goldsmith P. F., Liu S.-Y., Zhang H.-W., Meng F., Li D., Lo N., Guan X., Yuan J., Belloche A., Henkel C., Wyrowski F., Garay G., Ristorcelli I., Lee J.-E., Wang K., Bronfman L., Toth L. V., Schnee S., Qin S., Akhter S.	2015, PKAS 30, 79
2092	Dection of [CII] emission not associated with star-forming material in giant molecular clouds	Perez-Beaupuits J.-P.	2015, IAU Gen. Ass. 22, 2258547
2093	Spatially-resolved dust, molecular gas, and star formation maps of an exceptional strongly lensed giant arc at *z*=2	Schaerer D., Nakajima K., Dessauges-Zavadsky M., Walth G., Rujopakarn W., Richard J., Egami E.	2015, IAU Gen. Ass. 22, 2258419
2094	Coeval observations of a complete sample of flat-spectrum blazars with Effelsberg, IRAM 30m, and Planck	Rachen J. P., Fuhrmann L.	2015, IAU Gen. Ass. 22, 2258130
2095	Tracing the origin of warm water emission through the stages of low-mass star formation	Vilhelm Persson M., Jorgensen J. K., Coutens A., van Dishoeck E.	2015, IAU Gen. Ass. 22, 2258124
2096	Deep 2mm Surveys with GISMO : Searching for submillimeter galaxies at the highest redshifts	Staguhn J. G., Kovacs A., Karim A., Arendt R., Benford D. J., Decarli R., Dwek E., Fixsen D., Gene H., Irwin K., Moseley S. H., Sharp E., Walter F., Edward W.	2015, IAU Gen. Ass. 22, 2257764
2097	Filaments, ridges and the origin of high-mass stars and clusters in Cygnus X	Bontemps S., Schneider N., Motte F.	2015, IAU Gen. Ass. 22, 2257007
2098	Outflows Driven by a Potential Proto-Brown Dwarf Binary System IRAS 16253-2429	Hsieh T.-H., Lai S.-P., Belloche A., Wyrowski F.	2015, IAU Gen. Ass. 22, 2256664
2099	z>4 low luminosity dusty galaxy candidates in the Frontier Fields A2744, AS1063 and A370	Boone F., Schaerer D., Richard J., Clement B., Egami E., Rawle T., Lutz D., Weiss A., Staguhn J. G., Dessauges-Zavadsky M., Kneib J.-P., Combes F., Smail I., HLS Team	2015, IAU Gen. Ass. 22, 2256581
2100	Water, ammonia, methanol and complex molecules in the earliest phases of star formation	Caselli P.	2015, IAU Gen. Ass. 22, 2256481
2101	Molecular gas, stars, and dust in sub-L* star-forming galaxies at z~2: evidence for universal star formation and nonuniversal dust-to-gas ratio	Dessauges-Zavadsky M., Schaerer D., Combes F., Egami E., Swinbank A. M., Richard J., Sklias P., Rawle T. D.	2015, IAU Gen. Ass. 22, 2255083
2102	Gas kinematics of Lyman Alpha Blobs at *z*=2-3	Yang Y.	2015, IAU Gen. Ass. 22, 2254746
2103	Circumstellar molecular gas in extremely young planetary nebulae	Uscanga L., Rizzo J. R., Miranda L. F., Gomez J. F., Boumis P., Rodriguez M. I., Suarez O.	2015, IAU Gen. Ass. 22, 2253372
2104	Probing the water and CO snow lines in the young protostar NGC 1333-IRAS4B	Anderl S., Maret S., André P., Maury A., Belloche A., Cabrit S., Codella C., Lefloch B.	2015, IAU Gen. Ass. 22, 2252947
2105	New emerging results on molecular gas, stars, and dust at z~2, as revealed by low star formation rate and low stellar mass star-forming galaxies	Dessauges-Zavadsky M., Schaerer D., Combes F., Egami E., Swinbank M., Richard J., Sklias P., Rawle T. D.	2015, IAU Gen. Ass. 22, 2252304
2106	The ASAI View on our Chemical Origins	Lopez-Sepulcre A., Mendoza E., Lefloch B., Bachiller R., Ceccarelli C., Codella C., Boechat-Roberty H. M., vastel c., Cernicharo J.	2015, IAU Gen. Ass. 22, 2250928
2107	Water in the warm inner regions of Class 0 protostars	Coutens A., Jørgensen J. K., Persson M. V., van Dishoeck E., vastel c., Taquet V., Bottinelli S., Caux E., Harsono D., Lykke J. M.	2015, IAU Gen. Ass. 22, 2249617
2108	Pre-biotic molecules in shocks: the case of L1157	Mendoza E., Lefloch B., López-Sepulcre A., Ceccarelli C., Codella C., Boechat-Roberty H. M., Bachiller R.	2015, IAU Gen. Ass. 22, 2248299
2109	A higher efficiency of converting gas to stars in high-redshift starburst galaxies with ALMA and PdBI	Silverman J. D.	2015, IAU Gen. Ass. 22, 2246377
2110	Excitation Mechanisms for HCN (1-0) and HCO^+ (1-0) in Galaxies from the Great Observatories All-sky LIRG Survey	Privon G., Herrero-Illana R., Evans A., Iwasawa K., Perez-Torres M., Armus L., Diaz-Santos T., Murphy E., Stierwalt S., Aalto S., Mazzarella J., Barcos-Muñoz L., Borish J., Inami H., Kim D., Treister E., Surace J., Lord S., Conway J., Frayer D., Alberdi A.	2015, IAU Gen. Ass. 22, 2239308
2111	The IRAM 30m Nearby Galaxy Dense Gas Survey	Bigiel F.	2015, IAU Gen. Ass. 22, 2228516
2112	Maser emission of the most abundant SiO isotopomers in O-rich stars	Rizzo J. R., García Miró C., Cernicharo J.	2015, hsa8.conf 553
2113	The off-axis jet structure in Mrk 501 at mm-wavelengths	Koyama S., Kino M., Giroletti M., Doi A., Nagai H., Hada K., Niinuma K., Orienti M., Giovannini G., Ros E., Savolainen T., Pérez-Torres M. A., Krichbaum T. P.	2015, arXiv:1505.04433

2114	Herschel and IRAM-30m Observations of Comet C/2012 S1 (ISON) at 4.5 AU from the Sun	O'Rourke L., Bockelée-Morvan D., Biver N., Altieri B., Teyssier D., Jorda L., Debout V., Snodgrass C., Küppers M., A'Hearn M., Müller T., Farnham A.	2015, EGUGA 17, 14470
2115	Dust emission from the atomic and molecular gas in M 33: a changing β	Braine J., Tabatabaei F., Xilouris M.	2015, HiA 16, 617
2116	Molecular cloud structure and star formation in the W43 complex	Carlhoff P., Schilke P., Motte F., Nguyen-Luong Q.	2015, HiA 16, 592
2117	Molecular Outflows Driven by Young Brown Dwarfs And VLMs. New Clues from IRAM Interferometer Observations	Monin J.-L., Whelan E., Lefloch B., Dougados C.	2015, csss 18, 555
2118	EVLA Observation of Centimeter Continuum Emission from Protostars in Serpens South	Kern N. S., Tobin J. J., Keown J. A., Gutermuth R. A.	2015, AAS 225, 348.10
2119	High-resolution dust emission and the resolved star formation law in the z~4 submillimeter galaxy GN20	Hodge J., Riechers D. A., Decarli R., Walter F., Carilli C. L., Daddi E., Dannerbauer H.	2015, AAS 225, 251.11
2120	Triggered star-formation in the bright rimmed globule IC1396A	Patel N. A., Sicilia-Aguilar A., Goldsmith P.	2015, AAS 225, 211.03
2121	CO Line Ratios in Nearby Galaxies	Rosolowsky E., Leroy A. K., Usero A., Loeppky J., Walter F., Wilson C., Heracles Team N. T.	2015, AAS 225, 141.25
2122	Zooming into γ-ray loud galactic nuclei: broadband emission and structure dynamics of the blazar PKS 1502+106 and the narrow-line Seyfert 1 1H 0323+342	Karamanavis V.	2015, Thesis (University of Cologne, Germany)
2123	Study at radio wavelengths of circumstellar envelopes around red giants	Do Thi Hoai	2015, Thesis (Obs.de Paris, France, and Inst. of Physics, Hanoi, Vietnam)

IRAM (CO) AUTHORS

1980	Very extended cold gas, star formation and outflows in the halo of a bright quasar at z>6	Cicone C., Maiolino R., Gallerani S., Neri R., Ferrara A., Sturm E., Fiore F., Piconcelli E., Feruglio C.	2015, A&A 574, A14
1981	High resolution observations of HCN and HCO^+ J = 3-2 in the disk and outflow of Mrk 231. Detection of vibrationally excited HCN in the warped nucleus	Aalto S., Garcia-Burillo S., Muller S., Winters J. M., Gonzalez-Alfonso E., van der Werf P., Henkel C., Costagliola F., Neri R.	2015, A&A 574, A85
1982	Multimolecule ALMA observations toward the Seyfert 1 galaxy NGC 1097	Martín S., Kohno K., Izumi T., Krips M., Meier D. S., Aladro R., Matsushita S., Takano S., Turner J. L., Espada D., Nakajima T., Terashima Y., Fathi K., Hsieh P.-Y., Imanishi M., Lundgren A., Nakai N., Schinnerer E., Sheth K., Wiklind T.	2015, A&A 573, A116
1983	Chemistry in disks. IX. Observations and modelling of HCO^+ and DCO^+ in DM Tauri	Teague R., Semenov D., Guilloteau S., Henning T., Dutrey A., Wakelam V., Chapillon E., Pietu V.	2015, A&A 574, A137
1984	The hidden quasar nucleus of a WISE-selected, hyperluminous, dust-obscured galaxy at z ~ 2.3	Piconcelli E., Vignali C., Bianchi S., Zappacosta L., Fritz J., Lanzuisi G., Miniutti G., Bongiorno A., Feruglio C., Fiore F., Maiolino R.	2015, A&A 574, L9
1985	Properties of flat-spectrum radio-loud narrow-line Seyfert 1 galaxies	Foschini L., Berton M., Caccianiga A., Ciroi S., Cracco V., Peterson B. M., Angelakis E., Braito V., Fuhrmann L., Gallo L., Grupe D., Järvelä E., Kaufmann S., Komossa S., Kovalev Y. Y., Lähteenmäki A., Lisakov M. M., Lister M. L., Mathur S., Richards J. L., Romano P., Sievers A., Tagliaferri G., Tammi J., Tibolla O., Tornikoski M., Vercellone S., La Mura G., Maraschi L., Rafanelli P.	2015, A&A 575, A13
1986	Radio jet emission from GeV-emitting narrow-line Seyfert 1 galaxies	Angelakis E., Fuhrmann L., Marchili N., Foschini L., Myserlis I., Karamanavis V., Komossa S., Blinov D., Krichbaum T. P., Sievers A., Ungerechts H., Zensus J. A.	2015, A&A 575, A55
1987	Heating and cooling of the neutral ISM in the NGC 4736 circumnuclear ring	van der Laan T. P. R., Armus L., Beirao P., Sandstrom K., Groves B., Schinnerer E., Draine B. T., Smith J. D., Galametz M., Wolfire M., Croxall K., Dale D., Herrera Camus R., Calzetti D., Kennicutt R. C.	2015, A&A 575, A83
1988	Molecular shells in IRC+10216: tracing the mass loss history	Cernicharo J., Marcelino N., Agúndez M., Guélin M.	2015, A&A 575, A91
1989	A low-luminosity type-1 QSO sample. II. Tracing circumnuclear star formation in HE 1029-1831 with SINFONI	Busch G., Smajić S., Scharwächter J., Eckart A., Valencia-S. M., Moser L., Husemann B., Krips M., Zuther J.	2015, A&A 575, A128

1990	Detection of Keplerian dynamics in a disk around the post-AGB star AC Herculis	Bujarrabal V., Castro-Carrizo A., Alcolea J., Van Winckel H.	2015, A&A 575, L7
1991	Pressure distribution of the high-redshift cluster of galaxies CL J1226.9+3332 with NIKA	Adam R., Comis B., Macías-Pérez J.-F., Adane A., Ade P., André P., Beelen A., Belier B., Benoît A., Bideaud A., Billot N., Blanquer G., Bourrion O., Calvo M., Catalano A., Coiffard G., Cruciani A., D'Addabbo A., Désert F.-X., Doyle S., Goupy J., Kramer C., Leclercq S., Martino J., Mauskopf P., Mayet F., Monfardini A., Pajot F., Pascale E., Perotto L., Pointecouteau E., Ponthieu N., Revéret V., Ritacco A., Rodriguez L., Savini G., Schuster K., Sievers A., Tucker C., Zylka R.	2015, A&A 576, A12
1992	Passive galaxies as tracers of cluster environments at z ~ 2	Strazzullo V., Daddi E., Gobat R., Garilli B., Mignoli M., Valentino F., Onodera M., Renzini A., Cimatti A., Finoguenov A., Arimoto N., Cappellari M., Carollo C. M., Feruglio C., Le Floc'h E., Lilly S. J., Maccagni D., McCracken H. J., Moresco M., Pozzetti L., Zamorani G.	2015, A&A 576, L6
1993	No asymmetric outflows from Sagittarius A* during the pericenter passage of the gas cloud G2	Park J.-H., Trippe S., Krichbaum T. P., Kim J.-Y., Kino M., Bertarini A., Bremer M., de Vicente P.	2015, A&A 576, L16
1994	(Sub)millimetre interferometric imaging of a sample of COSMOS/AzTEC submillimetre galaxies. I. Multiwavelength identifications and redshift distribution	Miettinen O., Smolčić V., Novak M., Aravena M., Karim A., Masters D., Riechers D. A., Bussmann R. S., McCracken H. J., Ilbert O., Bertoldi F., Capak P., Feruglio C., Halliday C., Kartaltepe J. S., Navarrete F., Salvato M., Sanders D., Schinnerer E., Sheth K.	2015, A&A 577, A29
1995	CO excitation of normal star-forming galaxies out to z = 1.5 as regulated by the properties of their interstellar medium	Daddi E., Dannerbauer H., Liu D., Aravena M., Bournaud F., Walter F., Riechers D., Magdis G., Sargent M., Béthermin M., Carilli C., Cibinel A., Dickinson M., Elbaz D., Gao Y., Gobat R., Hodge J., Krips M.	2015, A&A 577, A46
1996	Nascent bipolar outflows associated with the first hydrostatic core candidates Barnard 1b-N and 1b-S	Gerin M., Pety J., Fuente A., Cernicharo J., Commerçon B., Marcelino N.	2015, A&A 577, L2
1997	Discovery of interstellar ketenyl (HCCO), a surprisingly abundant radical	Agúndez M., Cernicharo J., Guélin M.	2015, A&A 577, L5
1998	Measuring star formation with resolved observations: the test case of M 33	Boquien M., Calzetti D., Aalto S., Boselli A., Braine J., Buat V., Combes F., Israel F., Kramer C., Lord S., Relaño M., Rosolowsky E., Stacey G., Tabatabaei F., van der Tak F., van der Werf P., Verley S., Xilouris M.	2015, A&A 578, A8
1999	Evidence for feedback in action from the molecular gas content in the z ~ 1.6 outflowing QSO XID2028	Brusa M., Feruglio C., Cresci G., Mainieri V., Sargent M. T., Perna M., Santini P., Vito F., Marconi A., Merloni A., Lutz D., Piconcelli E., Lanzuisi G., Maiolino R., Rosario D., Daddi E., Bongiorno A., Fiore F., Lusso E.	2015, A&A 578, A11
2000	Sensitive survey for ^{13}CO, CN, H_2CO, and SO in the disks of T Tauri and Herbig Ae stars. II. Stars in Þ Ophiuchi and upper Scorpius	Reboussin L., Guilloteau S., Simon M., Grosso N., Wakelam V., Di Folco E., Dutrey A., Piétu V.	2015, A&A 578, A31
2001	Chemical footprint of star formation feedback in M 82 on scales of ~100 pc	Ginard D., Fuente A., García-Burillo S., Alonso-Albi T., Krips M., Gerin M., Neri R., Pilleri P., Usero A., Treviño-Morales S. P.	2015, A&A 578, A49
2002	The dust disk and companion of the nearby AGB star L Puppis. SPHERE/ZIMPOL polarimetric imaging at visible wavelengths	Kervella P., Montargès M., Lagadec E., Ridgway S. T., Haubois X., Girard J. H., Ohnaka K., Perrin G., Gallenne A.	2015, A&A 578, A77
2003	Chemical composition of the circumstellar disk around AB Aurigae	Pacheco-Vázquez S., Fuente A., Agúndez M., Pinte C., Alonso-Albi T., Neri R., Cernicharo J., Goicoechea J. R., Berné O., Wiesenfeld L., Bachiller R., Lefloch B.	2015, A&A 578, A81
2004	Widespread galactic CF^+ absorption: detection toward W49 with the Plateau de Bure Interferometer	Liszt H. S., Guzmán V. V., Pety J., Gerin M., Neufeld D. A., Gratier P.	2015, A&A 579, A12
2005	Lambda = 3 mm line survey of nearby active galaxies	Aladro R., Martín S., Riquelme D., Henkel C., Mauersberger R., Martín-Pintado J., Weiß A., Lefevre C., Kramer C., Requena-Torres M. A., Armijos-Abendaño R. J.	2015, A&A 579, A101
2006	Probing non-polar interstellar molecules through their protonated form: Detection of protonated cyanogen ($NCCNH^+$)	Agúndez M., Cernicharo J., de Vicente P., Marcelino N., Roueff E., Fuente A., Gerin M., Guélin M., Albo C., Barcia A., Barbas L., Bolaño R., Colomer F., Diez M. C., Gallego J. D., Gómez-González J., López-Fernández I., López-Fernández J. A., López-Pérez J. A., Malo I., Serna J. M., Tercero F.	2015, A&A 579, L10
2007	High-resolution imaging of the molecular outflows in two mergers: IRAS 17208-0014 and NGC 1614	García-Burillo S., Combes F., Usero A., Aalto S., Colina L., Alonso-Herrero A., Hunt L. K., Arribas S., Costagliola F., Labiano A., Neri R., Pereira-Santaella M., Tacconi L. J., van der Werf P. P.	2015, A&A 580, A35
2008	Temperatures of dust and gas in S 140	Koumpia E., Harvey P. M., Ossenkopf V., van der Tak F. F. S., Mookerjea B., Fuente A., Kramer C.	2015, A&A 580, A68
2009	Ionised outflows in z ~ 2.4 quasar host galaxies	Carniani S., Marconi A., Maiolino R., Balmaverde B., Brusa M., Cano-Díaz M., Cicone C., Comastri A., Cresci G., Fiore F., Feruglio C., La Franca F., Mainieri V., Mannucci F., Nagao T., Netzer H., Piconcelli E., Risaliti G., Schneider R., Shemmer O.	2015, A&A 580, A102

2010	The structure of the Cepheus E protostellar outflow: The jet, the bowshock, and the cavity	Lefloch B., Gusdorf A., Codella C., Eislöffel J., Neri R., Gómez-Ruiz A. I., Güsten R., Leurini S., Risacher C., Benedettini M.	2015, A&A 581, A4
2011	First 230 GHz VLBI fringes on 3C 279 using the APEX Telescope	Wagner J., Roy A. L., Krichbaum T. P., Alef W., Bansod A., Bertarini A., Güsten R., Graham D., Hodgson J., Märtens R., Menten K., Muders D., Rottmann H., Tuccari G., Weiss A., Wieching G., Wunderlich M., Zensus J. A., Araneda J. P., Arriagada O., Cantzler M., Duran C., Montenegro-Montes F. M., Olivares R., Caro P., Bergman P., Conway J., Haas R., Johansson J., Lindqvist M., Olofsson H., Pantaleev M., Buttaccio S., Cappallo R., Crew G., Doeleman S., Fish V., Lu R.-S., Ruszczyk C., SooHoo J., Titus M., Freund R., Marrone D., Strittmatter P., Ziurys L., Blundell R., Primiani R., Weintroub J., Young K., Bremer M., Sánchez S., Marscher A. P., Chilson R., Asada K., Inoue M.	2015, A&A 581, A32
2012	New observations and models of circumstellar CO line emission of AGB stars in the Herschel SUCCESS programme	Danilovich T., Teyssier D., Justtanont K., Olofsson H., Cerrigone L., Bujarrabal V., Alcolea J., Cernicharo J., Castro-Carrizo A., García-Lario P., Marston A.	2015, A&A 581, A60
2013	The jet and the disk of the HH 212 low-mass protostar imaged by ALMA: SO and SO_2 emission	Podio L., Codella C., Gueth F., Cabrit S., Bachiller R., Gusdorf A., Lee C.-F., Lefloch B., Leurini S., Nisini B., Tafalla M.	2015, A&A 581, A85
2014	Planck's dusty GEMS: The brightest gravitationally lensed galaxies discovered with the Planck all-sky survey	Cañameras R., Nesvadba N. P. H., Guery D., McKenzie T., König S., Petitpas G., Dole H., Frye B., Flores-Cacho I., Montier L., Negrello M., Beelen A., Boone F., Dicken D., Lagache G., Le Floc'h E., Altieri B., Béthermin M., Chary R., de Zotti G., Giard M., Kneissl R., Krips M., Malhotra S., Martinache C., Omont A., Pointecouteau E., Puget J.-L., Scott D., Soucail G., Valtchanov I., Welikala N., Yan L.	2015, A&A 581, A105
2015	Planck intermediate results. XXVII. High-redshift infrared galaxy overdensity candidates and lensed sources discovered by Planck and confirmed by Herschel-SPIRE	Planck Collaboration, Aghanim N., Altieri B., Arnaud M., Ashdown M., Aumont J., Baccigalupi C., Banday A. J., Barreiro R. B., Bartolo N., Battaner E., Beelen A., Benabed K., Benoit-Lévy A., Bernard J.-P., Bersanelli M., Bethermin M., Bielewicz P., Bonavera L., Bond J. R., Borrill J., Bouchet F. R., Boulanger F., Burigana C., Calabrese E., Canameras R., Cardoso J.-F., Catalano A., Chamballu A., Chary R.-R., Chiang H. C., Christensen P. R., Clements D. L., Colombi S., Couchot F., Crill B. P., Curto A., Danese L., Dassas K., Davies R. D., Davis R. J., de Bernardis P., de Rosa A., de Zotti G., Delabrouille J., Diego J. M., Dole H., Donzelli S., Doré O., Douspis M., Ducout A., Dupac X., Efstathiou G., Elsner F., Enßlin T. A., Falgarone E., Flores-Cacho I., Forni O., Frailis M., Fraisse A. A., Franceschi E., Frejsel A., Frye B., Galeotta S., Galli S., Ganga K., Giard M., Gjerløw E., González-Nuevo J., Górski K. M., Gregorio A., Gruppuso A., Guéry D., Hansen F. K., Hanson D., Harrison D. L., Helou G., Hernández-Monteagudo C., Hildebrandt S. R., Hivon E., Hobson M., Holmes W. A., Hovest W., Huffenberger K. M., Hurier G., Jaffe A. H., Jaffe T. R., Keihänen E., Keskitalo R., Kisner T. S., Kneissl R., Knoche J., Kunz M., Kurki-Suonio H., Lagache G., Lamarre J.-M., Lasenby A., Lattanzi M., Lawrence C. R., Le Floc'h E., Leonardi R., Levrier F., Liguori M., Lilje P. B., Linden-Vørnle M., López-Caniego M., Lubin P. M., Macías-Pérez J. F., MacKenzie T., Maffei B., Mandolesi N., Maris M., Martin P. G., Martinache C., Martínez-González E., Masi S., Matarrese S., Mazzotta P., Melchiorri A., Mennella A., Migliaccio M., Moneti A., Montier L., Morgante G., Mortlock D., Munshi D., Murphy J. A., Natoli P., Negrello M., Nesvadba N. P. H., Novikov D., Novikov I., Omont A., Pagano L., Pajot F., Pasian F., Perdereau O., Perotto L., Perrotta F., Pettorino V., Piacentini F., Piat M., Plaszczynski S., Pointecouteau E., Polenta G., Popa L., Pratt G. W., Prunet S., Puget J.-L., Rachen J. P., Reach W. T., Reinecke M., Remazeilles M., Renault C., Ristorcelli I., Rocha G., Roudier G., Rusholme B., Sandri M., Santos D., Savini G., Scott D., Spencer L. D., Stolyarov V., Sunyaev R., Sutton D., Sygnet J.-F., Tauber J. A., Terenzi L., Toffolatti L., Tomasi M., Tristram M., Tucci M., Umana G., Valenziano L., Valiviita J., Valtchanov I., Van Tent B., Vieira J. D., Vielva P., Wade L. A., Wandelt B. D., Wehus I. K., Welikala N., Zacchei A., Zonca A.	2015, A&A 582, A30
2016	The MAGNUM survey: positive feedback in the nuclear region of NGC 5643 suggested by MUSE	Cresci G., Marconi A., Zibetti S., Risaliti G., Carniani S., Mannucci F., Gallazzi A., Maiolino R., Balmaverde B., Brusa M., Capetti A., Cicone C., Feruglio C., Bland-Hawthorn J., Nagao T., Oliva E., Salvato M., Sani E., Tozzi P., Urrutia T., Venturi G.	2015, A&A 582, A63
2017	Exploring the molecular chemistry and excitation in obscured luminous infrared galaxies. An ALMA mm-wave spectral scan of NGC 4418	Costagliola F., Sakamoto K., Muller S., Martín S., Aalto S., Harada N., van der Werf P., Viti S., Garcia-Burillo S., Spaans M.	2015, A&A 582, A91
2018	The OH-streamer in Sagittarius A revisited: analysis of hydroxyl absorption within 10 pc from the Galactic centre	Karlsson R., Sandqvist A., Fathi K., Martín S.	2015, A&A 582, A118
2019	CO emission from EP Aquarii: Another example of an axi-symmetric AGB wind?	Nhung P. T., Hoai D. T., Winters J. M., Le Bertre T., Diep P. N., Phuong N. T., Thao N. T., Tuan-Anh P., Darriulat P.	2015, A&A 583, A64
2020	The multi-phase winds of Markarian 231: from the hot, nuclear, ultra-fast wind to the galaxy-scale, molecular outflow	Feruglio C., Fiore F., Carniani S., Piconcelli E., Zappacosta L., Bongiorno A., Cicone C., Maiolino R., Marconi A., Menci N., Puccetti S., Veilleux S.	2015, A&A 583, A99
2021	Probing highly obscured, self-absorbed galaxy nuclei with vibrationally excited HCN	Aalto S., Martín S., Costagliola F., González-Alfonso E., Muller S., Sakamoto K., Fuller G. A., García-Burillo S., van der Werf P., Neri R., Spaans M., Combes F., Viti S., Mühle S., Armus L., Evans A., Sturm E., Cernicharo J., Henkel C., Greve T. R.	2015, A&A 584, A42

2022	Chemical features in the circumnuclear disk of the Galactic center	Harada N., Riquelme D., Viti S., Jiménez-Serra I., Requena-Torres M. A., Menten K. M., Martín S., Aladro R., Martin-Pintado J., Hochgürtel S.	2015, A&A 584, A102
2023	Jet multiplicity in the proto-binary system NGC 1333-IRAS4A. The detailed CALYPSO IRAM-PdBI view	Santangelo G., Codella C., Cabrit S., Maury A. J., Gueth F., Maret S., Lefloch B., Belloche A., André P., Hennebelle P., Anderl S., Podio L., Testi L.	2015, A&A 584, A126
2024	Suppression of Star Formation in NGC 1266	Alatalo K., Lacy M., Lanz L., Bitsakis T., Appleton P. N., Nyland K., Cales S. L., Chang P., Davis T. A., de Zeeuw P. T., Lonsdale C. J., Martín S., Meier D. S., Ogle P. M.	2015, ApJ 798, 31
2025	A Detection of Molecular Gas Emission in the Host Galaxy of GRB 080517	Stanway E. R., Levan A. J., Tanvir N. R., Wiersema K., van der Laan T. P. R.	2015, ApJ 798, L7
2026	ALMA Observations of Warm Dense Gas in NGC 1614 - Breaking of the Star Formation Law in the Central Kiloparsec	Xu C. K., Cao C., Lu N., Gao Y., Diaz-Santos T., Herrero-Illana R., Meijerink R., Privon G., Zhao Y.-H., Evans A. S., König S., Mazzarella J. M., Aalto S., Appleton P., Armus L., Charmandaris V., Chu J., Haan S., Inami H., Murphy E. J., Sanders D. B., Schulz B., van der Werf P.	2015, ApJ 799, 11
2027	Resolving the Bright HCN(1-0) Emission toward the Seyfert 2 Nucleus of M51: Shock Enhancement by Radio Jets and Weak Masing by Infrared Pumping?	Matsushita S., Trung D.-V.-, Boone F., Krips M., Lim J., Muller S.	2015, ApJ 799, 26
2028	Blowin' in the Wind: Both "Negative" and "Positive" Feedback in an Obscured High-*z* Quasar	Cresci G., Mainieri V., Brusa M., Marconi A., Perna M., Mannucci F., Piconcelli E., Maiolino R., Feruglio C., Fiore F., Bongiorno A., Lanzuisi G., Merloni A., Schramm M., Silverman J. D., Civano F.	2015, ApJ 799, 82
2029	Combined CO and Dust Scaling Relations of Depletion Time and Molecular Gas Fractions with Cosmic Time, Specific Star-formation Rate, and Stellar Mass	Genzel R., Tacconi L. J., Lutz D., Saintonge A., Berta S., Magnelli B., Combes F., García-Burillo S., Neri R., Bolatto A., Contini T., Lilly S., Boissier J., Boone F., Bouché N., Bournaud F., Burkert A., Carollo M., Colina L., Cooper M. C., Cox P., Feruglio C., Förster Schreiber N. M., Freundlich J., Gracia-Carpio J., Juneau S., Kovac K., Lippa M., Naab T., Salome P., Renzini A., Sternberg A., Walter F., Weiner B., Weiss A., Wuyts S.	2015, ApJ 800, 20
2030	Chemically Distinct Nuclei and Outflowing Shocked Molecular Gas in Arp 220	Tunnard R., Greve T. R., Garcia-Burillo S., Graciá Carpio J., Fischer J., Fuente A., González-Alfonso E., Hailey-Dunsheath S., Neri R., Sturm E., Usero A., Planesas P.	2015, ApJ 800, 25
2031	Hops 383: an Outbursting Class 0 Protostar in Orion	Safron E. J., Fischer W. J., Megeath S. T., Furlan E., Stutz A. M., Stanke T., Billot N., Rebull L. M., Tobin J. J., Ali B., Allen L. E., Booker J., Watson D. M., Wilson T. L.	2015, ApJ 800, L5
2032	Spatially Resolved L-C_3H^+ Emission in the Horsehead Photodissociation Region: Further Evidence for a Top-Down Hydrocarbon Chemistry	Guzmán V. V., Pety J., Goicoechea J. R., Gerin M., Roueff E., Gratier P., Öberg K. I.	2015, ApJ 800, L33
2033	The Herschel Comprehensive (U)LIRG Emission Survey (HERCULES): CO Ladders, Fine Structure Lines, and Neutral Gas Cooling	Rosenberg M. J. F., van der Werf P. P., Aalto S., Armus L., Charmandaris V., Díaz-Santos T., Evans A. S., Fischer J., Gao Y., González-Alfonso E., Greve T. R., Harris A. I., Henkel C., Israel F. P., Isaak K. G., Kramer C., Meijerink R., Naylor D. A., Sanders D. B., Smith H. A., Spaans M., Spinoglio L., Stacey G. J., Veenendaal I., Veilleux S., Walter F., Weiß A., Wiedner M. C., van der Wiel M. H. D., Xilouris E. M.	2015, ApJ 801, 72
2034	A Search for Consistent Jet and Disk Rotation Signatures in RY Tau	Coffey D., Dougados C., Cabrit S., Pety J., Bacciotti F.	2015, ApJ 804, 2
2035	Constraining the Abundances of Complex Organics in the Inner Regions of Solar-type Protostars	Taquet V., López-Sepulcre A., Ceccarelli C., Neri R., Kahane C., Charnley S. B.	2015, ApJ 804, 81
2036	Si-bearing Molecules Toward IRC+10216: ALMA Unveils the Molecular Envelope of CWLeo	Velilla Prieto L., Cernicharo J., Quintana-Lacaci G., Agúndez M., Castro-Carrizo A., Fonfría J. P., Marcelino N., Zúñiga J., Requena A., Bastida A., Lique F., Guélin M.	2015, ApJ 805, L13
2037	Short GMC Lifetimes: An Observational Estimate with the PdBI Arcsecond Whirlpool Survey (PAWS)	Meidt S. E., Hughes A., Dobbs C. L., Pety J., Thompson T. A., García-Burillo S., Leroy A. K., Schinnerer E., Colombo D., Querejeta M., Kramer C., Schuster K. F., Dumas G.	2015, ApJ 806, 72
2038	Discovery of SiCSi in IRC+10216: A Missing Link between Gas and Dust Carriers of Si-C Bonds	Cernicharo J., McCarthy M. C., Gottlieb C. A., Agúndez M., Velilla Prieto L., Baraban J. H., Changala P. B., Guélin M., Kahane C., Martin-Drumel M. A., Patel N. A., Reilly N. J., Stanton J. F., Quintana-Lacaci G., Thorwirth S., Young K. H.	2015, ApJ 806, L3
2039	A Direct Constraint on the Gas Content of a Massive, Passively Evolving Elliptical Galaxy at $z = 1.43$	Sargent M. T., Daddi E., Bournaud F., Onodera M., Feruglio C., Martig M., Gobat R., Dannerbauer H., Schinnerer E.	2015, ApJ 806, L20
2040	Local Instability Signatures in ALMA Observations of Dense Gas in NGC 7469	Fathi K., Izumi T., Romeo A. B., Martín S., Imanishi M., Hatziminaoglou E., Aalto S., Espada D., Kohno K., Krips M., Matsushita S., Meier D. S., Nakai N., Terashima Y.	2015, ApJ 806, L34
2041	Signatures of Young Star Formation Activity within Two Parsecs of Sgr A*	Yusef-Zadeh F., Wardle M., Sewilo M., Roberts D. A., Smith I., Arendt R., Cotton W., Lacy J., Martin S., Pound M. W., Rickert M., Royster M.	2015, ApJ 808, 97

2042	The 2014 ALMA Long Baseline Campaign: An Overview	ALMA Partnership, Fomalont E. B., Vlahakis C., Corder S., Remijan A., Barkats D., Lucas R., Hunter T. R., Brogan C. L., Asaki Y., Matsushita S., Dent W. R. F., Hills R. E., Phillips N., Richards A. M. S., Cox P., Amestica R., Broguiere D., Cotton W., Hales A. S., Hiriart R., Hirota A., Hodge J. A., Impellizzeri C. M. V., Kern J., Kneissl R., Liuzzo E., Marcelino N., Marson R., Mignano A., Nakanishi K., Nikolic B., Perez J. E., Pérez L. M., Toledo I., Aladro R., Butler B., Cortes J., Cortes P., Dhawan V., Di Francesco J., Espada D., Galarza F., Garcia-Appadoo D., Guzman-Ramirez L., Humphreys E. M., Jung T., Kameno S., Laing R. A., Leon S., Mangum J., Marconi G., Nagai H., Nyman L.-A., Radiszcz M., Rodón J. A., Sawada T., Takahashi S., Tilanus R. P. J., van Kempen T., Vila Vilaro B., Watson L. C., Wiklind T., Gueth F., Tatematsu K., Wootten A., Castro-Carrizo A., Chapillon E., Dumas G., de Gregorio-Monsalvo I., Francke H., Gallardo J., Garcia J., Gonzalez S., Hibbard J. E., Hill T., Kaminski T., Karim A., Krips M., Kurono Y., Lopez C., Martin S., Maud L., Morales F., Pietu V., Plarre K., Schieven G., Testi L., Videla L., Villard E., Whyborn N., Zwaan M. A., Alves F., Andreani P., Avison A., Barta M., Bedosti F., Bendo G. J., Bertoldi F., Bethermin M., Biggs A., Boissier J., Brand J., Burkutean S., Casasola V., Conway J., Cortese L., Dabrowski B., Davis T. A., Diaz Trigo M., Fontani F., Franco-Hernandez R., Fuller G., Galvan Madrid R., Giannetti A., Ginsburg A., Graves S. F., Hatziminaoglou E., Hogerheijde M., Jachym P., Jimenez Serra I., Karlicky M., Klaasen P., Kraus M., Kunneriath D., Lagos C., Longmore S., Leurini S., Maercker M., Magnelli B., Marti Vidal I., Massardi M., Maury A., Muehle S., Muller S., Muxlow T., O'Gorman E., Paladino R., Petry D., Pineda J., Randall S., Richer J. S., Rossetti A., Rushton A., Rygl K., Sanchez Monge A., Schaaf R., Schilke P., Stanke T., Schmalzl M., Stoehr F., Urban S., van Kampen E., Vlemmings W., Wang K., Wild W., Yang Y., Iguchi S., Hasegawa T., Saito M., Inatani J., Mizuno N., Asayama S., Kosugi G., Morita K.-I., Chiba K., Kawashima S., Okumura S. K., Ohashi N., Ogasawara R., Sakamoto S., Noguchi T., Huang Y.-D., Liu S.-Y., Kemper F., Koch P. M., Chen M.-T., Chikada Y., Hiramatsu M., Iono D., Shimojo M., Komugi S., Kim J., Lyo A.-R., Muller E., Herrera C., Miura R. E., Ueda J., Chibueze J., Su Y.-N., Trejo-Cruz A., Wang K.-S., Kiuchi H., Ukita N., Sugimoto M., Kawabe R., Hayashi M., Miyama S., Ho P. T. P., Kaifu N., Ishiguro M., Beasley A. J., Bhatnagar S., Braatz J. A., III, Brisbin D. G., Brunetti N., Carilli C., Crossley J. H., D'Addario L., Donovan Meyer J. L., Emerson D. T., Evans A. S., Fisher P., Golap K., Griffith D. M., Hale A. E., Halstead D., Hardy E. J., Hatz M. C., Holdaway M., Indebetouw R., Jewell P. R., Kepley A. A., Kim D.-C., Lacy M. D., Leroy A. K., Liszt H. S., Lonsdale C. J., Matthews B., McKinnon M., Mason B. S., Moellenbrock G., Moullet A., Myers S. T., Ott J., Peck A. B., Pisano J., Radford S. J. E., Randolph W. T., Rao Venkata U., Rawlings M. G., Rosen R., Schnee S. L., Scott K. S., Sharp N. K., Sheth K., Simon R. S., Tsutsumi T., Wood S. J.	2015, ApJ 808, L1
2043	The 2014 ALMA Long Baseline Campaign: Observations of Asteroid 3 Juno at 60 Kilometer Resolution	ALMA Partnership, Hunter T. R., Kneissl R., Moullet A., Brogan C. L., Fomalont E. B., Vlahakis C., Asaki Y., Barkats D., Dent W. R. F., Hills R. E., Hirota A., Hodge J. A., Impellizzeri C. M. V., Liuzzo E., Lucas R., Marcelino N., Matsushita S., Nakanishi K., Pérez L. M., Phillips N., Richards A. M. S., Toledo I., Aladro R., Broguiere D., Cortes J. R., Cortes P. C., Espada D., Galarza F., Garcia-Appadoo D., Guzman-Ramirez L., Hales A. S., Humphreys E. M., Jung T., Kameno S., Laing R. A., Leon S., Marconi G., Mignano A., Nikolic B., Nyman L.-A., Radiszcz M., Remijan A., Rodón J. A., Sawada T., Takahashi S., Tilanus R. P. J., Vila Vilaro B., Watson L. C., Wiklind T., De Gregorio-Monsalvo I., Di Francesco J., Mangum J., Francke H., Gallardo J., Garcia J., Gonzalez S., Hill T., Kaminski T., Kurono Y., Lopez C., Morales F., Plarre K., Randall S., van kempen T., Videla L., Villard E., Andreani P., Hibbard J. E., Tatematsu K.	2015, ApJ 808, L2
2044	The 2014 ALMA Long Baseline Campaign: First Results from High Angular Resolution Observations toward the HL Tau Region	ALMA Partnership, Brogan C. L., Pérez L. M., Hunter T. R., Dent W. R. F., Hales A. S., Hills R. E., Corder S., Fomalont E. B., Vlahakis C., Asaki Y., Barkats D., Hirota A., Hodge J. A., Impellizzeri C. M. V., Kneissl R., Liuzzo E., Lucas R., Marcelino N., Matsushita S., Nakanishi K., Phillips N., Richards A. M. S., Toledo I., Aladro R., Broguiere D., Cortes J. R., Cortes P. C., Espada D., Galarza F., Garcia-Appadoo D., Guzman-Ramirez L., Humphreys E. M., Jung T., Kameno S., Laing R. A., Leon S., Marconi G., Mignano A., Nikolic B., Nyman L.-A., Radiszcz M., Remijan A., Rodón J. A., Sawada T., Takahashi S., Tilanus R. P. J., Vila Vilaro B., Watson L. C., Wiklind T., Akiyama E., Chapillon E., de Gregorio-Monsalvo I., Di Francesco J., Gueth F., Kawamura A., Lee C.-F., Nguyen Luong Q., Mangum J., Pietu V., Sanhueza P., Saigo K., Takakuwa S., Ubach C., van Kempen T., Wootten A., Castro-Carrizo A., Francke H., Gallardo J., Garcia J., Gonzalez S., Hill T., Kaminski T., Kurono Y., Liu H.-Y., Lopez C., Morales F., Plarre K., Schieven G., Testi L., Videla L., Villard E., Andreani P., Hibbard J. E., Tatematsu K.	2015, ApJ 808, L3
2045	The 2014 ALMA Long Baseline Campaign: Observations of the Strongly Lensed Submillimeter Galaxy HATLAS J090311.6+003906 at z = 3.042	ALMA Partnership, Vlahakis C., Hunter T. R., Hodge J. A., Pérez L. M., Andreani P., Brogan C. L., Cox P., Martin S., Zwaan M., Matsushita S., Dent W. R. F., Impellizzeri C. M. V., Fomalont E. B., Asaki Y., Barkats D., Hills R. E., Hirota A., Kneissl R., Liuzzo E., Lucas R., Marcelino N., Nakanishi K., Phillips N., Richards A. M. S., Toledo I., Aladro R., Broguiere D., Cortes J. R., Cortes P. C., Espada D., Galarza F., Garcia-Appadoo D., Guzman-Ramirez L., Hales A. S., Humphreys E. M., Jung T., Kameno S., Laing R. A., Leon S., Marconi G., Mignano A., Nikolic B., Nyman L.-A., Radiszcz M., Remijan A., Rodón J. A., Sawada T., Takahashi S., Tilanus R. P. J., Vila Vilaro B., Watson L. C., Wiklind T., Ao Y., Di Francesco J., Hatsukade B., Hatziminaoglou E., Mangum J., Matsuda Y., van Kampen E., Wootten A., de Gregorio-Monsalvo I., Dumas G., Francke H., Gallardo J., Garcia J., Gonzalez S., Hill T., Iono D., Kaminski T., Karim A., Krips M., Kurono Y., Lonsdale C., Lopez C., Morales F., Plarre K., Videla L., Villard E., Hibbard J. E., Tatematsu K.	2015, ApJ 808, L4

2046	ALMA Observations of the Submillimeter Dense Molecular Gas Tracers in the Luminous Type-1 Active Nucleus of NGC 7469	Izumi T., Kohno K., Aalto S., Doi A., Espada D., Fathi K., Harada N., Hatsukade B., Hattori T., Hsieh P.-Y., Ikarashi S., Imanishi M., Iono D., Ishizuki S., Krips M., Martín S., Matsushita S., Meier D. S., Nagai H., Nakai N., Nakajima T., Nakanishi K., Nomura H., Regan M. W., Schinnerer E., Sheth K., Takano S., Tamura Y., Terashima Y., Tosaki T., Turner J. L., Umehata H., Wiklind T.	2015, ApJ 811, 39
2047	First NuSTAR Observations of Mrk 501 within a Radio to TeV Multi-Instrument Campaign	Furniss A., Noda K., Boggs S., Chiang J., Christensen F., Craig W., Giommi P., Hailey C., Harisson F., Madejski G., Nalewajko K., Perri M., Stern D., Urry M., Verrecchia F., Zhang W., NuSTAR Team, Ahnen M. L., Ansoldi S., Antonelli L. A., Antoranz P., Babic A., Banerjee B., Bangale P., Barres de Almeida U., Barrio J. A., Becerra González J., Bednarek W., Bernardini E., Biasuzzi B., Biland A., Blanch O., Bonnefoy S., Bonnoli G., Borracci F., Bretz T., Carmona E., Carosi A., Chatterjee A., Clavero R., Colin P., Colombo E., Contreras J. L., Cortina J., Covino S., Da Vela P., Dazzi F., De Angelis A., De Caneva G., De Lotto B., de Oña Wilhelmi E., Delgado Mendez C., Di Pierro F., Dominis Prester D., Dorner D., Doro M., Einecke S., Eisenacher Glawion D., Elsaesser D., Fernández-Barral A., Fidalgo D., Fonseca M. V., Font L., Frantzen K., Fruck C., Galindo D., García López R. J., Garczarczyk M., Garrido Terrats D., Gaug M., Giammaria P., Godinov', N., González Muñoz A., Guberman D., Hanabata Y., Hayashida M., Herrera J., Hose J., Hrupec D., Hughes G., Idec W., Kellermann H., Kodani K., Konno Y., Kubo H., Kushida J., La Barbera A., Lelas D., Lewandowska N., Lindfors E., Lombardi S., Longo F., López M., López-Coto R., López-Oramas A., Lorenz E., Majumdar P., Makariev M., Mallot K., Maneva G., Manganaro M., Mannheim K., Maraschi L., Marcote B., Mariotti M., Martínez M., Mazin D., Menzel U., Miranda J. M., Mirzoyan R., Moralejo A., Nakajima D., Neustroev V., Niedzwiecki A., Nievas Rosillo M., Nilsson K., Nishijima K., Orito R., Overkemping A., Paiano S., Palacio J., Palatiello M., Paneque D., Paoletti R., Paredes J. M., Paredes-Fortuny X., Persic M., Poutanen J., Prada Moroni P. G., Prandini E., Puljak I., Reinthal R., Rhode W., Ribó M., Rico J., Rodriguez Garcia J., Saito T., Saito K., Satalecka K., Scapin V., Schultz C., Schweizer T., Shore S. N., Sillanpää A., Sitarek J., Snidaric I., Sobczynska D., Stamerra A., Steinbring T., Strzys M., Takalo L., Takami H., Tavecchio F., Temnikov P., Terzi', T., Tescaro D., Teshima M., Thaele J., Torres D. F., Toyama T., Treves A., Verguilov V., Vovk I., Will M., Zanin R., MAGIC Collaboration, Archer A., Benbow W., Bird R., Biteau J., Bugaev V., Cardenzana J. V., Cerruti M., Chen X., Ciupik L., Connolly M. P., Cui W., Dickinson H. J., Dumm J., Eisch J. D., Falcone A., Feng Q., Finley J. P., Fleischhack H., Fortin P., Fortson L., Gerard L., Gillanders G. H., Griffin S., Griffiths S. T., Grube J., Gyuk G., Håkansson N., Holder J., Humensky T. B., Johnson C. A., Kaaret P., Kertzman M., Kieda D., Krause M., Krennrich F., Lang M. J., Lin T. T. Y., Maier G., McArthur S., McCann A., Meagher K., Moriarty P., Mukherjee R., Nieto D., O'Faoláin de Bhróithe A., Ong R. A., Park N., Petry D., Pohl M., Popkow A., Ragan K., Ratliff G., Reyes L. C., Reynolds P. T., Richards G. T., Roache E., Santander M., Sembroski G. H., Shahinyan K., Staszak D., Telezhinsky I., Tucci J. V., Tyler J., Vassiliev V. V., Wakely S. P., Weiner O. M., Weinstein A., Wilhelm A., Williams D. A., Zitzer B., The VERITAS Collaboration, Vince O., Fuhrmann L., Angelakis E., Karamanavis V., Myserlis I., Krichbaum T. P., Zensus J. A., Ungerechts H., Sievers A., F-Gamma Consortium T., Bachev R., Böttcher M., Chen W. P., Damljanovic G., Eswaraiah C., Güver T., Hovatta T., Hughes Z., Ibryamov S. I., Joner M. D., Jordan B., Jorstad S. G., Joshi M., Kataoka J., Kurtanidze O. M., Kurtanidze S. O., Lähteenmäki A., Latev G., Lin H. C., Larionov V. M., Mokrushina A. A., Morozova D. A., Nikolashvili M. G., Raiteri C. M., Ramakrishnan V., Readhead A. C. R., Sadun A. C., Sigua L. A., Semkov E. H., Strigachev A., Tammi J., Tornikoski M., Troitskaya Y. V., Troitsky I. S., Villata M.	2015, ApJ 812, 65
2048	Velocity-resolved [CII] Emission and [CII]/FIR Mapping along Orion with Herschel	Goicoechea J. R., Teyssier D., Etxaluze M., Goldsmith P. F., Ossenkopf V., Gerin M., Bergin E. A., Black J. H., Cernicharo J., Cuadrado S., Encrenaz P., Falgarone E., Fuente A., Hacar A., Lis D. C., Marcelino N., Melnick G. J., Müller H. S. P., Persson C., Pety J., Röllig M., Schilke P., Simon R., Snell R. L., Stutzki J.	2015, ApJ 812, 75
2049	A Higher Efficiency of Converting Gas to Stars Pushes Galaxies at z ~ 1.6 Well Above the Star-forming Main Sequence	Silverman J. D., Daddi E., Rodighiero G., Rujopakarn W., Sargent M., Renzini A., Liu D., Feruglio C., Kashino D., Sanders D., Kartaltepe J., Nagao T., Arimoto N., Berta S., Béthermin M., Koekemoer A., Lutz D., Magdis G., Mancini C., Onodera M., Zamorani G.	2015, ApJ 812, L23
2050	A Multi-wavelength Polarimetric Study of the Blazar CTA 102 during a Gamma-Ray Flare in 2012	Casadio C., Gómez J. L., Jorstad S. G., Marscher A. P., Larionov V. M., Smith P. S., Gurwell M. A., Lähteenmäki A., Agudo I., Molina S. N., Bala V., Joshi M., Taylor B., Williamson K. E., Arkharov A. A., Blinov D. A., Borman G. A., Di Paola A., Grishina T. S., Hagen-Thorn V. A., Itoh R., Kopatskaya E. N., Larionova E. G., Larionova L. V., Morozova D. A., Rastorgueva-Foi E., Sergeev S. G., Tornikoski M., Troitsky I. S., Thum C., Wiesemeyer H.	2015, ApJ 813, 51
2051	The Multi-phase Cold Fountain in M82 Revealed by a Wide, Sensitive Map of the Molecular Interstellar Medium	Leroy A. K., Walter F., Martini P., Roussel H., Sandstrom K., Ott J., Weiss A., Bolatto A. D., Schuster K., Dessauges-Zavadsky M.	2015, ApJ 814, 83
2052	The Peculiar Distribution of CH_3CN in IRC +10216 Seen by ALMA	Agúndez M., Cernicharo J., Quintana-Lacaci G., Velilla Prieto L., Castro-Carrizo A., Marcelino N., Guélin M.	2015, ApJ 814, 143
2053	Modeling the Molecular Gas in NGC 6240	Tunnard R., Greve T. R., Garcia-Burillo S., Graciá Carpio J., Fuente A., Tacconi L., Neri R., Usero A.	2015, ApJ 815, 114
2054	Variations in the Star Formation Efficiency of the Dense Molecular Gas across the Disks of Star-forming Galaxies	Usero A., Leroy A. K., Walter F., Schruba A., García-Burillo S., Sandstrom K., Bigiel F., Brinks E., Kramer C., Rosolowsky E., Schuster K.-F., de Blok W. J. G.	2015, AJ 150, 115

2055	Simultaneous multifrequency radio observations of the Galactic Centre magnetar SGR J1745-2900	Torne P., Eatough R. P., Karuppusamy R., Kramer M., Paubert G., Klein B., Desvignes G., Champion D. J., Wiesemeyer H., Kramer C., Spitler L. G., Thum C., Güsten R., Schuster K. F., Cognard I.	2015, MNRAS 451, L50
2056	WASP-14 b: transit timing analysis of 19 light curves	Raetz S., Maciejewski G., Seeliger M., Marka C., Fernández M., Güver T., Göğüş E., Nowak G., Vaňko M., Berndt A., Eisenbeiss T., Mugrauer M., Trepl L., Gelszinnis J.	2015, MNRAS 451, 4139
2057	A high-resolution wide-field radio survey of M51	Rampadarath H., Morgan J. S., Soria R., Tingay S. J., Reynolds C., Argo M. K., Dumas G.	2015, MNRAS 452, 32
2058	Evidences for a large hot spot on the disk of Betelgeuse (α Ori)	Montargès M., Kervella P., Perrin G., Chiavassa A., Le Bouquin J. B.	2015, IAUS 307, 273
2059	Gas inflow and AGN-driven outflow in M51	Querejeta M., Meidt S. E., Schinnerer E., García-Burillo S., Pety J., Hughes A., Meier D., Bigiel F., Kreckel K., Blanc G.	2015, IAUS 309, 338
2060	Physics and chemistry of UV illuminated gas: the Horsehead case	Guzmán V., Pety J., Gratier P., Goicoechea J. R., Gerin M., Roueff E., Teyssier D.	2015, Highlights of Astronomy 16, 593
2061	The Multi-Scale Environment of RS Cnc from CO and HI Observations	Hoai D. T., Matthews L. D., Winters J. M., Nhung P. T., Gérard E., Libert Y., Le Bertre T.	2015, ASPC 497, 119
2062	On the Central Symmetry of the Circumstellar Envelope of RS Cnc	Nhung P. T., Hoai D. T., Winters J. M., Darriulat P., Gérard E., Le Bertre T.	2015, ASPC 497, 133
2063	VLT/NACO Imaging of the Nearest AGB Star, L Puppis	Montargès M., Kervella P., Ridgway S. T., Perrin G., Chesneau O.	2015, ASPC 497, 209
2064	Search for ammonia in comet C/2012 S1 (ISON)	Faggi S., Codella C., Tozzi G. P., Comoretto G., Crovisier J., Nesti R., Panella D., Boissier J., Brucato J. R., Bolli P., Massi F., Tofani G.	2015, Planetary & Space Sci. 118, 173
2065	The European ALMA Regional Centre Network: A Geographically Distributed User Support Model	Hatziminaoglou E., Zwaan M., Andreani P., Barta M., Bertoldi F., Brand J., Gueth F., Hogerheijde M., Maercker M., Massardi M., Muehle S., Muxlow T., Richards A., Schilke P., Tilanus R., Vlemmings W., Afonso J., Messias H.	2015, The Messenger 162, 24
2066	The Convection of Close Red Supergiant Stars Observed With Near-Infrared Interferometry	Montargès M., Kervella P., Perrin G., Chiavassa A., Aurière M.	2015, EAS 71, 243
2067	The Nearby AGB Star L Puppis: The Birth Of a Planetary Nebula?	Kervella P., Montargès M., Lagadec E.	2015, EAS 71, 211
2068	The distribution and excitation of CHOH in comet C/2012 K1 (PanSTARRS) from ALMA	Milam S. N., Cordiner M. A., Boissier J., Charnley S. B., Remijan A., Mumma M., Villanueva G., Paganini L., Bockelee-Morvan D., Crovisier J., Biver N., Bonev B., Kuan Y.-J., Lis D.	2015, DPS 47, 506.05
2069	Long Wavelength Observations of Thermal Emission from Pluto and Charon with ALMA	Butler B. J., Gurwell M., Lellouch E., Moullet A., Moreno R., Bockelee-Morvan D., Biver N., Fouchet T., Lis D., Stern A., Young L., Young E., Weaver H., Boissier J., Stansberry J.	2015, DPS 47, 210.04
2070	Detection of HCN in Pluto's atmosphere	Lellouch E., Gurwell M., Butler B., Moullet A., Moreno R., Bockelée-Morvan D., Biver N., Fouchet T., Lis D., Stern A., Young L., Young E., Weaver H., Boissier J., Stansberry J.	2015, DPS 47, 105.07
2071	Detection of Atmospheric CO on Pluto with ALMA	Gurwell M., Lellouch E., Butler B., Moullet A., Moreno R., Bockelée-Morvan D., Biver N., Fouchet T., Lis D., Stern A., Young L., Young E., Weaver H., Boissier J., Stansberry J.	2015, DPS 47, 105.06
2072	Ethyl alcohol and sugar in comet C/2014 Q2 (Lovejoy)	Biver N., Bockelée-Morvan D., Moreno R., Crovisier J., Colom P., Lis D. C., Sandqvist A., Boissier J., Despois D., Milam S. N.	2015, Science Advances 1, 1500863
2073	First Polarised Light with the NIKA Camera	Ritacco A., Adam R., Adane A., Ade P., André P., Beelen A., Belier B., Benoît A., Bideaud A., Billot N., Bourrion O., Calvo M., Catalano A., Coiffard G., Comis B., D'Addabbo A., Désert F.-X., Doyle S., Goupy J., Kramer C., Leclercq S., Macías-Pérez J. F., Martino J., Mauskopf P., Maury A., Mayet F., Monfardini A., Pajot F., Pascale E., Perotto L., Pisano G., Ponthieu N., Rebolo-Iglesias M., Revéret V., Rodriguez L., Savini G., Schuster K., Sievers A., Thum C., Triqueneaux S., Tucker C., Zylka R.	2015, Journal of Low Temperature Physics, Online First, 19-Oct-2015
2074	A molecular survey of comet C/2014 Q2 (Lovejoy) at radio wavelengths	Biver N., Moreno R., Boissier J., Lis D., Bockelée-Morvan D., Crovisier J., Colom P., Paubert G., Milam S., Sandqvist A., Hjalmarson A., Lundin S., Karlsson T., Battelino M., Frisk U., Murtagh D., Nordh L.	2015, EPSC 10, EPSC2015-486
2075	Molecular Gas and Radio Jet Interaction: a Case Study of the Seyfert 2 AGN M51	Matsushita S., Trung D.-V., Boone F., Krips M., Lim J., Muller S.	2015, Pub. of the Korean Astr. Soc. 30, 439
2076	Giant Molecular Cloud Populations in Nearby Galaxies	Hughes A., Meidt S., Leroy A., Dobbs C., Schinnerer E., Colombo D., Wong T., Pety J.	2015, IAU Gen. Ass. 22, 2258072
2077	Anatomy of a Spiral Arm: Gas, Dust and Star Formation	Schinnerer E., Meidt S., Pety J., Leroy A., Hughes A., Colombo D.	2015, IAU Gen. Ass. 22, 2257628
2078	Star Formation Regulation on Molecular Cloud Scale	Schinnerer E., Meidt S., Hughes A., Colombo D., Pety J., Querejeta M., Leroy A.	2015, IAU Gen. Ass. 22, 2257438
2079	Intensity ratios: a cautionary tale	Green C.-E., Cunningham M., Green J., Dawson J., Jones P., Lopez-Sanchez A., Verdes-Montenegro L., Henkel C., Baan W., Martin S.	2015, IAU Gen. Ass. 22, 2255894
2080	Dense circum-nuclear molecular gas in starburst galaxies	Green C.-E., Cunningham M., Green J., Dawson J., Jones P., Lopez-Sanchez A., Verdes-Montenegro L., Henkel C., Baan W., Martin S.	2015, IAU Gen. Ass. 22, 2255865
2081	Measuring the distribution and excitation of cometary volatiles using ALMA	Cordiner M. A., Charnley S. B., Milam S., Mumma M. J., Villanueva G., Paganini L., Bockelee-Morvan D., Biver N., Crovisier J., Boissier J., Remijan A. J., Kuan Y.-J., Chuang Y.-L.	2015, IAU Gen. Ass. 22, 2255335

2082	Shedding light on the formation of disks and multiple systems: small- scale properties of Class 0 protostars from the CALYPSO IRAM-PdBI interferometric survey	Maury A., André P., Maret S., Belloche A., Gueth F., Cabrit S., Codella C., Anderl S., Santangelo G.	2015, IAU Gen. Ass. 22, 2254840
2083	Resolved star formation relations at high redshift from the IRAM PHIBSS program	Freundlich J., Combes F., Tacconi L., Cooper M., Genzel R., Neri R.	2015, IAU Gen. Ass. 22, 2247399
2084	Molecules in action: Extragalactic ISM at high resolution	Martin S.	2015, IAU Gen. Ass. 22, 2241940
2085	On the central symmetry of the circumstellar envelope of RS Cnc	Nhung P. T., Thi Hoai D., Winters J. M., Darriulat P., Gérard E., Le Bertre T.	2015, Research in Astron. and Astrophys. 15, 713
2086	Localizing the γ rays from blazar PKS 1502+106	Karamanavis V., Fuhrmann L., Krichbaum T. P., Angelakis E., Hodgson J., Myserlis I., Nestoras I., Zensus J. A., Ungerechts H., Sievers A.	2015, arXiv:1504.02314
2087	5 year Global 3-mm VLBI survey of Gamma-ray active blazars	Hodgson J. A., Krichbaum T. P., Marscher A. P., Jorstad S. G., Marti-Vidal I., Lindqvist M., Bremer M., Sanchez S., de Vicente P., Zensus J. A.	2015, arXiv:1504.03136
2088	The chemistry of molecular anions in circumstellar sources	Agúndez M., Cernicharo J., Guélin M.	2015, AIPC 1642, 362
2089	Short GMC lifetimes: an observational estimate with the PdBI Arcsecond Whirlpool Survey (PAWS)	Meidt S., Hughes A., Dobbs C. L., Pety J., Thompson T. A., Garcia-Burillo S., Leroy A. K., Schinnerer E., Colombo D., Querejeta M., Kramer C., Schuster K., Dumas G.	2015, AAS 225, 446.08
2090	An ALMA detection of circumnuclear molecular gas in M87	Vlahakis C. E., Leon S., Martin S.	2015, AAS 225, 324.07
2091	Line Ratio Diagnostics Along the Disc of Two Edge-on Lenticular Galaxies, NGC 4710 and NGC 5866	Topal S., Bureau M., Davis T. A., Young L., Krips M.	2015, AAS 225, 127.03
2092	(134340) Pluto	Lellouch E., Gurwell M., Butler B., Moullet A., Moreno R., Bockelee-Morvan D., Biver N., Fouchet T., Lis D., Stern A., Young L., Young E., Weaver H., Boissier J., Stansberry J.	2015, IAUC 9273, 1
2093	Significant Decrease in Intensity and Variability of Millimeter Emission from V404 Cyg	Tetarenko A., Sivakoff G. R., Bremer M., Miller-Jones J. C., Mooley K., Fender R., Staley T., Anderson G.	2015, Astronomer's Telegram No. 7740

Committees

EXECUTIVE COUNCIL

R. Bachiller, OAN-IGN, Spain
A. Barcia Cancio, CAY, Spain
R. Genzel, MPE, Germany
J. Gomez-Gonzalez, IGN, Spain
S. Guilloteau, CNRS, France
K. Menten, MPIfR, Germany
D. Mourard, CNRS-INSU, France
J.L. Puget, IAS, France
M. Schleier, MPG, Germany

SCIENTIFIC ADVISORY COMMITTEE

F. Boulanger, IAS, France
R. Moreno, LESIA, France
M. Tafalla, OAN, Spain
M. Gerin, ENS, France
P. Planesas, OAN, Spain
A. Weiss, MPIfR, Germany
G.J. Stacey, Cornell Univ., USA
L. Tacconi, MPE, Germany
F. Wyrowski, MPIfR, Germany

PROGRAM COMMITTEE

J. Alcolea, OAN, Spain
A. Bolatto, Maryland, USA
C. Codella, INAF, Italy
J. Goicoechea, CSIC, Spain
K. Kohno, IAT, Japan
C. Vastel, IRAP, France
A. Beelen, IAS, France
N. Brouillet, OASU, France
R. Davé, Western Cape Univ., SA
L. Hartmann, Michigan, USA
H. Linz, MPIA, Germany
A. Blain, Leicester Univ., UK
V. Bujarrabal, OAN, Spain
R. Davies, MPE, Germany
C. Henkel, MPIfR, Germany
A. Usero, OAN, Spain

AUDIT COMMISSION

M. L. Inisan-Ehret, CNRS, France
G. Maar, MPG, Germany

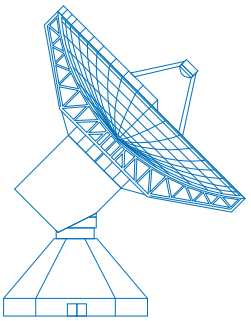

30-meter telescope, Pico Veleta

7 x 15-meter interferometer, NOEMA

The Institut de Radioastronomie Millimétrique (IRAM) is a multi-national scientific institute covering all aspects of radio astronomy at millimeter wavelengths. IRAM operates two observatories - a 30-meter telescope on Pico Veleta in the Sierra Nevada and NOEMA, an interferometer of seven 15-meter antennas on the Plateau de Bure in the French Alps.

IRAM was founded in 1979 by two national research organizations: the CNRS and the Max-Planck-Gesellschaft – the Spanish Instituto Geográfico Nacional, initially an associate member, became a full member in 1990.

The technical and scientific staff of IRAM develops instrumentation and software for the specific needs of millimeter radioastronomy and for the benefit of the international astronomical community.

IRAM's scientists conduct forefront research in several domains of astrophysics, from nearby star-forming regions to objects at cosmological distances.

IRAM Partner Organizations:
Centre National de la Recherche Scientifique (CNRS) – Paris, France
Max-Planck-Gesellschaft (MPG) – München, Deutschland
Instituto Geográfico Nacional (IGN) – Madrid, España

iram
Institut de
Radioastronomie
Millimétrique